"FEDERICO II" UNIVERSITY OF NAPLES

PhD PROGRAM IN NEUROSCIENCE

XXXI CYCLE

PhD Thesis:

IDENTIFICATION OF THE ROLE PLAYED BY Na^+/Ca^{2+} EXCHANGER 1 (NCX1) IN HIPPOCAMPAL-DEPENDENT ANXIETY, SPATIAL LEARNING AND MEMORY CONSOLIDATION THROUGH GENETIC MODIFIED MICE AND NEWLY SYNTHESIZED COMPOUNDS

Tutor

Dr. Pasquale Molinaro

Candidate

Dr. Silvia Natale

ACADEMIC YEAR 2017-2018

SUMMARY

ABSTRACT

The Na^+/Ca^{2+} exchanger 1 (NCX1), which is highly expressed in the hippocampus, cortex, and amygdala, regulates Akt1 phosphorylation. Since Akt1 is part of the PTEN/Akt1/CREB signaling pathway, which participates in synaptic plasticity and long-term memory, we investigated whether NCX1 expression/activity might also be involved in some hippocampal-dependent learning and memory processes. To test this hypothesis, we used two genetically-modified mice to selectively overexpress (*NCX1.4*^{over}) or downregulate (*NCX1*^{ko}) NCX1 in hippocampal, cortical, and amygdala neurons and a newly synthesized selective NCX1 stimulating compound, named CN-PYB2. Both *NCX1.4*^{over} and CN-PYB2-treated mice showed increased phosphorylated CaMKII levels in the hippocampus and improved long-term spatial learning and memory performance. By contrast, *NCX1*^{ko} mice displayed a decrease in both. In addition, both *NCX1.4*^{over} and CN-PYB2-treated mice also displayed an increase in context-dependent anxiety.

Altogether, these results demonstrate that neuronal NCX1 participates in hippocampal-amygdala memory consolidation and promote anxiety behavior.

1. INTRODUCTION

1.1 MEMORY PROCESS

1.1.1 HISTORY OF THE RESEARCH IN SYNAPTIC PLASTICITY AND MEMORY CONSOLIDATION

Memory is defined as the capacity of brain to storage new pieces of information. The memory process is not a single faculty of mind but it is composed by multiple kinds of learning, each one processed by different brain regions. Studies in memory classification began in 1804 when Mine de Biran described for the first time three types of memories: (a) mechanical memory, (b) sensitive memory and (c) representative memory (Maine de Biran, 1929). In 1890 James W. explained in two different chapters memory and habits; in 1923 McDougall distinguished between explicit and implicit recognition and Tolman in 1948 reaching the theory that there is more than one kind of learning (James, 1890; Tolman, 1948). However, the main milestone in the memory research is represented by the case of the patient H.M., a severely amnesic man that was able to learn hand-eye coordination skill in absence of most of brain structure related to memory (Milner et al., 1968). Thanks to the increasing research in memory, to date it is widely accepted that it can be mainly classified in declarative and non-declarative memories. Declarative memory is the capacity of conscious to recollect fact and events and depending on structures in the medial temporal lobe and midline diencephalon (Squire et al., 2004). Non-declarative memory is referred to the collection of non-conscious abilities including simple

conditioning, priming, skills and habits, each one dependent on amygdala, neocortex and striatum respectively (Squire, 1992).

1.1.2 BRAIN STRUCTURES INVOLVED IN MEMORY FORMATION

To date, it is known that the most important cerebral regions involved in memory formation are the medial temporal lobe of cerebral cortex, amygdala, hippocampus, cingulate gyrus, thalamus and hypothalamus. The brain structures responsible of the "storage information" are interrelated through neural circuits. The cerebral cortex is subdivided into four lobes each one participates in different kinds of learning. The frontal lobe, known as prefrontal cortex, is involved in conscious though and in higher mental functions such as decision-making and it is important in processing short-term memory and in retaining long-term memories (Matthews, 2015). The parietal lobe integrates sensory information and participates in determining spatial sense and navigation; temporal lobe is involved in the senses of smell and sound and in processing of semantics and the occipital lobe is mainly involved in the sense of sight. The amygdala is essentially associated to memory consolidation, emotional learning and fear mediated responses (Roozendaal et al., 2009). Finally, the hippocampus is important for the conversion of short-term to long-term memory (Wong, 1997). Interestingly, hippocampus is divided in two subregions dorsal and ventral that are differently involved in several cognition processes. In particular, dorsal hippocampus participates in the spatial memory, since it is enriched with "place cells" that are responsible for modeling of cognitive maps representing the surrounding environment (Moser et al., 2015; Cobar et al., 2017). On the other hand, the ventral hippocampus is involved in contextual anxiety since it is enriched with

"anxiety cells", that increase their cytosolic Ca^{2+} concentration ($[Ca^{2+}]_i$) in response to anxiety-dependent contexts (Jimenez et al., 2018).

1.1.3 BIOCHEMISTRY OF MEMORY: LONG TERM POTENTIANTION (LTP) AND MOLECULAR PATWAYS

The molecular storage of learning and memory in the brain is highly correlated to the changes in the strength and numbers of connections among neurons. This phenomenon is called "synaptic plasticity" and the potentiation of synaptic connection responds differently to specific stimulations (HEBB and KONZETT, 1949). Studies in hippocampal neurons suggest that a weak train of stimulations induces post-tetanic potentiation (PTP), whereas an intermediate train of stimulations induces short term potentiation (STP) and a strong train of stimulations induces the long-term potentiation (LTP) (Bliss and Collingridge, 1993). The effect of PTP lasts in the range of several minutes, STP decays within 1 hour and LTP is sustained for a much longer period (Bliss and Gardner-Medwin, 1973; Walters and Byrne, 1984; Zucker and Regehr, 2002). The LTP could be delivered by a "tetanus" which means a train of 50-100 stimuli at 100 Hz (Figurov et al., 1996), by a more modest stimulus such as "theta-burst stimulation" (several bursts of 4 shocks at 100 Hz delivered at an interval of 200 ms) (Larson et al., 1986) or by a "primed burst stimulation" (a single priming stimulus followed at 200 ms by 4 shocks at 100 Hz) (Rose and Dunwiddie, 1986; Otto et al., 1991). The LTP is characterized by three basic properties: cooperativity, means the intensity and pattern of tetanic stimulation; associativity, the input could be active at the same or separate time; and input-specificity, LTP could occur only in a synapse of a neuron. The effects of LTP are expressed in the potentiation of long-

term memory (Lynch, 2004). The molecular mechanisms occurred during LTP process are dependent on the stimulation of NMDA glutamate receptors, Ca^{2+} entry and the activation of specific molecular pathways (Miyamoto, 2006). Studies performed in Ca^{2+}/Calmodulin-dependent protein kinase II (CaMKII) mutant mice, or experiments performed on hippocampal slices after a theta-burst stimulation suggest a crucial role of the active form of the CaMKII during LTP (Silva et al., 1992; Fukunaga et al., 1993; Fukunaga et al., 1995). The generation of knockout mice for the cyclic AMP responsive element binding protein (CREB) suggests that the phosphorylation and activation of this protein is important for the induction of the LTP (Bourtchuladze et al., 1994) since it promotes the transcription of genes involved in the consolidation of synaptic plasticity (Lüscher et al., 2000). Moreover, it is known that the activation CREB could be directly regulated by CaMKII phosphorylation (Sun et al., 1994) or by AKT phosphorylation (Du and Montminy, 1998). At present, both CaMKII and CREB are considered as molecular markers of memory (Mizuno et al., 2002; Kandel, 2012).

1.2 THE Na^+ AND Ca^{2+} EXCHANGER (NCX)

1.2.1 BIOCHEMICAL CHARACTHERIZATION OF NCX

The Na^+ and Ca^{2+} exchanger (NCX) is an important plasma membrane transporter that mediates the antiporter of Na^+ and Ca^{2+} (Reeves and Hale, 1984; Fujioka et al., 2000; Kang and Hilgemann, 2004). The exchanger is expressed in three isoforms NCX1, NCX2 and NCX3, each one is coded by three different genes (Nicoll et al., 1990; Li et al., 1994; Nicoll et al., 1996). NCX1 is composed of 938 amino acids and has a theoretical molecular mass of 120 kDa, NCX2 and NCX3 consists of 921 and 927 amino acids with a predicted molecular weight of 102 and 105 kDa, respectively.

It is widely accepted that NCX mediates the antiporter of Ca^{2+} and Na^+ ions across plasma membrane with a stoichiometry 1:3, even if it could vary from 1:1 to 1:4 depending on intracellular Na^+ and Ca^{2+} concentration (Blaustein and Lederer, 1999; Philipson and Nicoll, 2000). NCX could operate in *forward* mode by coupling extrusion of Ca^{2+} to the influx of Na^+ and in *reverse* mode by mediating the extrusion of Na^+ and the intrusion of Ca^{2+} (Annunziato et al., 2004).

1.2.2 TISSUE-SPECIFIC DISTRIBUTIONS OF NCX ISOFORMS

The three NCX isoforms show a peculiar distribution in different tissues. In particular, the isoform NCX1 is expressed in brain, heart, skeletal muscle, smooth muscle, kidney, eye, secretory and blood cells, whereas NCX3 has been found in neuronal and skeletal muscle tissues (Quednau et al., 1997) and NCX2 is predominantly expressed in CNS (Jeon et al., 2003).

NCX1, NCX2 and NCX3 genes are differently expressed in neurons and glia of all areas of the central nervous system (CNS) (Papa et al., 2003). In particular,

pyramidal neurons of motor cortex layer III and V are enriched in NCX1, whereas NCX2 is intensively localized in the somatosensory cortical area. Immunohistochemistry experiments revealed differential expression of NCX isoforms in hippocampal subregions. NCX1 isoform is mainly localized in the granule cell layer and in dentate gyrus, the area of hippocampus receiving cortical projections; both NCX1 and NCX3 are expressed in the CA3 region, whereas only NCX3 is mainly found in the CA1 region. In the amygdala both NCX1 and NCX3 are localized in the lateral nucleus and basolateral nuclei (Canitano et al., 2002).

1.2.3 THE IMPORTANCE OF NCX UNDER PATHOLOGICAL AND PHISYOLOGICAL CONDITIONS

The Na^+ and Ca^{2+} exchanger is involved under different physiological and pathological conditions by regulating sodium and calcium homeostasis. Under physiological condition, for example, NCX is important in the contraction of cardiac myocytes (Bridge et al., 1990; Crespo et al., 1990), in mastocytes it participates in the cellular activation (Aneiros et al., 2005), in neurons it is involved in action potential and neurotransmitters release, and in glia it could regulate cellular activation (Boscia et al., 2009) and oligodendrocyte differentiation (Boscia et al., 2011). The Na^+ and Ca^{2+} exchanger is also involved in pathological diseases characterized by a dysregulation of Ca^{2+} homeostasis, such as stroke, Alzheimer, Parkinson and multiple sclerosis diseases (Herchuelz et al., 2002; Pannaccione et al., 2002; Molinaro et al., 2008b). In stroke, it has been discovered that an increase in NCX activity could limit the severity of ischemic damage by coping with the increase of $[Ca^{2+}]_i$ (Annunziato et al., 2007). The analysis of NCX isoforms in synaptosomal

preparation from parietal cortex of normal aged controls and late stage Alzheimer's disease patient revealed an upregulation of NCX2 and a downregulation of NCX3 suggesting a possible role of this protein in the progression of the disease (Sokolow et al., 2011).

NCX2 and NCX3 plasmalemmal proteins regulate the mitochondrial protein kinase PINK1, involved in Parkinson disease, and their activity prevent the neurodegeneration of dopaminergic neurons by regulating the accumulation of mitochondrial $[Ca^{2+}]_i$ (Wood-Kaczmar et al., 2013). In multiple sclerosis NCX have been implicated in the impairment of axonal and neuronal functions.

1.2.4 PHARMACOLOGICAL MODULATION NCX

Since the discovery of the roles of NCX under different physiological and pathological conditions, many studies have been dedicated to its pharmacological modulation (Annunziato et al., 2004). Several organic and inorganic compounds have been identified as modulators of NCX activity, however most of them are inhibitors (Watano et al., 1999; Iwamoto et al., 2004; Secondo et al., 2009b; Molinaro et al., 2016), subdivided in 16 chemical classes, or possesses some nonspecific effects on others ion channels or receptors (Pintado et al., 2000; Reuter et al., 2002b). A new cell penetrating peptide, consistent of the endogenous region 562-688aa of the exchanger, was developed to prevent, by steric hindrance, the interaction between P1 and XIP domains involved in the autoinhibition of the exchanger (Molinaro et al., 2015). Thus, this regulatory peptide exerts a stimulatory effect on NCX1 activity. Recently, a new chemical compound named neurounina-1 (Molinaro et al., 2013) was synthesized by the modification of the chemical structure of SM-15811, one of

the most potent inhibitor of NCX activity (Hasegawa et al., 2003). Neurounina-1 is able to increase NCX1 and NCX2 activity, in both *forward* and *reverse* modes of operation, with an EC_{50} in the low nanomolar range, whereas it has no effects on NCX3 activity. This new compound shows a neuroprotective effect on experimental model of cerebral ischemia. In order to obtain drugs selective for each NCX isoform, twenty new compounds were generated by different modifications on the chemical backbone of neurounina-1. In the present work these compounds were screened for their effects on NCX1, NCX2 and NCX3 activity.

1.2.5 NCX GENETIC MODIFIED MICE

In order to study the role of all three NCX isoforms under some physiological or pathological conditions NCX1, NCX2 and NCX3 genetically modified mice were generated. In 2000, four independent laboratories generated NCX1 knock-out mice, but this mouse dye in utero 9.5 days post-coitum because of the loss of spontaneous heartbeat (Cho et al., 2000; Wakimoto et al., 2000; Koushik et al., 2001; Reuter et al., 2002a) Then, in 2004, Henderson *et al.*, overcame this limitation with the generation of a conditioned NCX1 knock-out mouse by means of Cre/LoxP technique. The knock-out of NCX2 or NCX3 isoform is compatible with life and survive until old age. Further studies in NCX1 genetic modified mice show that the overexpression of NCX1 in cortex and hippocampus reduces the ischemic volume and ameliorates focal and general deficits after transient middle cerebral artery occlusion, whereas, opposite results are obtained in NCX1 knockout mice. Moreover, the overexpression of NCX1 is accompanied by an enhancement of phosphorylation levels of Akt1 in

neuronal cells in both *in vitro* and *in vivo* models (Secondo et al., 2015; Molinaro et al., 2016; Secondo et al., 2018b).

Moreover, since NCX plays a role in the regulation of $[Ca^{2+}]_i$ concentration at synaptic level of hippocampal neurons (Reuter and Porzig, 1995; Bouron and Reuter, 1996) the role of NCX2 and NCX3 in learning and memory performance were investigated by the use of NCX2 and NCX3 knock-out mice, respectively. The deletion of NCX2 in hippocampal neurons significantly prolongs the time required for clearance of increased $[Ca^{2+}]_i$ and consequently increases LTP and synaptic plasticity consolidation. Furthermore, NCX2 knock-out mice show an improvement of their performance in hippocampal-depended learning and memory tasks such as Barnes maze, contextual conditioning and novel object recognition test (Jeon et al., 2003). On the other hand, the knock-out of NCX3 worsens LTP and impairs basal synaptic transmission in hippocampus. For this reason, NCX3 knockout mice show a reduction of CaMKII expression and a reduction of learning and memory performance in Barnes maze, novel object and context depended fear conditioning assay (Molinaro et al., 2011).

To date, there is no evidence of the role played by NCX1 in learning and memory performance, but previous studies show that NCX1 increases the phosphorylation of Akt, a protein involved in signalling pathways important for the long-term potentiation and in the improvement of memory consolidation (Sui et al., 2008; Giese and Mizuno, 2013). In the present work we analyse the effects of NCX1 on learning and memory tasks by modulating its activity with a new selective activator, and its expression with the generation of two genetic modified mice that, upon tamoxifen administration show

a selective overexpression, or knockout, of NCX1 isoform (Molinaro et al., 2016) in neurons of hippocampus, cortex and amygdala.

2. AIMS

The Na^+/Ca^{2+} exchanger 1 (NCX1) participates in the maintenance of cytosolic Ca^{2+} homeostasis and is highly expressed in the hippocampus, cortex, and amygdala (Canitano et al., 2002; Papa et al., 2003), three brain regions involved in spatial learning and memory and social behavior. This appear to be very interesting since: (a) NCX1 expression/activity regulates Akt1 phosphorylation in neuronal cells (Secondo et al., 2015; Molinaro et al., 2016; Secondo et al., 2018a); (b) NCX1 might increase CREB phosphorylation via the PTEN/Akt/CREB signaling pathway by increasing Akt1 phosphorylation; (c) NCX1 might affect calmodulin kinase II (CaMKII) activation via the Ca^{2+}/calmodulin/CaMKII pathway by regulating cytosolic neuronal Ca^{2+} clearance; (d) activation of both CaMKII and CREB proteins plays a pivotal role in spatial learning and memory performance and anxiety behavior (Carlezon et al., 2005; Lo Iacono and Gross, 2008).

On the basis of these assumptions, we investigated the role of NCX1 in spatial learning, memory and anxiety behavior by means of two complementary strategies: (i) two genetically modified mouse strains for NCX1 and (ii) the design and synthesis of a newly compound, named CN-PYB2, that selectively increases NCX1 activity. In particular, upon tamoxifen administration, the two genetically modified mouse strains, display a selective increase ($NCX1.4^{over}$), or decrease ($NCX1^{ko}$), in NCX1 expression in hippocampal, cortical and amygdala neurons (Molinaro et al., 2016).

All genetically modified mice for NCX1 and CN-PYB2-treated C57BL/6 mice were analyzed in several hippocampal-dependent tasks to evaluate the physiological role of NCX1 in promoting spatial learning, memory, and anxiety behavior, and in

activating of some molecular markers involved in synaptic plasticity including CaMKII and CREB.

3. MATERIALS AND METHODS

3.1 PROCEDURES FOR THE SYNTHESIS OF 5-(2-CHLOROPHENYL)-7-NITRO-1-(PYRROLIDIN-1-YLMETHYL)-1H-BENZO[E][1,4]DIAZEPIN-2(3H)-ONE 2,2,2-TRIFLUOROACETATE (COMPOUND 2)

The compound was obtained as following the synthetic procedure reported for neurounina-1 (Molinaro et al., 2013), starting from clonazepam and pyrrolidine. Yield 67.8%. ESI-MS calcd for $C_{20}H_{19}ClN_4O_3$ 398,8 found $[M+H]^+$ 400,5. Final compound was converted to the corresponding trifluoroacetate salt by dissolving in 0.1% trifluoroacetic acid (TFA) in H_2O/acetonitrile (60:40 [v/v]). Finally, the obtained solution was frozen and lyophilized to yield the desired salt (mp 169.1 °C). The final product was analyzed by NMR spectroscopy. In particular, results showed ^{1}H NMR (400 MHz, DMSO-d6) δ 1.80-1.90 (m, 4H), 2.00-2.10 (m, 4H), 3.75 (s, 2H), 4.27 (s, 2H), 7.47-7.57 (m, 4H), 7.78 (s, 1H), 7.82 (d, 1H), 8.41 (d, 1H); ^{13}C-NMR (400 MHz, DMSO-d6): δ 168.69; 168.30; 143.95; 142.37; 137.79; 132.37; 132.33; 132.26; 130.25; 127.98; 127.72; 127.28; 125.45; 122.96; 60.70; 55.39; 54.35; 22.82; where "s" was used for singlet and "m" was used for multiplet. The ^{1}H and ^{13}C NMR spectra were recorded on a Varian Mercury Plus 400 MHz instrument (Varian Inc., Palo Alto, CA). Purity of the product (>99.5%) was assessed by analytical reversed-phase high-performance liquid chromatography (HPLC) using the conditions previously reported in literature for neurounina-1 (Molinaro et al., 2013).

3.2 EXPERIMENTAL GROUPS

Both genetically modified mouse lines, viz, neuronal specific NCX1.4 overexpressing mice (*NCX1.4*^{over}) and NCX1 knock-out (*NCX1*^{ko}) mice, were generated by our research group as previously described (Molinaro et al., 2016). Wild-type C57BL/6 mice were purchased from Charles River (Italy). *NCX1*^{ko}, *NCX1.4*^{over} and C57BL/6 mouse strains, aged 8–12 weeks and weighing 20–25 g, were housed under diurnal lighting conditions (light 6:00 a.m. to 6:00 p.m.).

In this study, 105 genetically modified and 75 C57BL/6 male mice were used for experimental procedures. In particular, animals for each experimental group were randomly selected from the respective mouse genotypes. Fifteen animals, randomly selected for each genotype, were considered to be sufficient per each experimental group to demonstrate any variation in behavioral tests.

To induce genomic DNA recombination, both *NCX1*^{ko}, *NCX1.4*^{over} were treated with tamoxifen for 5 days as previously reported (Molinaro et al., 2016) and used after at least one week of drug wash-out. C57BL/6 mice were treated with saline solution (vehicle) or with 32 µg/kg of Compound 2 solution by i.p. injections. In vivo toxicity was evaluated by a single i.p. administration of a saline solution containing 32 µg/kg of Compound 2. Variations of body weight, temperature, and abnormal behavior was monitored for 15 days.

All experiments were carried out in blind manner, the people who performed the experiments and analyzed the data were not aware of the pharmacological treatment. All protocols and procedures of the handling of animals were performed on male mice according to the international guidelines for animal research and approved by the Animal Care Committee of “Federico II” University of Naples, Italy.

3.3 MEASUREMENT OF Na^+-DEPENDENT $^{45}Ca^{2+}$ EFFLUX

NCX-mediated $^{45}Ca^{2+}$ efflux was measured as previously described (Molinaro et al., 2013). Briefly, cells were loaded with 5 µM $^{45}Ca^{2+}$ (80 MBq/ml) together with 1 µM ionomycin for 60 seconds in normal Krebs (in mM): 5.5 KCl, 145 NaCl, 1.2 $MgCl_2$, 1.5 $CaCl_2$, 10 glucose, and 10 Hepes-NaOH (pH 7.4). Next, cells were exposed either to a Ca^{2+} and Na^+-free solution—a condition that blocks both intracellular $^{45}Ca^{2+}$ efflux and extracellular Ca^{2+} influx— or to a Ca^{2+}-free plus 0.5 mM EGTA containing 145 mM Na^+, a condition that promotes $^{45}Ca^{2+}$ efflux. Thapsigargin (1 µM) was present in both solutions. $^{45}Ca^{2+}$ efflux was started by using Ca^{2+}-free, Na^+-containing solution plus 0.5 mM EGTA. Cells were exposed to this solution, which promotes $^{45}Ca^{2+}$ efflux, for 10 seconds. At the time chosen (10 seconds), a very low efflux was detected in wild-type BHK cells. Na^+-dependent $^{45}Ca^{2+}$ efflux was estimated by subtracting $^{45}Ca^{2+}$ efflux in Ca^{2+}- and Na^+-free solution from that in Ca^{2+}-free solution. Cells were subsequently lysed with 0.1 N NaOH, and aliquots were taken to determine radioactivity. The EC_{50} values for Compound 2 were obtained by fitting the data with the equation $a + b \times \exp(-x/t)$, where a is the maximal response, b is the basal response, x is the drug concentration, and t is the EC_{50}.

3.4 PROTEIN EXPRESSION ANALYSIS

Whole-cell protein extracts from adult hippocampus or cortex were obtained and processed as previously described (Molinaro et al., 2008a). Briefly, nitrocellulose-membranes were incubated with anti-CREB (mouse monoclonal, 1:1000, Cell Signaling), anti-pCREB Ser133 (rabbit polyclonal, 1:1000 Millipore), anti-Phospho-CaM Kinase II T286 (rabbit polyclonal, 1:1000, abcam), anti-Phospho-CaM Kinase II

T305 (rabbit polyclonal, 1:1000, Bioss antibodies) or anti-Tubulin (mouse monoclonal, 1:10.000, Sigma) antibodies.

These nitrocellulose-membranes were first washed with 0.1% Tween 20, and then incubated with the corresponding secondary antibodies for 1h (GE Healthcare Bio-Sciences). Immunoreactive bands were detected with electrochemiluminescence (GE Healthcare Bio-Sciences). The optical density of the bands (normalized with Tubulin or Creb) was determined by Chemi-Doc Imaging System (Bio-Rad).

3.5 CELL CULTURES

Baby hamster kidney (BHK) cells stably transfected with canine cardiac NCX1.1, rat brain NCX2.1, and NCX3.3 were a generous gift from Dr. Kenneth D. Philipson (University of California, Los Angeles, CA). All BHK cell lines were grown on plastic dishes in a mix of Dulbecco's modified Eagle's medium and Ham's F-12 medium (1:1) (Life Technologies, San Giuliano Milanese, Italy) supplemented with 5% fetal bovine serum, 100 U/ml penicillin, and 100 mg/ml streptomycin (Sigma-Aldrich, St. Louis, MO). Cells were cultured in a humidified 5% CO_2 atmosphere, and the culture medium was changed every 2 days. For microfluorimetric and electrophysiologic studies, cells were seeded on glass coverslips (Thermo Fisher Scientific, Springfield, NJ) coated with poly-L-lysine (30 mg/ml) (Sigma-Aldrich) and used at least 12h after seeding.

Human embryonic kidney-293 (HEK293) cells were cultured in DMEM–Dulbecco's Modified Eagle Medium (Gibco) containing 10% fetal bovine serum, penicillin (50 U/ml) and streptomycin (50 µg/ml), 2 mM Glutamine in a humidified atmosphere at 37°C with 5% CO_2. HEK293 cells endogenously express ASIC1a channels

(Gunthorpe et al., 2001). For electrophysiological experiments, cells were seeded on glass coverslips (Glaswarenfabrik Karl Hecht KG, Sondheim, Germany) coated with poly-L-lysine (50 µg/mL) and used after 24-72 hours in culture (Sigma-Aldrich, St. Louis, MO) to assess the effects of Compound 2 on ASIC1a currents.

3.6 $[Ca^{2+}]_i$ MEASUREMENT

$[Ca^{2+}]_i$ was measured by single-cell computer-assisted video imaging (Secondo et al., 2007). Briefly, BHK cells, grown on glass coverslips, were loaded with 6 mM Fura-2 acetoxymethyl ester (Fura-2 AM) for 30 minutes at 37°C in normal Krebs solution containing the following (in mM): 5.5 KCl, 160 NaCl, 1.2 $MgCl_2$, 1.5 $CaCl_2$, 10 glucose, and 10 Hepes-NaOH (pH 7.4). At the end of the Fura-2 AM loading period, the coverslips were placed into a perfusion chamber (Medical Systems, Greenvale, NY) mounted onto the stage of an inverted Zeiss Axiovert 200 microscope (Carl Zeiss, Oberkochen, Germany) equipped with a FLUAR 40X oil objective lens. The experiments were carried out with a digital imaging system composed of MicroMax 512BFT cooled CCD camera (Princeton Instruments, Trenton, NJ), LAMBDA 10-2 filter wheeler (Sutter Instruments, Novato, CA), and Meta-Morph/MetaFluor Imaging System software (Universal Imaging, West Chester, PA). After loading, cells were alternatively illuminated at wavelengths of 340 nm and 380 nm by a xenon lamp. The emitted light was passed through a 512-nm barrier filter. Fura-2 fluorescence intensity was measured every 3 seconds. Forty to sixty-five individual cells were selected and monitored simultaneously from each coverslip. All the results are presented as cytosolic Ca^{2+} concentration. Since K_D for Fura-2 was assumed to be 224 nm, the equation of Grynkiewicz (Grynkiewicz et al., 1985) was

used for calibration. NCX activity was evaluated as Ca^{2+} uptake through the reverse mode by switching the normal Krebs medium to Na^+-deficient $NMDG^+$ medium named Na^+-free (in mM): 5.5 KCl, 147 NMDG, 1.2 $MgCl_2$, 1.5 $CaCl_2$, 10 glucose, and 10 Hepes-Trizma (pH 7.4), in the presence of thapsigargin, the irreversible and selective inhibitor of the sarco(endo)plasmic reticulum Ca^{2+}-ATPase (SERCA) (Secondo et al., 2007).

Compound 2 was incubated with cells for 30 minutes before NCX activity was studied. Each EC50 of Compound 2 was obtained by fitting the data with the equation $a + b \times \exp(-x/t)$, where *a* is the maximal response, *b* is the basal response, *x* is the drug concentration, and *t* is the EC_{50}.

3.7 ELECTROPHYSIOLOGY

NCX Currents. NCX currents (I_{NCX}) were recorded, by patch-clamp technique in whole-cell configuration (Secondo et al., 2007; Molinaro et al., 2013) in BHK cells stably transfected with NCX1 exposed either to Compound 2 or its vehicle.

Currents were filtered at 5 kHz and digitized using a Digidata 1322A interface (Molecular Devices, Sunnyvale, CA). Data were acquired and analyzed using the pClamp software (version 9.0; Molecular Devices). In brief, I_{NCX} were recorded starting from a holding potential of -70 mV up to a short-step depolarization at +60 mV (60 ms) (Secondo et al., 2009a). Then, a descending voltage ramp from +60 mV to -120 mV was applied. The current recorded in the descending portion of the ramp (from +60 mV to -120 mV) was used to plot the current-voltage (I-V) relation curve. The magnitudes of I_{NCX} were measured at the end of +60mV (reverse mode) and at the end of -120 mV (forward mode), respectively. To isolate I_{NCX}, the same cells of all

experimental groups were recorded first for total currents and then for currents in the presence of Ni^{2+} (5 mM), a selective blocker of I_{NCX}. Compound 2-induced I_{NCX} increase was calculated as follows: (I_{NCX} Compound 2/I_{NCX} control) x 100.

External Ringer solution contained the following (in mM unless otherwise specified): 126 NaCl, 1.2 $NaHPO_4$, 2.4 KCl, 2.4 $CaCl_2$, 1.2 $MgCl_2$, 10 glucose, and 18 $NaHCO_3$, 20 TEA, 10 nM TTX, and 10 mM nimodipine (pH 7.4). The dialyzing pipette solution contained the following (in mM): 100 potassium gluconate, 10 TEA, 20 NaCl, 1 Mg-ATP, 0.1 $CaCl_2$, 2 $MgCl_2$, 0.75 EGTA, and 10 Hepes, adjusted to pH 7.2 with CsOH. TEA (20 mM) and Cs were included to block delayed outward rectifier K^+ components; nimodipine (10 mM) and TTX (50nM) were added to external solution to block L-type Ca^{2+} channels and TTX sensitive Na^+ channels, respectively. The quantifications of I_{NCX} were normalized for membrane capacitance and expressed as a percentage of controls as previously reported (Molinaro et al., 2008a; Molinaro et al., 2011), whereas the representative traces of I_{NCX} are expressed as picoamps per millivolt (pA/mV).

Asic Currents. ASIC1a currents were measured on HEK293 by means of the patch-clamp technique in the whole-cell configuration. Electrophysiological recordings were carried out at room temperature (20–24°C), using an Axopatch 200B amplifier controlled using the pClamp 10 software (Axon Instruments, Union City, CA, USA). The holding potential was -70 mV, traces were filtered at 5kHz and currents were digitized using a Digidata 1322A interface (Axon Instruments, Union City, CA, USA). The extracellular solutions contained (in mM) 140 NaCl, 5 KCl, 2 $CaCl_2$, 2 $MgCl_2$, 10 HEPES, pH was adjusted to 7.4 using NaOH or HCl. For solution with pH 6.0, glycine 10 mM and MES instead of HEPES were used for more reliable pH buffering.

Pipettes had a resistance of 2–4 MΩ when filled with the intracellular solution, which contained (in mM): 30 NaCl, 120 KCl, 2 $MgCl_2$, 10 HEPES with or without EGTA, pH was adjusted to 7.3 using NaOH or HCl. The ASIC1a channel was activated by shifting the pH of the external solution from pH 7.4 to pH 6.0. Fast extracellular solution exchange was performed using a commercially available automated fast solution exchange system (Warner Instruments SF-77B). In particular, a rapid reduction of extracellular pH from 7.4 to pH 6.0 (10 seconds) evoked large transient inward currents. Between two-three stimulation cells were kept in a bath solution (pH 7.4) for at least 40 seconds. After that, Compound 2 was pre-applied in extracellular solution pH 7.4 for 40 seconds and co-applied in extracellular solution pH 6.0 for 10 seconds (approximately 50 seconds between pH stimulations).

3.8 DETERMINATION OF MITOCHONDRIAL ACTIVITY

Mitochondrial dysfunction was evaluated with the MTT method (Molinaro et al., 2013). In brief, after the experimental procedures, BHK cells were washed with normal Krebs solution and incubated with a MTT solution (0.5 mg/ml in phosphate-buffered saline). This yellow water-soluble tetrazolium salt is converted into a water-insoluble purple formazan by the succinate dehydrogenase system of the active mitochondria. Therefore, the amount of formazan produced is proportional to the number of cells with mitochondria that are still alive. After 1h of incubation at 37°C, cells were dissolved in 1 ml of DMSO, in which the rate of MTT reduction was measured by a spectrophotometer at a wavelength of 540 nm. Data are expressed as percentage of mitochondrial dysfunction versus sham-treated cultures.

3.9 IMMUNOHISTOCHEMISTRY AND IMAGE ANALYSIS

Immunostaining and confocal immunofluorescence procedures were performed as previously described (Anzilotti et al., 2015). Animals were anesthetized and transcardially perfused with saline solution containing 0.01 ml heparin, followed by 4% paraformaldehyde in 0.1 mol/l PBS saline solution. Brains were rapidly removed on ice and postfixed overnight at +4°C and cryoprotected in 30% sucrose in 0.1 M phosphate buffer (PB) with sodium azide 0.02% for 24 h at 4°C. Next, brains were sectioned frozen on a sliding cryostat at 40 μm thickness, in rostrum-caudal direction. Afterwards, free floating serial sections were incubated with PB Triton X 0.3% and blocking solution (0.5% milk, 10% FBS, 1% BSA) for 1 h and 30 min. The sections were incubated overnight at +4 °C with the following primary antibodies: mouse monoclonal anti-NeuN (Millipore, Milan, Italy), mouse monoclonal anti-NCX1 (Swant, Bellinzona, Switzerland), rabbit polyclonal anti-phospho-CREB S133 (Millipore, Cat #06-519), mouse monoclonal anti-phospho-CaMKII T286 (Abcam, ab32678).

The sections were then incubated with the corresponding florescent-labeled secondary antibodies, Alexa 488/Alexa 594 conjugated antimouse/antirabbit IgGs (Molecular Probes, Invitrogen S.R.L., Milan, Italy). Nuclei were counterstained with Hoechst (Sigma-Aldrich, Milan, Italy). Images were observed using a Zeiss LSM700 META/laser scanning confocal microscope (Zeiss, Oberkochen, Germany). Single images were taken with an optical thickness of 0.7 m and a resolution of 1024 × 1024. In double-labeled sections, the pattern of immune reactivity for both antigens was identical to that seen in single-stained material. Control double-immunofluorescence staining entailed the replacement of the primary antisera with normal serum (data not

shown). To minimize a possible cross-reactivity between IgGs in double immunolabeling experiments, the full complement of secondary antibodies was maintained but the primary antisera were replaced with normal serum or only one primary antibody was applied (data not shown). In addition, the secondary antibodies were highly preadsorbed to the IgGs of numerous species. Tissue labeling without primary antibodies was also tested to exclude autofluorescence. No specific staining was observed under these control conditions, thus confirming the specificity of the immunosignals.

To obtain an indirect measure of the amount of pCaMKII_T286, NCX1, and pCREB_S133 in neurons, image analysis of NeuN was performed by NIH image software by measuring the intensity of fluorescent NCX1, pCaMKII_T286 and pCREB_S133 immunolabeling in 60 NeuN positive neurons for each group. The intensity of NCX1 CaMKII_T286 and pCREB_S133 immunoreactivity was expressed in arbitrary units (Anzilotti et al., 2018).

3.10 BEHAVIORAL STUDIES AND HORMONAL MEASUREMENTS

At the age between 2-3 months, mice were behaviorally tested. Experiments were performed during the light phase between 11:00 a.m. and 3:00 p.m. During behavioral tests, animal movements were recorded by 2 cameras (resolution 640x480 pixels) and analyzed by a dedicated software operating in video tracking mode (Anymaze) and manually by an experimental researcher. The system tracked the animal's head as well as its centre of gravity and tail. The results therefore included measures specific to the position of the animal and movements. The animal was considered to be immobile if it doesn't change location and at least 65% of its

body remains static for a period of 2000ms or more. The system detected periods when the animal is freezing for at least 250ms. Experiment's treatment groups were coded in blind with the experimental researcher involved in the score definition.

For hormone assay, mice were sacrificed by CO_2 and blood was collected from heart in ice-cooled centrifugal tubes. Serum corticosterone levels were measured in serum by Elisa (VetforLab, Pozzuoli, Italy) at 6:00 a.m., 12:00 p.m., 6:00 p.m. and 12:00 a.m. under non-stressful conditions, or approximately 60m or 24h after foot-shock. Serum corticosterone levels at 12:00 p.m. were used as control group for 1h and 24h after foot-shock groups.

3.11 OPEN-FIELD EXPLORATION AND NOVEL OBJECT RECOGNITION MEMORY TASK

Open field and novel object recognition task were performed as previously described (Molinaro et al., 2011). Briefly, the open field apparatus (50x50 cm, 40 cm high) was placed in a homogenously lit experimental room with several large-scale environmental visual cues. Ninety animals (13 *NCX1.4*^{over}, 12 *NCX1.4*$^{+/+}$, 17 *NCX1*^{ko}, 19 *NCX1*$^{+/+}$, 14 compound 2-treated C57BL/6, 15 vehicle-treated C57BL/6) were individually placed in the apparatus and were allowed to explore it for 5 min. Several parameters, including total traveled distance, were measured by using an automated tracking software (Anymaze). The time spent by animals in three concentric areas was automatically measured as an index of anxious behavior (Kassed and Herkenham, 2004; Kazlauckas et al., 2005). The same apparatus was also used for the object recognition task. Compound 2, or vehicle, was administered once 30m before the begin of the test by i.p. injection.

Novel object recognition memory task was performed 30m after open field test, thus no additional drug administration was provided for this test neither in training, 1h nor 24h session. During the training trial, two objects were placed in the box and animals were allowed to explore them for 5 min. A mouse was considered to be exploring the object when its head was facing the object within 27mm of distance. Following retention intervals (1h and 24h), animals were placed back to the box with two objects in the same locations, but one of the familiar objects was replaced by a novel object and then were allowed to explore the two objects for 5 min. The preference percentage, ratios of the amount of time spent exploring any one of two objects or the novel one over the total time spent exploring both objects, were used to assess the recognition memory.

3.12 ROTAROD

Motor coordination and balance were assessed using a five-station mouse rotarod apparatus (Ugo Basile; Milan, Italy). In each station, the rod was 6 cm in length and 3 cm in diameter. Mice were trained to maintain balance at increasing speed from 4 to 14 rpm for three consecutive trials over 60 s. The test sessions were conducted by three trials of rotarod over 60 s under the same conditions of the training session. The maximum latency of 60 s was assigned to the mice that did not fall at all (Giampà et al., 2010). Compound 2, or vehicle, was administered by i.p. 30m before the test session. Data were expressed as mean of the three trials in the test session.

3.13 ELEVATED ZERO MAZE AND DARK/LIGHT BOX

The elevated-O-maze is a modification of the plus-maze and displays the advantage of lacking the ambiguous central area of the elevated plus-maze. Zero maze consisted of a circular path with an outer diameter of 122 cm and with a catwalk of 10 cm wide. With regard to mice's natural aversion towards elevated and open spaces (Shepherd et al., 1994; Kulkarni et al., 2007) the catwalk was positioned at a height of 40 cm and divided into four subsections: two "closed" (wall height: 30 cm) and two "open" quadrants. Testing took place approximately at 12:00 a.m. with equal lighting conditions that provided a maze surface free of distracting shadows. Compound 2, or vehicle, was administered by i.p. 30m before the test. After at least 30m of habituation to the experiment room, each mouse was placed alternately into the center of one of the open quadrants and video-recorded for 5m. The time spent in the open quadrants was expressed as percentage of the respective wild-type or vehicle group.

Dark/light box apparatus consisted of two transparent polyvinylchloride boxes (22x38 cm, 15cm height). One of the boxes was covered and darkened, whereas the other box was well lighted. The two boxes contained some dust-free sawdust bedding and are linked by a window (10 cm wide, 6.5 cm height). The subjects were individually tested from 11 a.m. to 3 p.m. in two sessions: before (naïve) and after (post-shock) a single foot-shock. Mice were placed in the lit box at the beginning of the test. The amount of time spent in the lit box and the number of transitions across the two boxes were automatically and manually recorded. A mouse whose four paws were in the new area was considered having changed box. During the video-recording, the

experimenters were not present in the room. Analysis was performed post-hoc on videorecording movie.

3.14 BARNES CIRCULAR MAZE TASK

Apparatus. The behavioral apparatus used in this experiment consisted of a white circular platform (1.22 m diameter) elevated 80 cm above the floor, with 36 equally spaced holes (each 5 cm diameter) around the periphery (5 cm from the perimeter). Only one hole led to a dark escape box (5 cm x 5 cm x 11 cm) that was fixed in relation to the distal environmental cues and contained some dust-free sawdust bedding. The platform surface was brightly illuminated from above to motivate to escape in the dark box (Bach et al., 1995; Seeger et al., 2004).

Procedure. Mice were gently picked up from the tail and placed in the middle of the platform. The direction faced by the animals at the start position was random and changed from trial to trial. After 5 min, if the mice did not find the goal they were gently directed toward the correct hole and allowed to descend into the escape box where they were left for 1 min (Bach et al., 1995; Seeger et al., 2004). The following 5 test trials (one trial per day) were performed under same conditions. Each trial ended when the mouse entered the goal escape box or after a maximum time of 5 min. The amount of time it took the mice to enter the escape hole (escape latency) was recorded (Bach et al., 1995; Seeger et al., 2004).

3.15 TRACE FEAR CONDITIONING

The trace fear conditioning procedure is a modified form of tone (delay) fear conditioning because it demands a “trace interval” between the unconditioned

stimulus (US) and conditioned stimulus (CS). Unlike delay tone conditioning, the acquisition of trace fear conditioning is sensitive to hippocampal lesions (McEchron et al., 1998; Desmedt et al., 2003; Bangasser et al., 2006) and to genetic modifications of the hippocampus (Huerta et al., 2000; D'Adamo et al., 2002). In this test a fear-conditioning shock chamber (17x17 cm, 25 cm height) containing a stainless-steel rod floor (2.5 mm diameter, spaced 1 cm apart, Ugo Basile Inc.) and a digital camera to monitor animal movements were used in a soundproof box (Ugo Basile Inc.). The apparatus for on-line tracking and stimulus/shock delivery was controlled using anymaze software v5.31.

Briefly, for the conditioning (Lu et al., 1997; Jeon et al., 2003), mice were first placed in the fear-conditioning apparatus chamber for 3 min (habituation phase), and, then, a 15 s acoustic CS (1000 Hz, 80 dB) was delivered. The tone intensity and frequency, previously tested in C57BL/6 mice, did not evoke freezing before conditioning although short orienting reactions showed their ability to perceive the sound. After 15 s from the end of the acoustic stimulus, a 0.5mA shock (0.8 s duration) of unconditioned stimulus was applied to the floor grid. This protocol was performed one time per animal. Compound 2, or vehicle, was administered 30m before the habituation phase.

Context test of trace fear conditioning was measured 30m after the conditioning procedure. Animals were tested for their context freezing response and afterward for their response to the tone in a different context.

Context freezing response was measured placing the animals for 5m in the same apparatus used for conditioning in absence of electrical or acoustical stimuli. Behavior was recorded with a digital camera and analyzed by software (anymaze) for

the freezing behavior, defined as complete absence of somatic movements except for respiratory movements.

To assess the tone test in trace fear conditioning, the animals were placed in a different context (novel chamber, odor, floor, and visual cues) 30m after the context test, and their behavior was monitored for 6 min. All experimental groups were observed for 3m before the tone (pre-CS) and 3m (CS) during the tone in the new context. Fear response was quantified by measuring the duration of freezing behavior. Freezing behavior was defined as a total lack of movement, apart from respiration.

3.16 STATISTICAL ANALYSIS

Values are expressed as means ±S.E.M. Statistical analysis was performed with paired or unpaired Student's t test, Kruskal-Wallis one or two Way ANOVA followed by Dunn's test with all pairwise multiple comparison procedures or Student-Newman-Keuls post-hoc test. Statistical significance was accepted at the 95% confidence level ($p < 0.05$).

4. RESULTS

4.1 NEWLY SYNTHESIZED COMPOUNDS MODULATING NCX ACTIVITY

Twenty newly compounds have been synthesized by different modifications on the chemical backbone of neurounina-1 (7-nitro-5-phenyl-1-(pyrrolidin-1-ylmethyl)-1H-benzo[e][1,4]diazepin-2(3H)-one) (Figure 1). The benzodiazepinonic derivatives are obtained by the addition of cyclic amine via an acetic spacer (compounds I-VIII) or by an ethylic spacer (in compound 4 and compounds IX-XVI) to the position 1 of neurounina-1 (Figure 1). Moreover, compounds 2 and 3 were generated by the addition of a chloride residue in position 2 and 7, respectively (Figure 1).

The effects of newly synthesized compounds on all three NCX isoforms were evaluated with $^{45}Ca^{2+}$ radiotracer, fura-2-monitored Ca^{2+} increase and patch clamp in whole cell configuration methods (Figure 2) on BHK cells singly transfected with NCX1, NCX2 or NCX3. Among the twenty new compounds, five of them were selected: compounds 2 and 3 that are able to increase NCX1 activity (Figure 2A); compounds II and IX that are inhibitors of NCX2 activity (Figure 2B); and compound III for its effect as activator on NCX3 (Figure 2C). The concentration effect-curves evaluated on each NCX isoform revealed that compounds 2 and 3 show an EC_{50} of 1.4 nM and 1.3 nM on NCX1 (Figure 3), respectively. Compounds IX inhibited NCX2 activity with an EC_{50} of 2,9 nM and Compound II modulated both NCX1 and NCX2 activity (Figure 4). Compound III increases NCX3 and NCX1 activity but no EC_{50} was calculated (Figure 5).

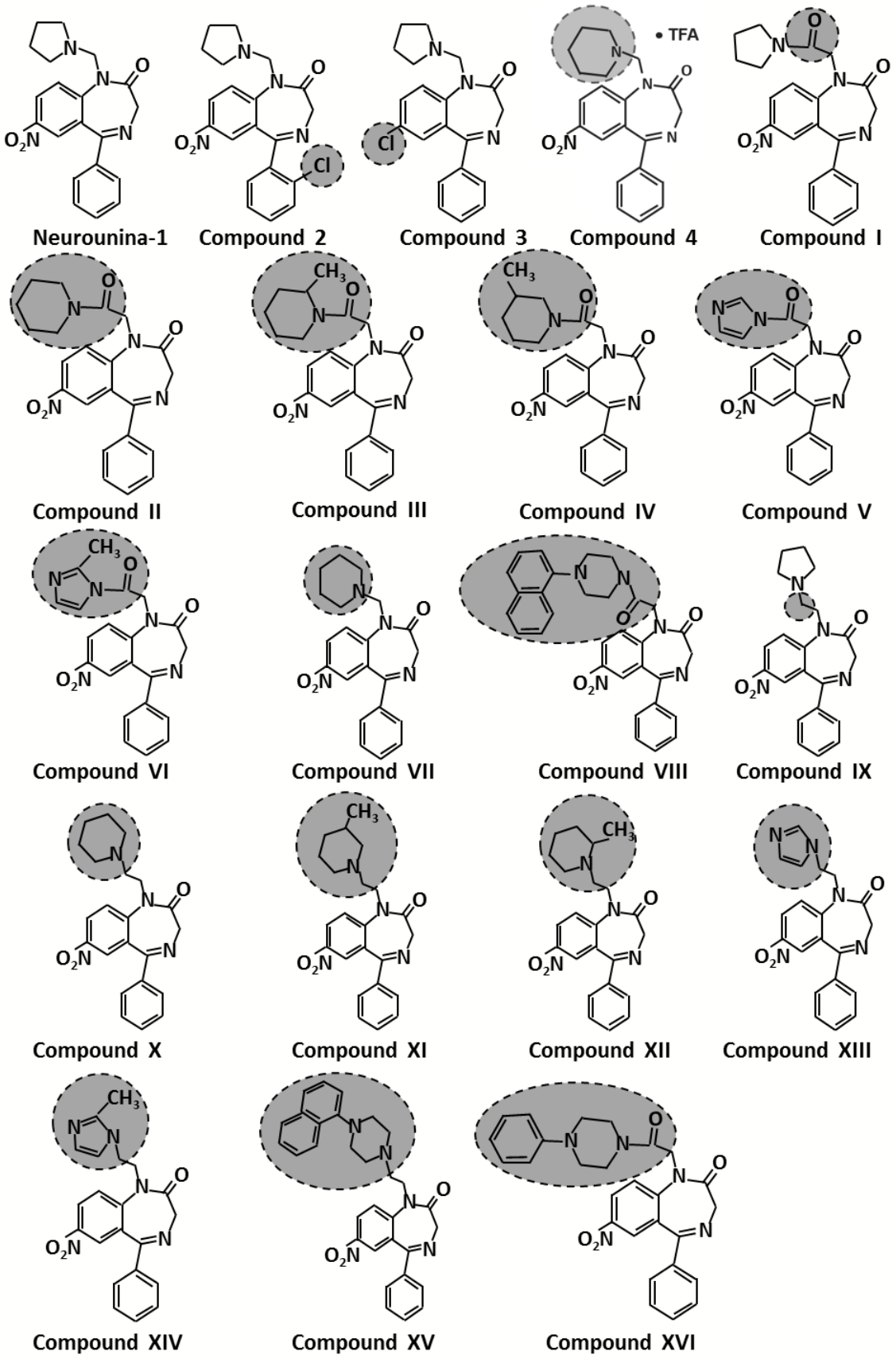

***Figure 1**. Chemical structure of twenty derivatives of neurounina-1.*

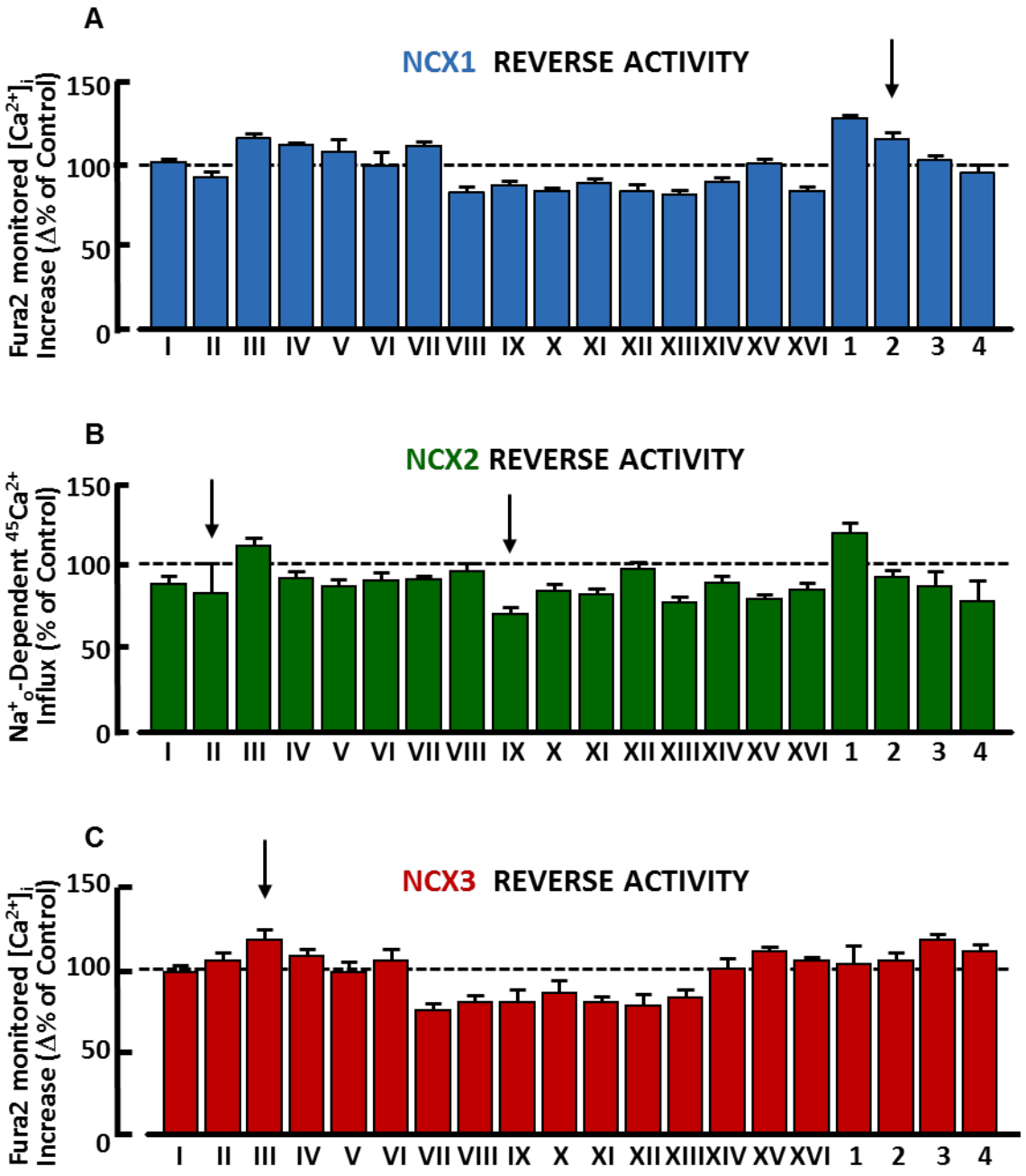

Figure 2. *Effects of newly synthesized compounds on the three NCX isoforms.*

(A) and (C) Effects of new compounds on NCX1 or NCX3 activity evaluated with single cell Fura-2 monitored Ca^{2+} technique.

(B) Effects of new compounds on NCX2 activity evaluated with $^{45}Ca^{2+}$ radiotracer assay. Arrows show selected compound for in vivo experiments.

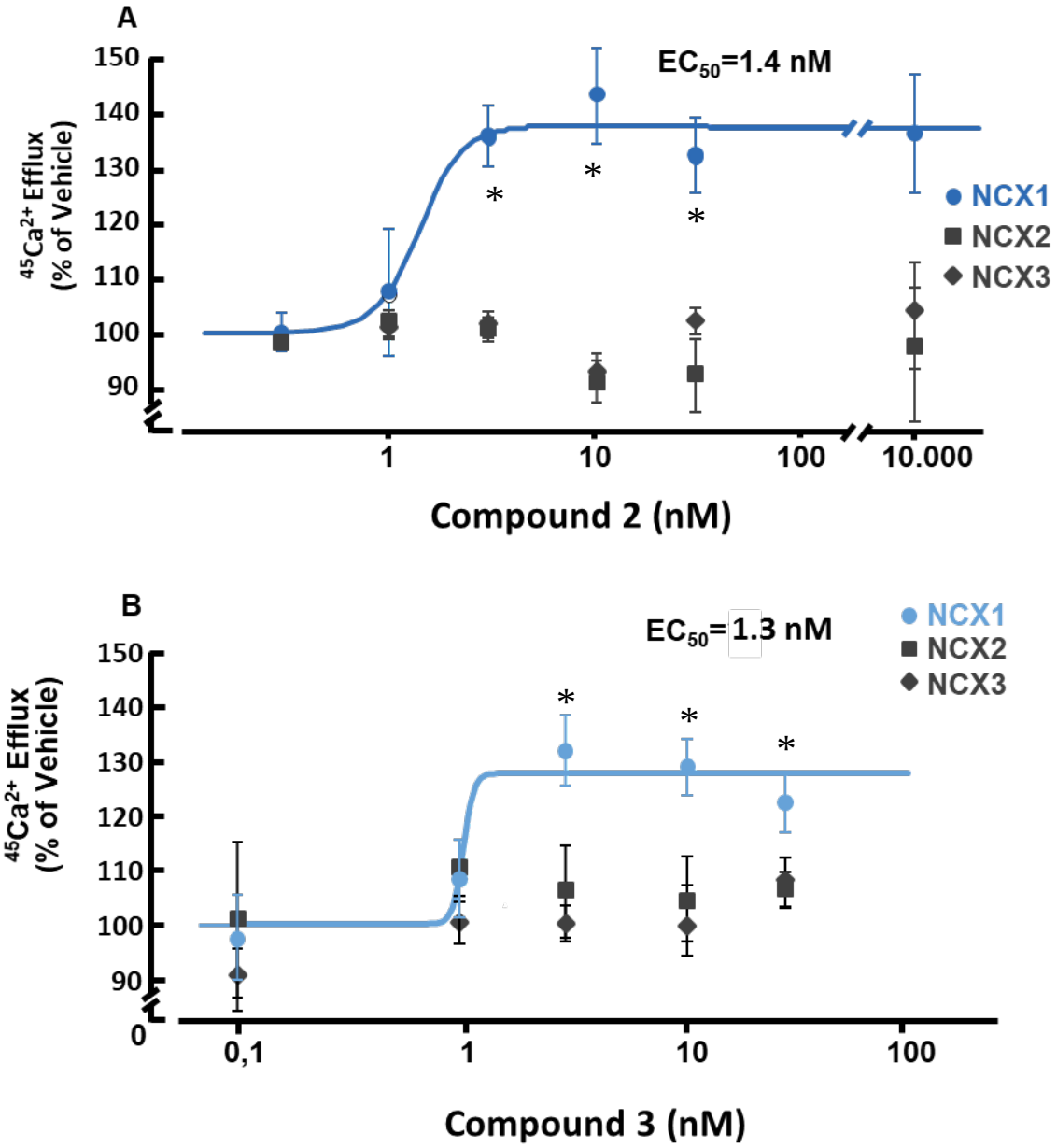

Figure 3. *Dose-effect curves of compounds 2 and 3.*

*Concentration-response curves of compound 2 (A) and compound 3 (B) on Na^+-dependent $^{45}Ca^{2+}$ efflux in BHK cells expressing NCX1, NCX2 or NCX3. *, $p < 0.05$ vs respective NCX2 and NCX3, two-way ANOVA followed by Newman-Keuls' test. Compound 2, $F(2,144) = 20.34$, $p<0.0001$; Compound 3, $F(2, 114) = 7.224$, $p=0.0011$.*

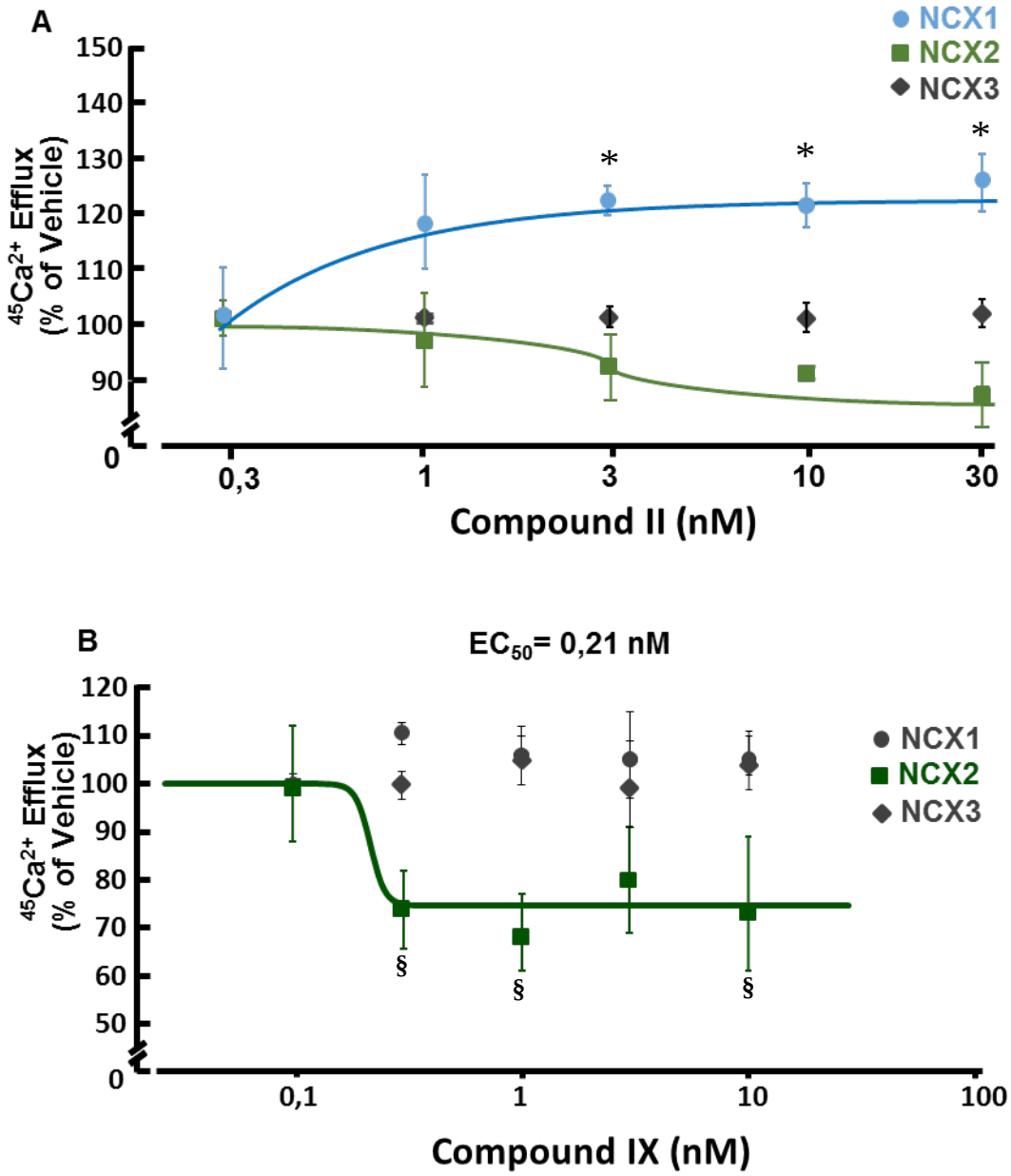

Figure 4. *Dose-effect curves of compounds II and IX.*

*Concentration-response curves of compound II (A) or compound IX (B) on Na^+-dependent $^{45}Ca^{2+}$ efflux in BHK cells expressing NCX1, NCX2 or NCX3. *, $p < 0.05$ vs respective NCX2 and NCX3; §, $p < 0.05$ vs respective NCX1 and NCX3. Two-way ANOVA followed by Newman-Keuls' test. Compound II, $F(2,127) = 41.08$, $p<0.0001$; Compound IX, $F(2, 62) = 8.027$, $p=0.0008$.*

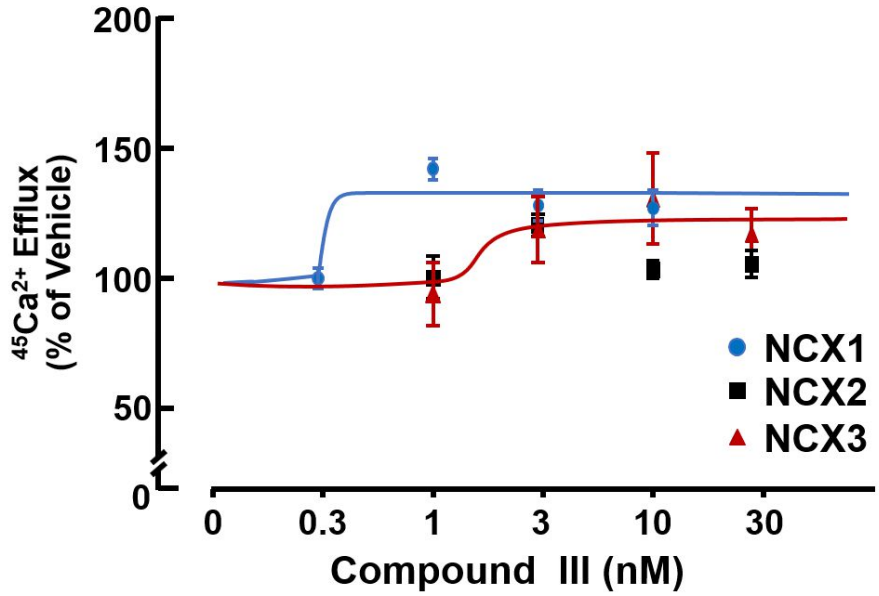

Figure 5 *Dose-effect curves of compound III.*

Concentration-response curves of compound III on Na^+-dependent $^{45}Ca^{2+}$ efflux in BHK cells expressing NCX1, NCX2 or NCX3.

4.2 COMPOUNDS 2 AND IX AMELIORATE LEARNING AND MEMORY PERFOMANCE IN NOVEL OBJECT RECOGNITION TEST

Ten nM and 10 µM of each selected compound did not decrease mitochondrial activity on BHK cells as measured with MTT assay (Figure 6A). Moreover, a single i.p. injection of 32 µg/kg of compound 2, 3, II, III or IX did not cause body weight loss after one and two weeks (Figure 6B), signs of suffering, and evident toxic effects on several organs such as liver, kidney, pancreas and gut. Furthermore, the total distance travelled and the total time mobile in open field test (Figure 7 A and B) and the latency to fall in rotarod test (Figure 9) did not reveal impairment of locomotor activity for mice treated with each compound. Moreover, compounds did not affect the number of entries in open zone and the percentage of time spent by mice in open zone of zero maze test (Figure 8 A and B).

In novel object recognition test each mouse group were equally motivated to explore the two objects during the training phase (Figure 10, Figure 11, Figure 12). One hour and 24 hours later, when one object was replaced with a new one, mice treated with compound 2 (Figure 10A) and compound IX (Figure 11B) spent more time exploring the novel object, as compared with vehicle-treated mice. Compound 3-treated mice ameliorated learning and memory performance only 24h after the training session (Figure 10B). On the other hand, mice treated with compound II (Figure 11A) and III (Figure 12) displayed the same performance of exploration of vehicle treated mice.

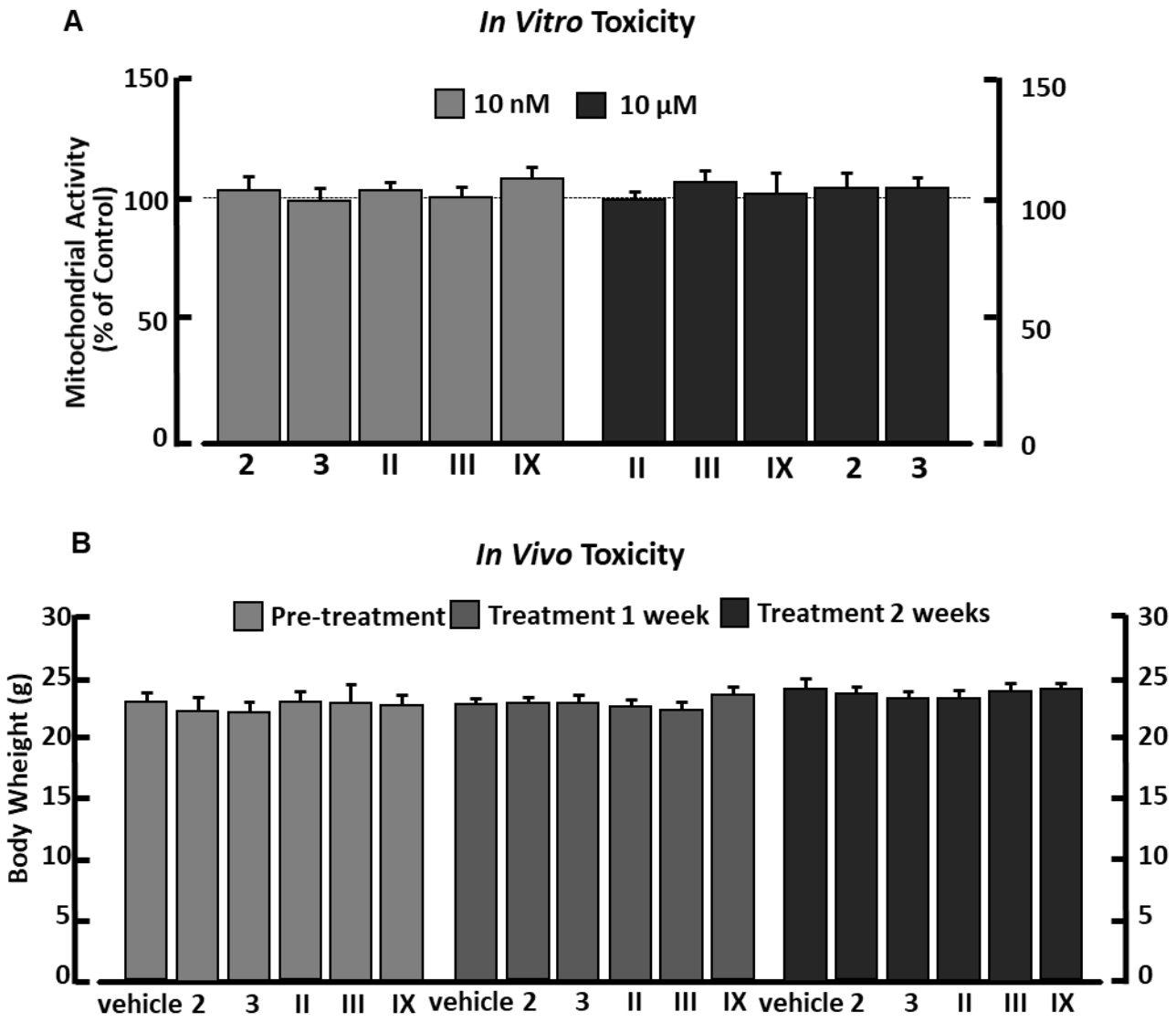

Figure 6. *In vitro and in vivo toxicity evaluated for the five selected compounds.*

(A) Mitochondrial activity of BHK cells incubated with vehicle, 10 nM or 10 µM of compounds 2, 3, II, III and IX. ANOVA followed by Tukey's post-hoc test.

(B) Mouse weight measured 7 days or 14 days after a single i.p. injection of vehicle or 32 µg/kg of compounds 2, 3, II, III and IX. ANOVA followed by Tukey's post-hoc test

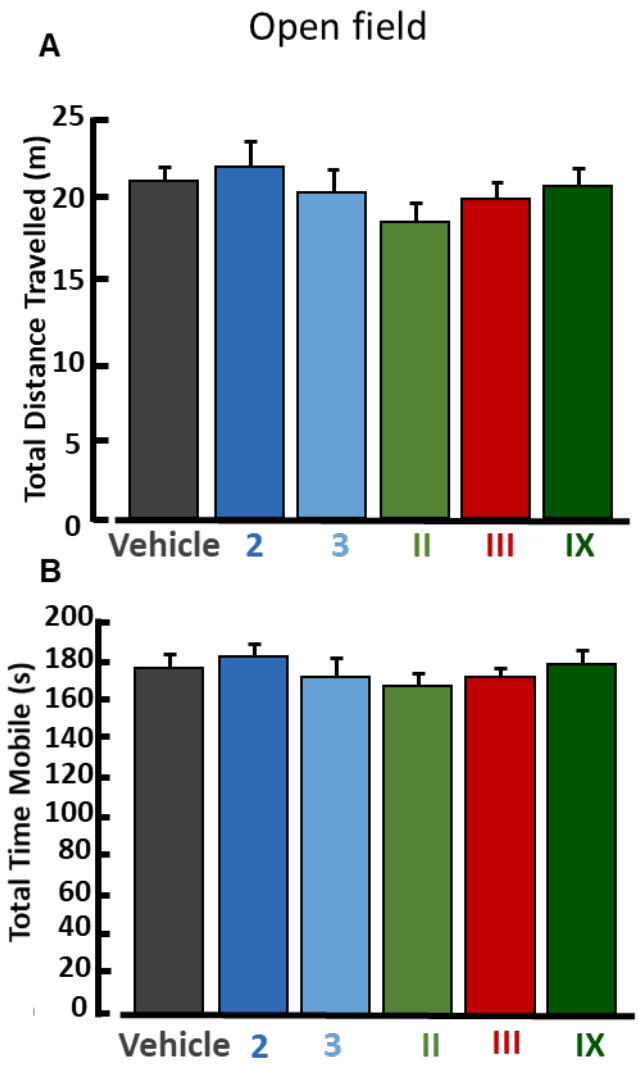

Figure 7. *Locomotor activity examined in the open field test.*

(A) Quantification of total distance travelled in open field test in mice treated with vehicle (20.84m ± 0.86, n=15), compound 2 (21.65m ± 1.63, n=14), compound 3 (20.10m ± 1.38, n=15), compound II (18.26m ± 1.22, n=15) compound III (19.67m ± 1.05, n=15), compound IX (20.54m ± 1.05, n=15). ANOVA followed by Tukey's post-hoc test.

(B) Quantification of total time spent moving in open field test expressed in seconds in mice treated with vehicle (178.03s ± 5.68, n=15), compound 2 (182.44s ± 7.9, n=14), compound 3 (174.01s ± 7.66, n=15), compound II (167.01s ± 8.6, n=15) compound III (172.00s ± 4.79, n=15), compound IX (179.33s ± 6.06, n=15). ANOVA followed by Tukey's post-hoc test.

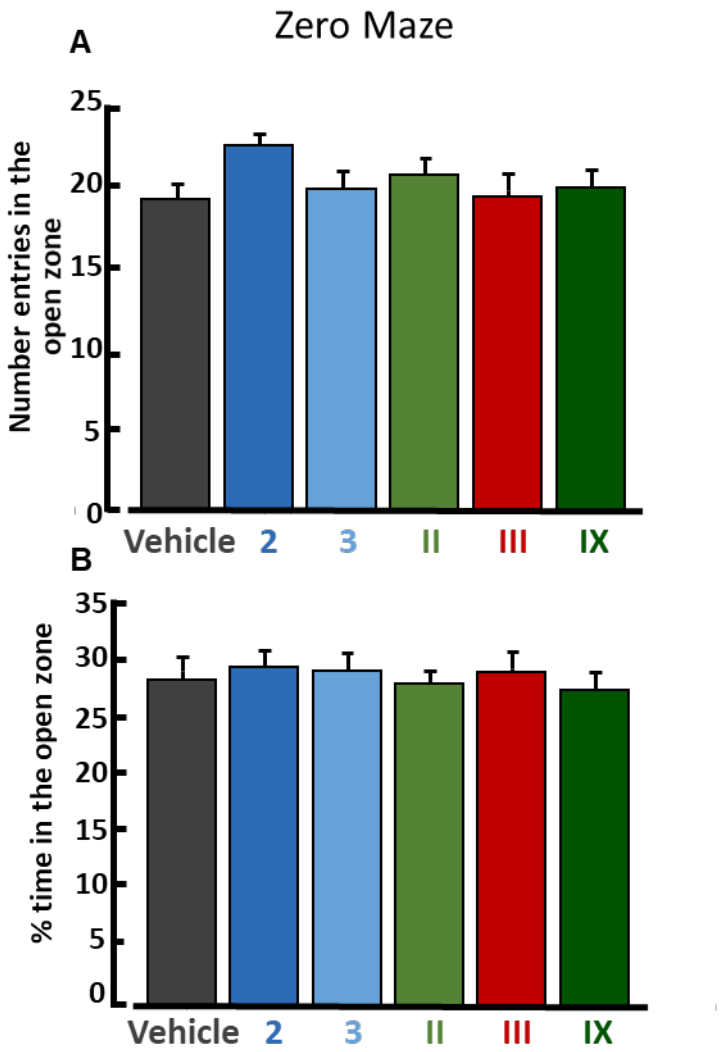

***Figure 8**. Anxiety levels examined in zero maze test.*

(A) Results of number of entries in the open zone of zero maze apparatus in mice treated with vehicle (19.33 ± 0.81 n=15), compound 2 (22.57 ± 0.75 n=14), compound 3 (19.93 ± 1.13 n=15), compound II (20.93 ± 0.75 n=15) compound III (19.53 ± 1.42 n=15), compound IX (20.00 ± 1.02 n=15). ANOVA followed by Tukey's post-hoc test

(B) Quantification of total time spend in the open zone of zero maze apparatus expressed as percentage of vehicle-treated control group vehicle (29.12% ± 1.89 n=15), compound 2 (29.91% ± 1.85 n=14), compound 3 (29.70% ± 1.66 n=15), compound II (28.45% ± 1.52 n=15) compound III (29.61% ± 1.88 n=15), compound IX (28.08% ± 1.60 n=15). ANOVA followed by Tukey's post-hoc test.

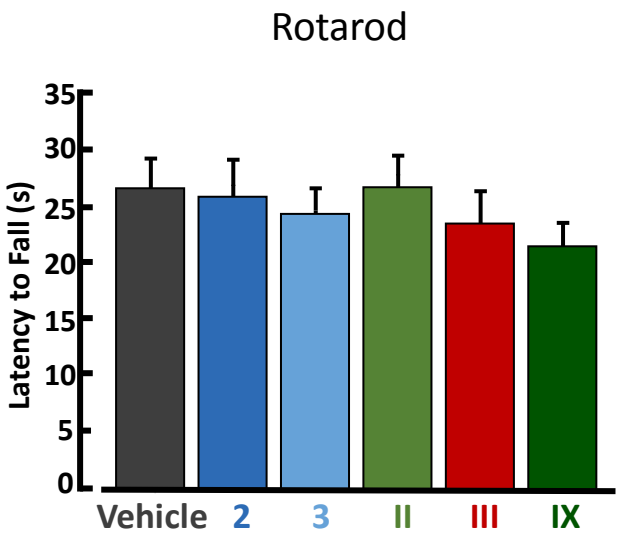

***Figure 9**. Evaluation of locomotor activity with rotarod test.*

Average of time latency to fall in wild-type mice treated with vehicle (27s ± 2.8 n=15), compound 2 (26s ± 2.4 n=14), compound 3 (24s ± 2.5 n=14), compound II (27s ± 2.8 n=15), compound III (24s ± 2.9 n=15) or compound IX (22 ± 2.1 n=15) in rotarod task. ANOVA followed by Tukey's post-hoc test.

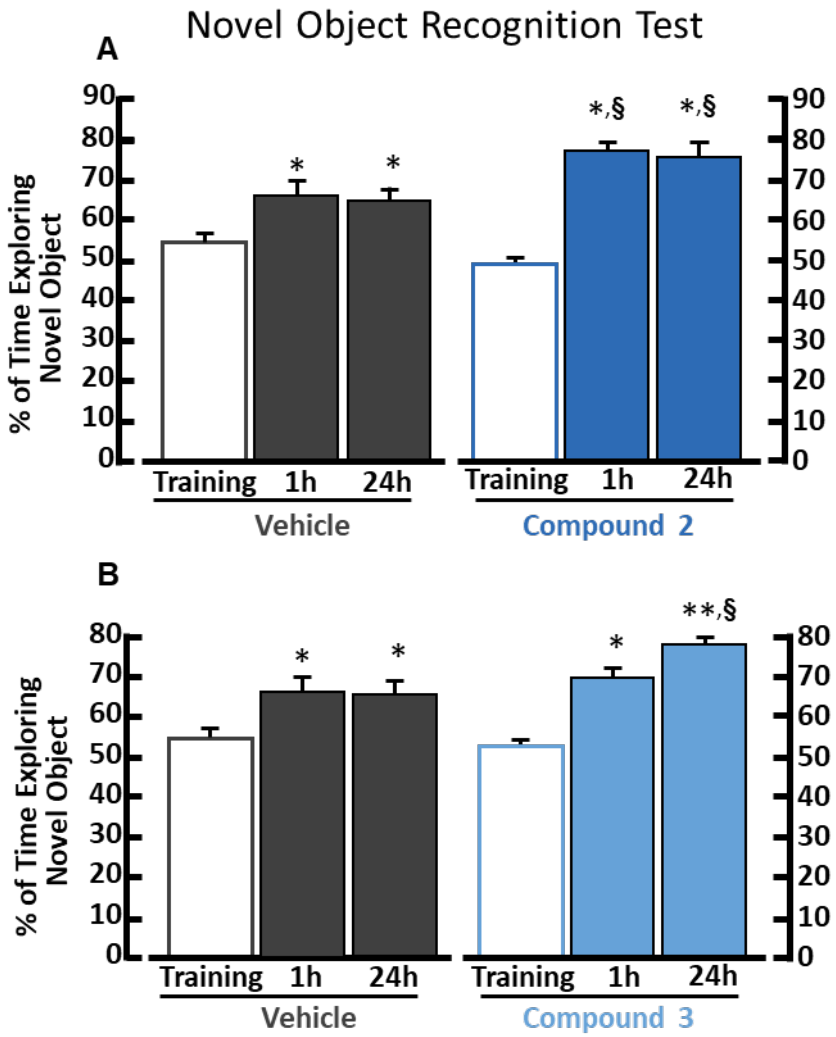

Figure 10. *Novel object recognition test of mice treated with compound 2 or 3.*

*(A) Mean exploratory preference during training session and each retention time in vehicle-treated (n=15) *p<0.05 vs training, ANOVA followed by Tukey's post-hoc test. F(2,42) = 6,30, p=0.004 on the left; and compound 2-treated (n=14) mice. ANOVA followed by Tukey's post-hoc test. F(2,39) = 42,62, p<0.001 on the right. [§], p<0.05 vs vehicle-treated group, Unpaired Student's t test.*

*(B) Mean exploratory preference during training session and each retention time in vehicle-treated (n=15) *p<0.05 vs training, ANOVA followed by Tukey's post-hoc test. F(2,42) = 6,30, p=0.004 on the left; and compound 3-treated (n=15) mice*p<0.05 vs training, ANOVA followed by Tukey's post-hoc test. F(2,42) = 48,19, p<0.001 on the right. [§], p<0.05 vs vehicle-treated group, Unpaired Student's t test.*

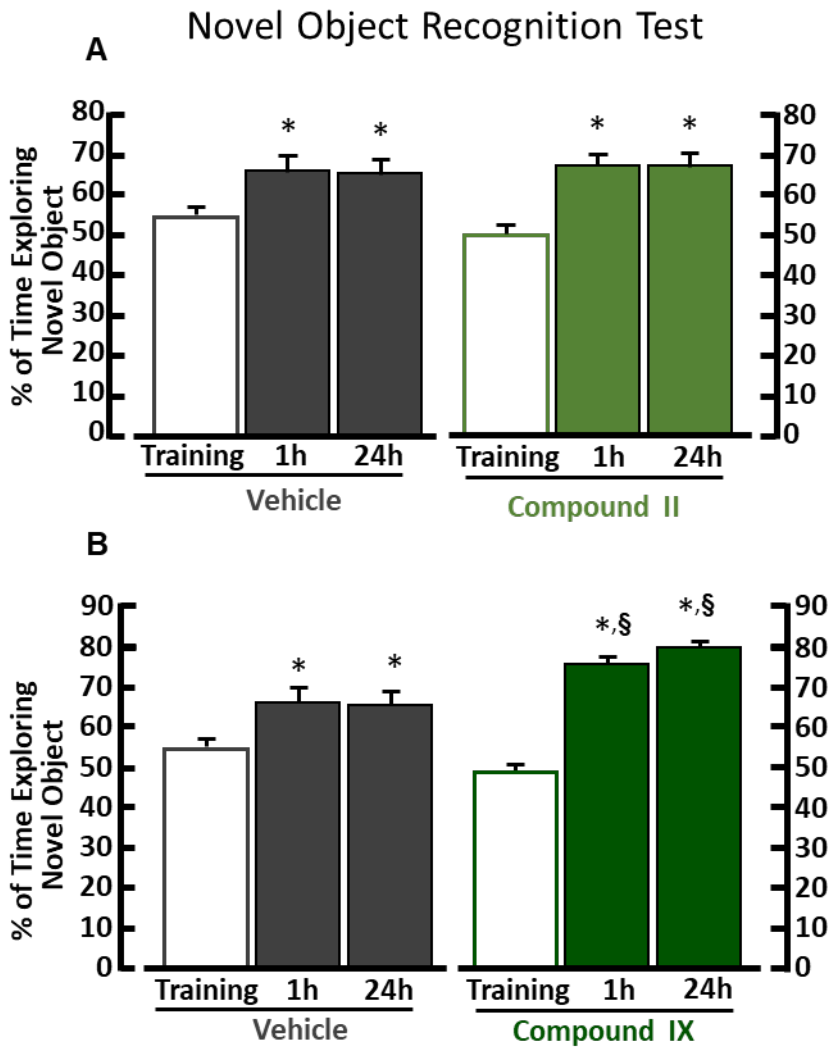

***Figure 11**. Novel object recognition test of mice treated with compound II or IX.*

*(A) Mean exploratory preference during training session and each retention time in vehicle-treated (n=15) *p<0.05 vs training, ANOVA followed by Tukey's post-hoc test. F(2,42) = 6,30, p=0.004 on the left; and compound II-treated (n=14) mice*p<0.05 vs training, ANOVA followed by Tukey's post-hoc test. F(2,42) = 19,08, p<0.001 on the right.*

*(B) Mean exploratory preference during training session and each retention time in vehicle-treated (n=15) *p<0.05 vs training, ANOVA followed by Tukey's post-hoc test. F(2,42) = 6,30, p=0.004 on the left; and compound IX-treated (n=15) mice*p<0.05 vs training, ANOVA followed by Tukey's post-hoc test. F(2,42) = 82,44, p<0.004 on the right. §, p<0.05 vs vehicle-treated group. Unpaired Student's t test.*

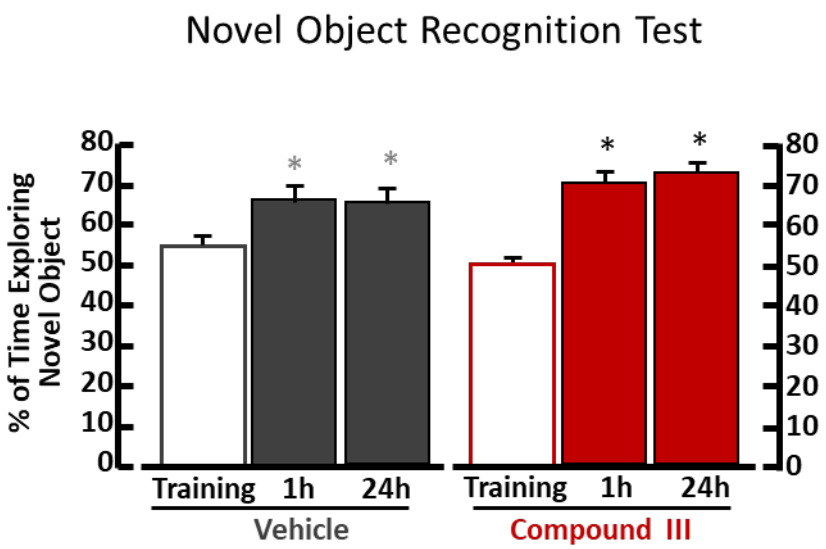

***Figure 12**. Novel object recognition test of mice treated with compound III.*

*Mean exploratory preference during training session and each retention time in vehicle-treated (n=15) *p<0.05 vs training, ANOVA followed by Tukey's post-hoc test. F(2,42) = 6,30, p=0.004 on the left; and compound III-treated (n=14) mice*p<0.05 vs training, ANOVA followed by Tukey's post-hoc test. F(2,42) = 29,25, p<0.001 on the right.*

4.3 COMPOUNDS 2, II AND IX AMELIORATE SPATIAL MEMORY IN BARNES MAZE AND TRACE FEAR CONDITIONING TESTS

The treatment with compounds 2, 3 II, III or IX did not ameliorate spatial learning during trial 1-5 of Barnes maze test (Figure 13, Figure 14, Figure 15). Indeed, experimental groups treated with compound 2 or III required more time to find the escape box as compared with vehicle-treated mice on the trial two (Figure 13A, Figure 15). On the other hand, during the memory recall phase (trial 6) the escape box was removed, and mice previously treated with compound 2, II or IX spent significantly more time in the probe zone, where before was located the escape box, as compared with vehicle-treated mice (Figure 16 B, Figure 17 E). The treatment with compound 2, or II, induced an increase of the number of entries in the probe zone (Figure 16 C, Figure 17 C), but only mice treated with compound 2 significantly increased the time spent in the correct quadrant, Q1 (Figure 16 A). However, mice treated with compound 3, or III, did not ameliorate spatial memory during the trial 6 of Barnes maze test (Figure 16 D-E, Figure 18 A-B).

In the trace fear conditioning test compound 2-treated group increased fear response in the same environment where mice 30 minutes before received the foot-shock (context trial 30m) (Figure 19 A). Moreover, in the cue test, mice treated with compound II showed a significant increase freezing behavior in the new environment, when subjected to the acoustic stimulus (CS) 60 min training session (Figure 20 C). In addition, 24 h after the training session vehicle group did not recognize the CS whereas compounds 2, II and IX significantly increased freezing behavior when subjected to the CS in the new environment (Figure 21).

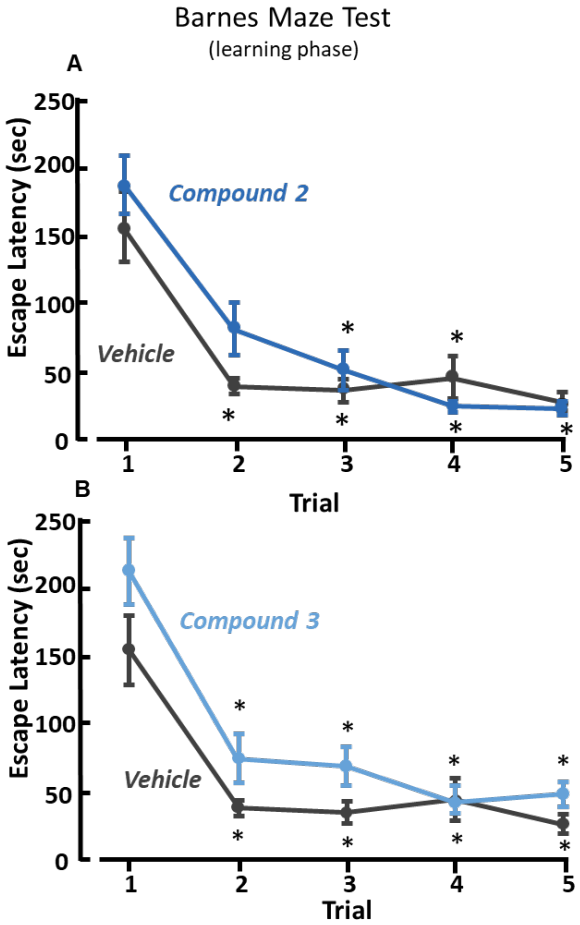

***Figure 13**. Learning phase of Barnes maze test in mice treated with compound 2 or 3. Results of time to find the escape box during learning phase (trial 1-5) of Barnes maze test in compound 2-treated (n=15) (A) compound 3-treated (n=14) (B) and vehicle-treated (n=14) C57BL/6 mice. *, p<0.05 vs trial 1, ANOVA followed by Dunn's post-hoc test. Treatment F(5,79)=1.5548, p=0.183.*

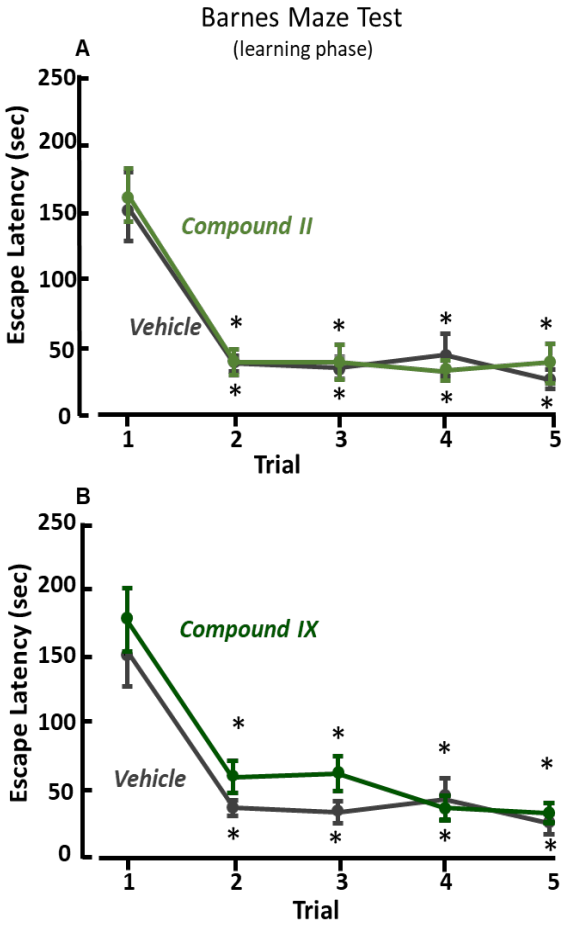

Figure 14. *Barnes maze test (learning phase) of mice treated with compound II and IX. Results of time to find the escape box during learning phase (trial 1-5) of Barnes maze test in compound II-treated (n=15) (A), compound IX-treated (n=14) (B), and vehicle-treated (n=14) C57BL/6 mice. *, p<0.05 vs trial 1, ANOVA followed by Dunn's post-hoc test. Treatment F(5,79)=1.5548, p=0.183*

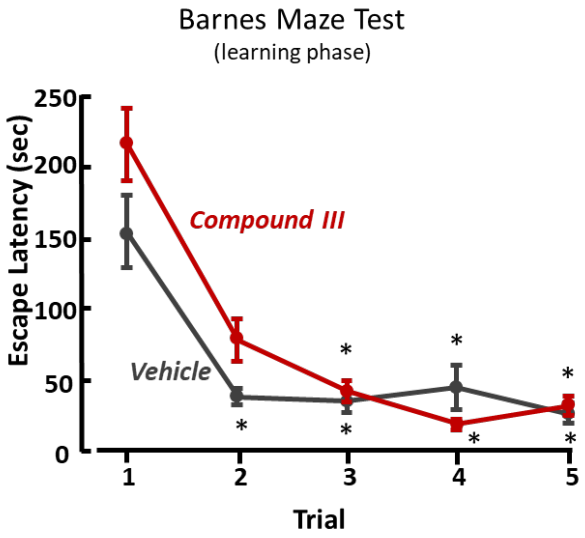

***Figure 15**. Barnes maze test (learning phase) of mice treated with compound III.*

*Results of time to find the escape box during learning phase (trial 1-5) of Barnes maze test in compound III-treated (n=15) and vehicle-treated (n=14) C57BL/6 mice. *, p<0.05 vs trial 1, ANOVA followed by Dunn's post-hoc test. Treatment F(5,79)=1.5548, p=0.183*

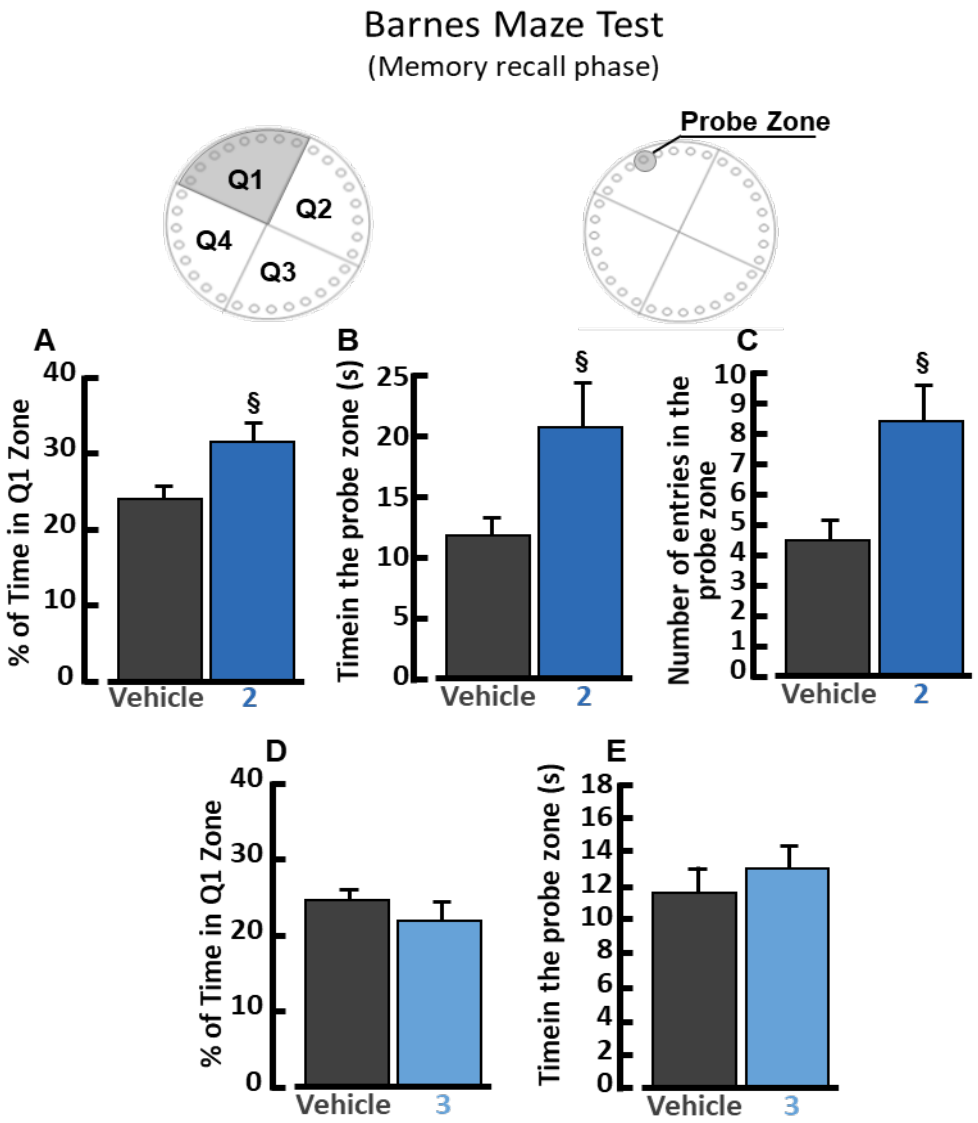

***Figure 16**. Barnes maze test (learning phase) of mice treated with compound 2 or 3.*

(A and D) Quantification of time spend in Q1 during trial 6 by mice treated with vehicle (24.11% ± 1.73, n=14), compound 2 (31.77% ± 2.41, n=15) (A), or compound 3 (21.66% ± 2.44, n=14) (D). Time is expressed as percentage of test duration. [§], p<0.05 vs vehicle treated mice, unpaired Student's t test.

(B and E) Quantification of time spent in the probe zone by mice treated with vehicle (11.61s ± 1.62, n=14), compound 2 (19.74s ± 2.39, n=15) (B), or compound 3 (14.07 ± 2.11, n=14) (E) during trial 6, expressed as percentage of test duration. [§], p<0.05 vs respective vehicle treated mice, unpaired Student's t test.

(C) Results of the number of entries in the probe zone during trial 6 of Barnes maze test in vehicle (4.5 ± 0.7, n= 14) and compound 2 (8.27 ± 1.36, n=15) groups. Unpaired Student's t test.

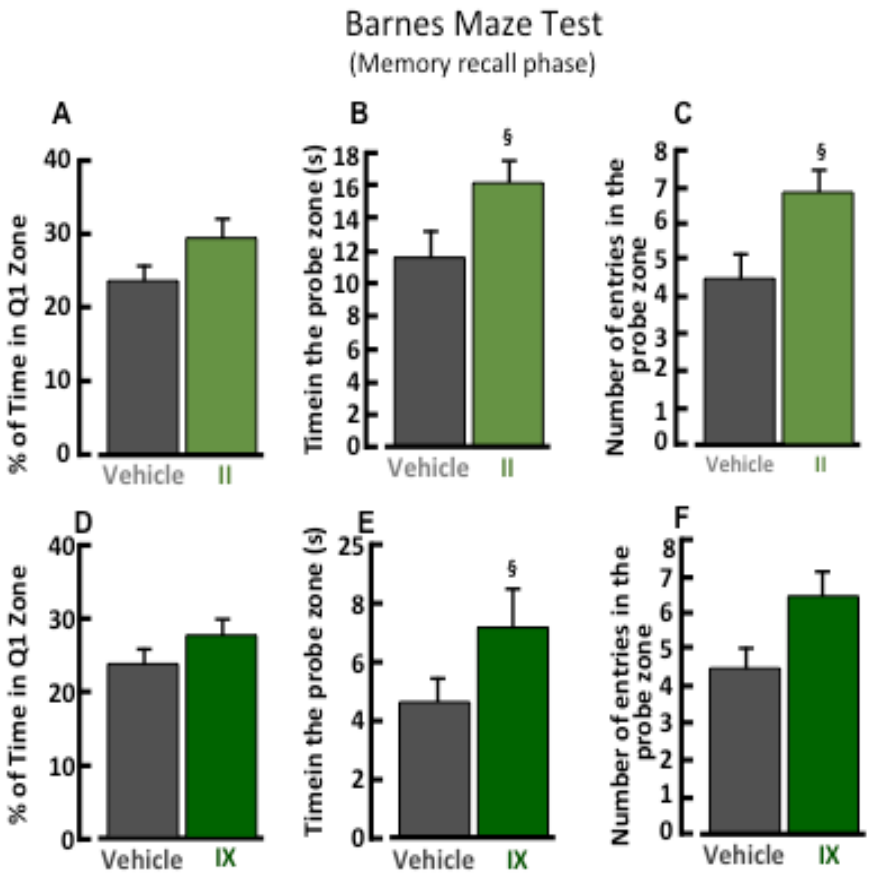

Figure 17. *Barnes maze test (learning phase) of mice treated with compound II or IX.*

(A and D) Quantification of time spend in Q1 during trial 6 by mice treated with vehicle (24,11% ± 1.73, n=14), compound II (29.62% ± 2.43, n=15) (A) or compound IX (28.48% ± 2.42, n=13) (D). Time is expressed as percentage of test duration.

(B and E) Quantification of time spent in the probe zone by mice treated with vehicle (11.61s ± 1.62, n=14), compound II (16.16 ± 1.42 n=15) (B) or compound IX (18.2s ± 2.78, n=13) (D) during trial 6, expressed as percentage of test duration. §*, p<0.05 vs respective vehicle-treated mice, unpaired Student's t test.*

(C and F) Results of the number of entries in the probe zone by vehicle-treated (4.5 ± 0.7, n=14), compound II-treated (6.8 ± 0.63, n=15) (C) or compound IX-treated (6.46 ± 0.67, n=13) (F) mice during trial 6 of Barnes maze. Unpaired Student's t test.

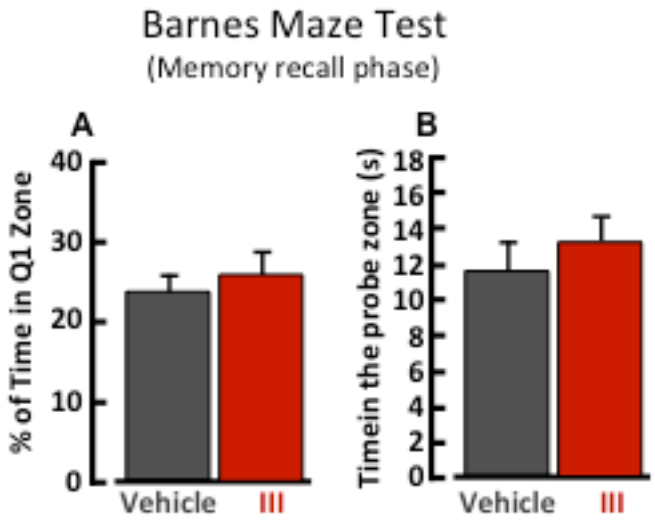

***Figure 18**. Barnes maze test (learning phase) of mice treated with compound III.*

(A) Quantification of time spend in Q1 during trial 6 by mice treated with vehicle (24.11% ± 1.73 n=14) or compound III (26.27% ± 2.21 n=15). Time is expressed as percentage of test duration.

(B) Quantification of time spent in probe zone during trial 6 of Barnes maze by vehicle (11.61s ± 1.61 n=14) or compound III (13.06 ± 1.38 n=15) group.

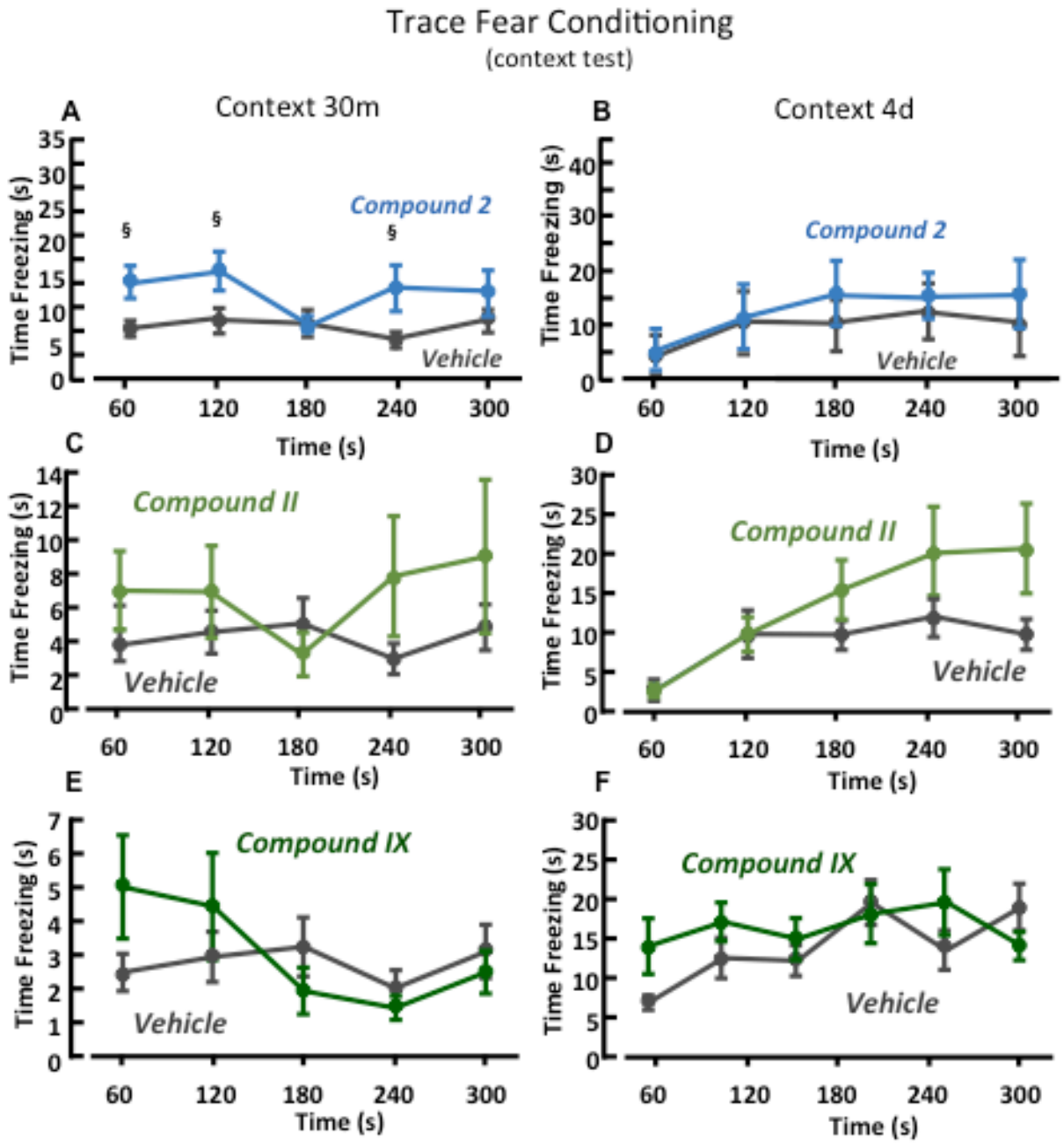

***Figure 19**. Contextual fear conditioning for the three selected compounds.*

(A, C and E) Quantification of freezing time of vehicle (n=24), compound 2 (n=24) (A), compound II (n=15) (C), and compound IX (n=15) (E) measured in the same environment where 30 minutes before they received a foot-shock during the training phase. Freezing time is expressed as total seconds in freezing behavior. §, p<0.05 vs corresponding

segment of vehicle group, ANOVA followed by Dunn's post-hoc test. Treatment F(5,103) = 1.0404, p=0.398; Segment of Test F(4,412)=7.4888, p<0.0001.

(B, D and F) Quantification of freezing time in the same environment where vehicle (n= 24), compound 2 (n=24) (B), compound II (n=15) (D), and compound IX (n=15) (F) groups received the foot-shock 4 days before. Freezing time is expressed as total seconds in freezing behavior. Treatment F(5,83) = 1.9952, p=0.088; Segment of Test F(4,332)=31.2681, p<0.0001.

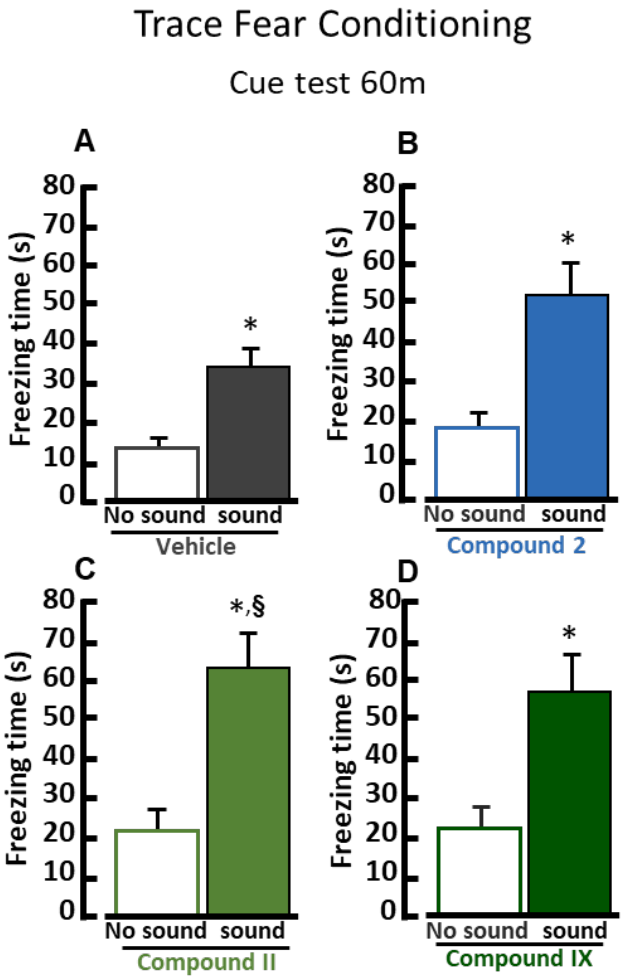

***Figure 20**. Cue trial (1h) of trace fear conditioning test for the three selected compounds.*

*(A) Quantification of freezing behavior in a new environment, 1h after the training, under basal conditions (empty histogram) and in presence of the CS (full histogram) for mice treated with vehicle (13.81s ± 2.22, 34.37s ± 4.63, n=25). *, p<0.05 vs vehicle group "no sound", unpaired Student's t test.*

*(B) Quantification of freezing behavior in a new environment, 1h after the training, under basal conditions (empty histogram) and in presence of the CS (full histogram) for mice treated with compound 2 (18.61s ± 3.27, 52.04s ± 7.6 n= 24). *, p<0.05 vs "no sound" group, unpaired Student's t test.*

(C) Quantification of freezing behavior in a new environment, 1h after the training, under basal conditions (empty histogram) and in presence of the CS (full histogram) for mice

*treated with compound II (20.76s ± 4.87, 61.59s ± 8.94 n=15). *, p<0.05 vs "no sound" group, unpaired Student's t test. §, p<0.05 vs "sound" group, unpaired Student's t test.*

*(D) Quantification of freezing behavior in a new environment, 1h after the training, under basal conditions (empty histogram) and in presence of the CS (full histogram) for mice treated with compound IX (22.81s ± 5.41, 56.84 ± 9.67, n=15). *, p<0.05 vs "no sound" group, unpaired Student's t test.*

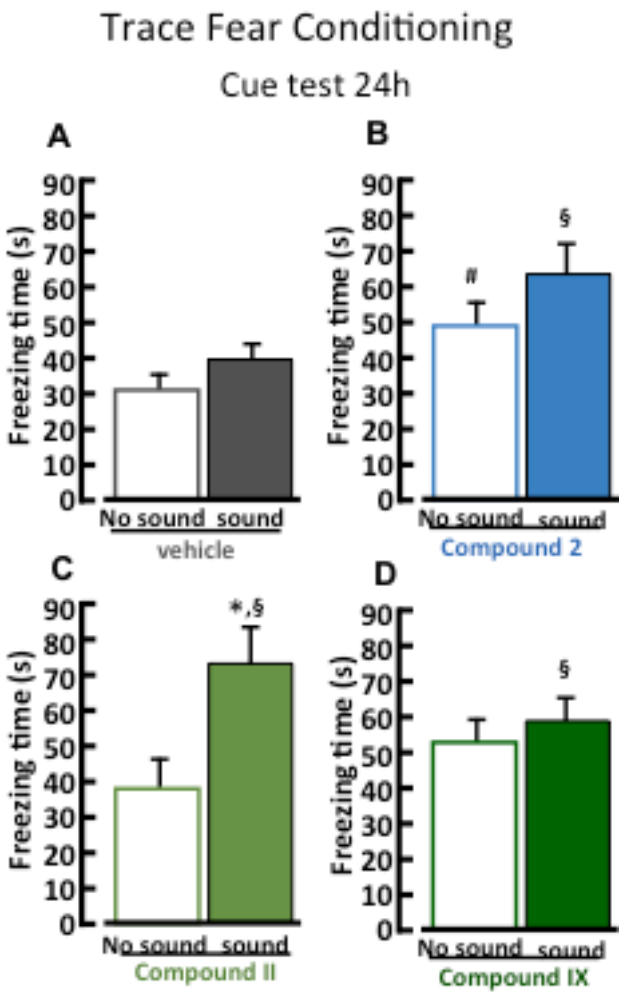

***Figure 21**. Cue trial (24h) of trace fear conditioning test for the three selected compounds.*

(A) Quantification of freezing behavior in a new environment, 24h after the training, under basal conditions (empty histogram) and in presence of the CS (full histogram) for mice treated with vehicle (31.68s ± 4.53, 39.47s ± 5.07 n=20).

(B) Quantification of freezing behavior in a new environment, 1h after the training, under basal conditions (empty histogram) and in presence of the CS (full histogram) for mice treated with compound 2 (50.33s ± 5.31, 63.54s ± 6.97 n=19). §, p<0.05 vs vehicle "sound" group, unpaired Student's t test; $^{\#}$, p<0.05 vs vehicle "no sound" group, unpaired Student's t test.

*(C) Quantification of freezing behavior in a new environment, 1h after the training, under basal conditions (empty histogram) and in presence of the CS (full histogram) for mice treated with compound II (39.07s ± 8.48, 73.89s ± 11.69 n=15). *, p<0.05 vs "no sound"*

control group, unpaired Student's t test; §, p<0.05 vs vehicle "sound" group, unpaired Student's t test.

(D) Quantification of freezing behavior in a new environment, 1h after the training, under basal conditions (empty histogram) and in presence of the CS (full histogram) for mice treated with compound IX (53.43s ± 7.73, 59.18s ± 7.42, n= 15). §, p<0.05 vs vehicle "sound" group, unpaired Student's t test.

4.4 COMPOUND 2 SELECTIVELY INCREASES NCX1 ACTIVITY

Analysis of Na^+ dependent-$^{45}Ca^{2+}$ efflux in BHK cells singly transfected with each NCX isoform showed that 10 nM of compound 2 selectively increases NCX1 activity (Figure 22). Moreover, concentration-effect curve performed with fura-2 techniques displayed an EC_{50} in the low nanomolar range (1.4 nM) for compound 2 (Figure 23B). The stimulatory effect of compound 2 in NCX1 activity was also confirmed by patch clamp in whole cell configuration technique in both *forward* and *reverse* modes of operation (Figure 24 A and B). Compound 2 till the concentration of 10 μM did not affect ASIC1a currents (Figure 25), a channel involved in the control of anxiety and spatial memory and that is also regulated by several drugs targeting NCX1.

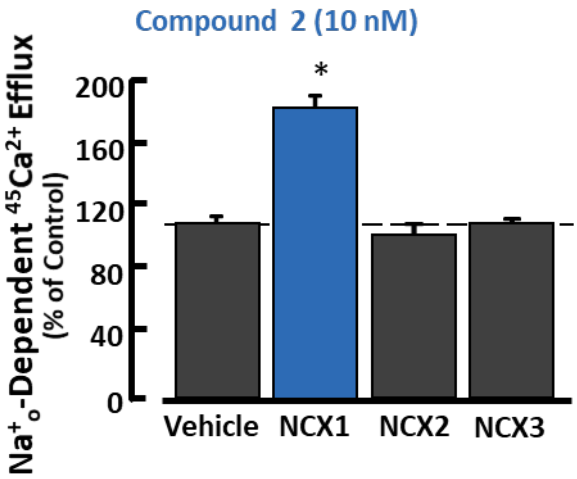

***Figure 22**. Compound 2 selectively increases NCX1 activity.*

*Quantification of NCX1, NCX2 and NCX3 activity measured trough Na^+-dependent $^{45}Ca^{2+}$ efflux in BHK cells treated with 10 nM of compound 2. F(3,12) = 16,53, *p<0.001;*

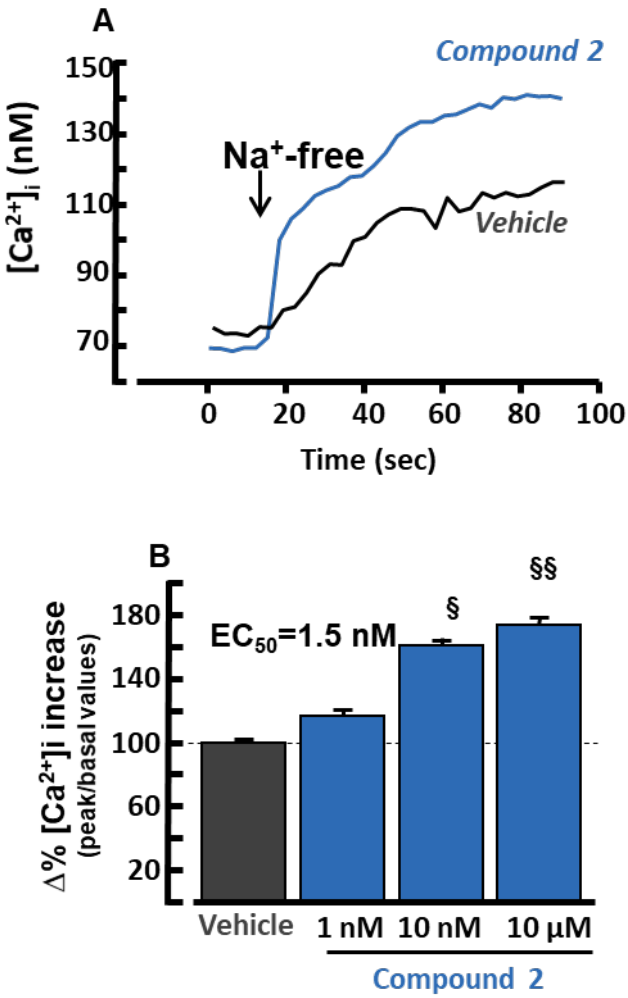

Figure 23. *Concentration-response curve of compound 2 on NCX1 activity measured by Fura-2 technique.*

(A) Superimposed traces representing the effect of compound 2 or vehicle on Na^+-free-induced $[Ca^{2+}]_i$ increase in BHK-NCX1 cells.

(B) Quantification of the effect of compound 2 on NCX1 activity measured by single-cell Fura-2 AM microfluorimetry in BHK-NCX1 cells (n=60 cells for each group). Data are calculated as Δ% of plateau/basal $[Ca^{2+}]_i$ values after Na^+ free addition. §, $p<0.05$ vs vehicle and 1 nM, §§, $p<0.05$ vs all groups, ANOVA followed by Student-Newman-Keuls post-hoc test.

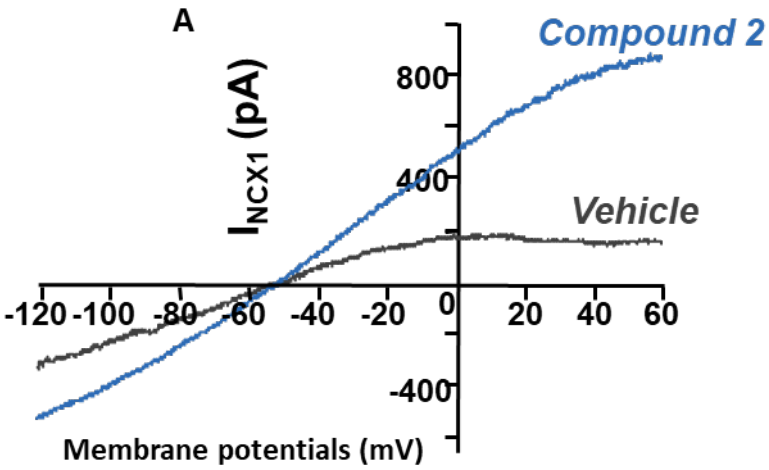

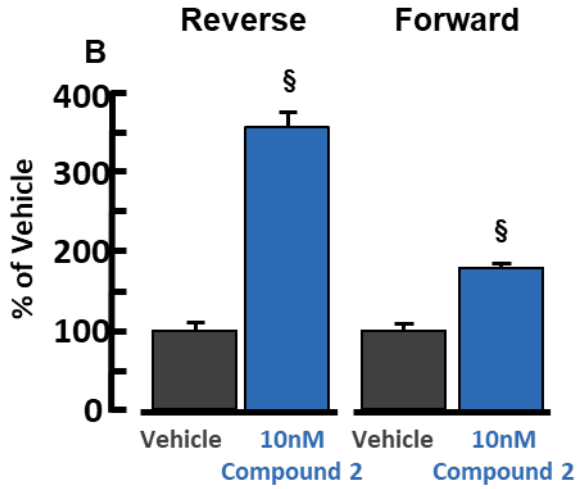

Figure 24. *Effect of compound 2 on NCX1 activity in reverse and forward modes of operation measured by patch-clamp technique in whole cell configuration.*

(A) Superimposed traces on I_{NCX1} currents recorded from BHK-NCX1 cells treated with vehicle or 10 nM of compound 2.

(B) Quantification of the effects of 10 nM compound 2 on NCX1 currents in reverse and forward modes of operation. §, $p<0.05$ vs respective vehicle control group, unpaired Student's t test.

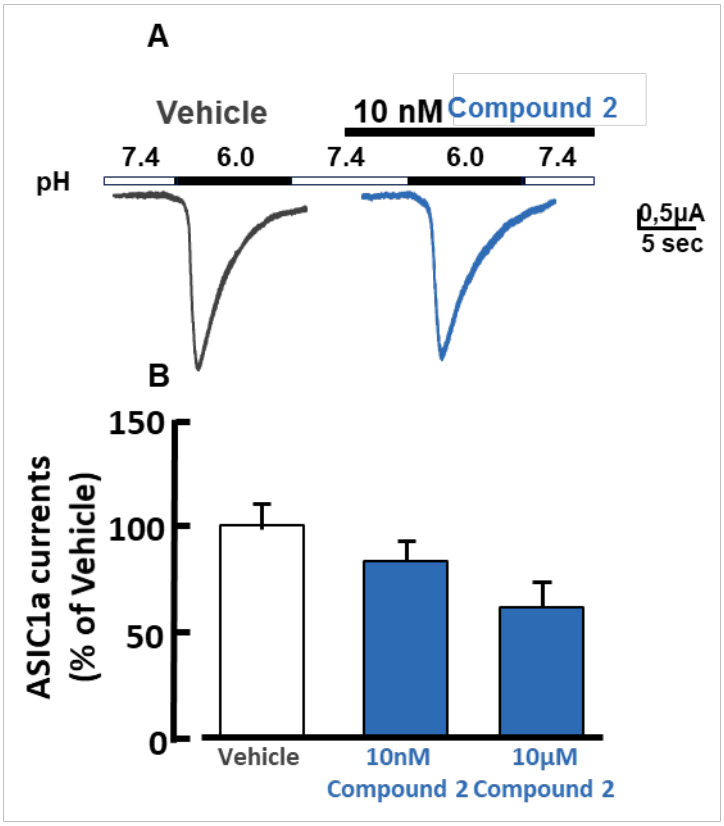

Figure 25. *Effects of compound 2 on ASIC1a currents measured by patch-clamp in whole cell technique.*

(A) Representative traces of the effects of compound 2, or vehicle, on ASIC1a currents activated by shifting the pH of external solution from pH 7.4 to 6.0.

(B) Quantification of ASIC1a currents in presence of vehicle, 10 nM or 10 µM of compound 2 expressed as percentage of vehicle group.

4.5 COMPOUND 2 INCREASES ANXIETY RESPONSE

Corticosterone levels measured in peripheral blood of C57BL/6 mice 6:00 a.m., 12:00 p.m., 18:00 p.m. and 12:00 a.m. revealed a regular circadian rhythm (Figure 26 A). Compound 2-treated mice spent less time in the external zone, more time in the intermediate zone (Figure 26 B) and increased their total time freezing as compared with vehicle-treated mice (Figure 26 C), in the open field test. However, here were no differences of the time spent in light zone for both experimental groups in the dark/light box test under basal conditions. Furthermore, compound 2-treated mice significantly reduced the time of residence in the light zone as compared with vehicle-treated mice after a slightly foot-shock (Figure 27 A). In addition, both mouse groups increased plasma corticosterone levels 1h after the foot-shock, whereas compound 2-treated group showed significant lower levels as compared with vehicle group 24h later (Figure 27 B).

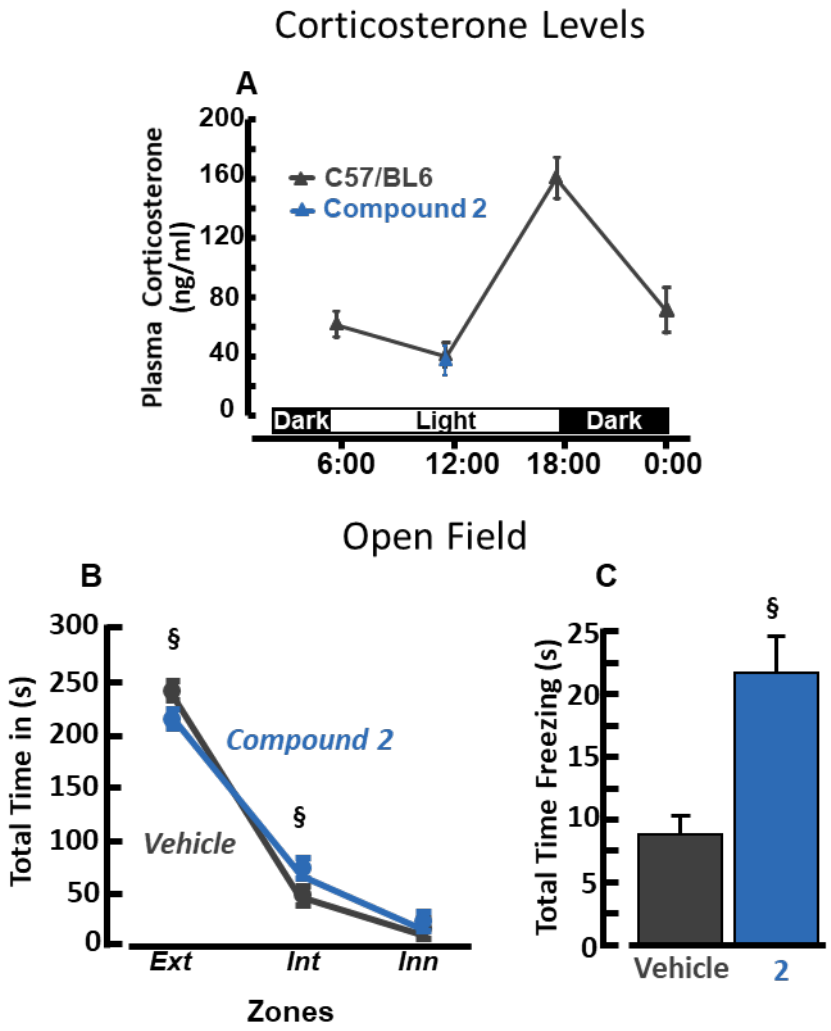

***Figure 26**. Effects of compound 2 on anxiety levels under basal conditions.*

(A) Concentration of corticosterone measured in peripheral blood of C57BL/6 or C57BL/6 treated with compound 2 at different time points.

(B) Quantification of total time spent in external, intermediate or inner zones of open field arena by vehicle-treated (n=15) or compound 2-treated (n=14) mice. Time is expressed in seconds. §, p<0.05 vs vehicle group, unpaired Student's t test.

(C) Quantification of total time spent in freezing behavior during the open field test expressed in seconds. §, p<0.05 vs vehicle-treated mice, unpaired Student's t test.

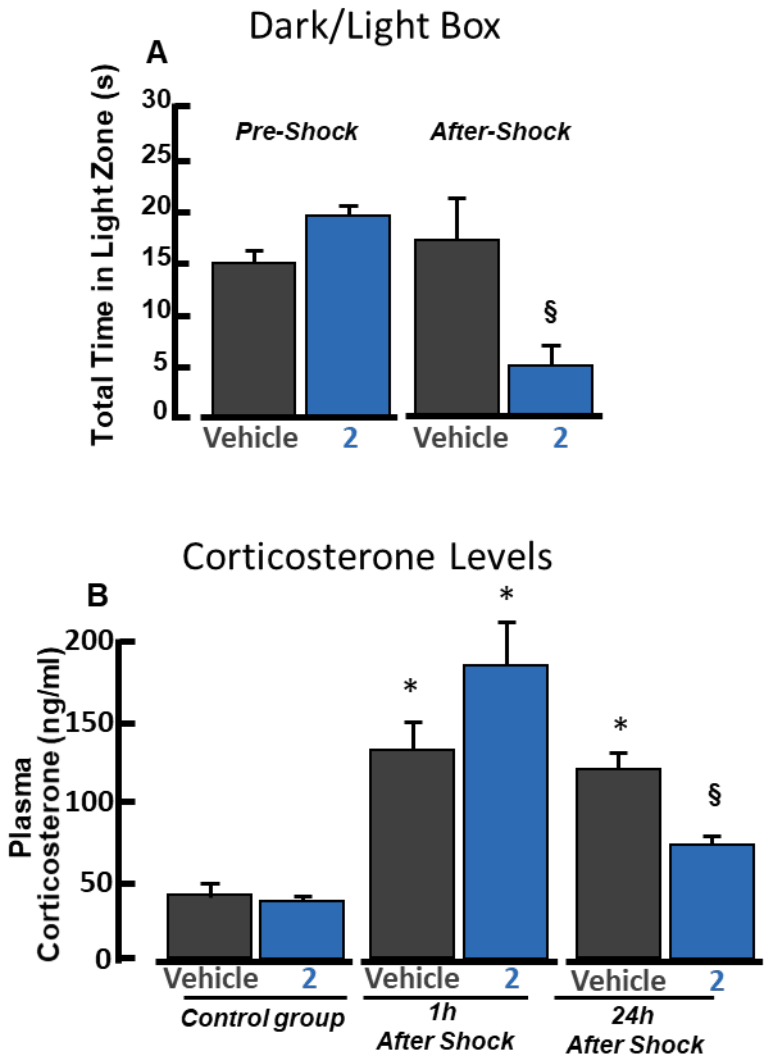

***Figure 27**. Effects of compound 2 on anxiety levels after foot-shock.*

(A) Quantification of total time spent in the light box during pre-shock session (vehicle=14; compound 2=15) and during post-shock session (vehicle=10; compound 2=10) expressed in seconds. [§], p<0.05 vs vehicle treated group, unpaired Student's t test.

*(B) Concentration of corticosterone measured in peripheral blood of C57BL/6s mice treated with vehicle (n=5) or compound 2 (n=5) under control conditions, corresponding to the 12:00 p.m. measurement, and after 1h or 24 hours after the foot-shock. . *, p<0.05 vs respective Vehicle-treated group, Unpaired Student's t test [§], p<0.05 vs respective control group, Unpaired Student's t test.*

4.6 COMPOUND 2-TREATED MICE INCREASE PHOSPHORYLATED CaMKII LEVELS IN THEIR HIPPOCAMPUS

pCaMKII_T286 and pCREB were evaluated in cortex and hippocampus of mice treated with compound 2 or vehicle by western blot assay. In particular, pCaMKII_T286 levels significantly increased in hippocampus of compound 2-treated mice (Figure 28A) and no change in the total amount of pCREB was detected in the same brain region (Figure 28B). Moreover, western blots revealed no change in pCaMKII_T286 or pCREB total amount in cortex of treated mice (Figure 28 A and B).

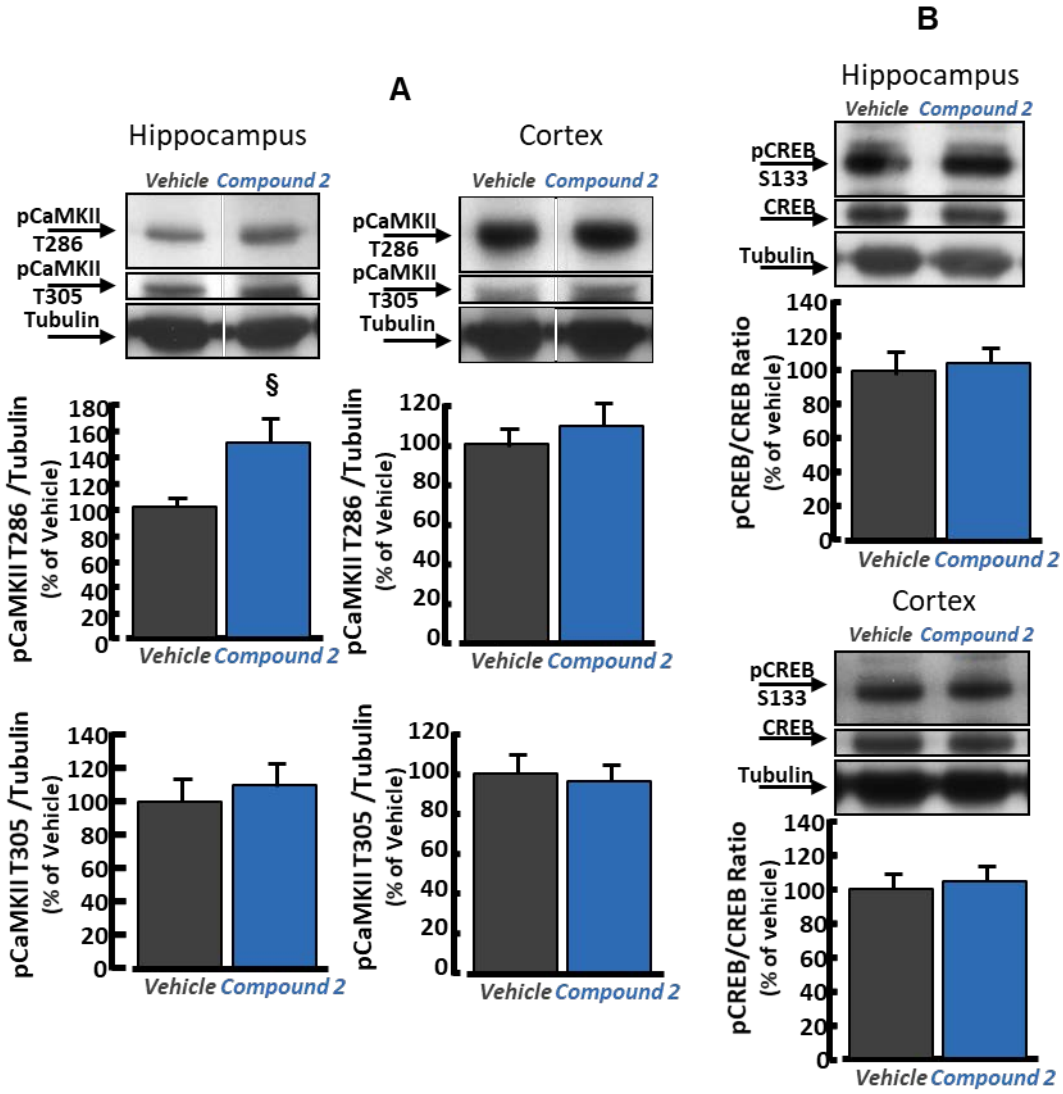

Figure 28. *Quantification of phosphorylated CaMKII and CREB in hippocampus and cortex of mice treated with compound 2 or vehicle.*

(A) Quantification of pCaMKII_T286 and pCAMKII_T305 in hippocampus (on the left) and in cortex (on the right) of mice treated with compound 2, or vehicle, normalized for tubulin and expressed as percentage of vehicle-treated group. §*, $p<0.05$ vs vehicle-treated mouse group, unpaired Student's t test.*

(B) Quantification of pCREB in hippocampus (on the top) and in cortex (on the bottom) of mice treated with compound 2, or vehicle, normalized for total CREB and expressed as percentage of vehicle-treated group.

4.7 KNOCK-OUT OR OVEREXPRESSION OF NCX1 IN NEURONS OF HIPPOCAMPUS, AMYGDALA AND CORTEX AFFECT THE PHOSPHORYLATION OF CREB AND CaMKII

The immunofluorescence analysis did not show any significant morphological abnormalities in the hippocampus, striatum, cortex and amygdala of *NCX1*^{ko} and *NCX1.4*^{over} mice as showed by NeuN neuronal marker (Figure 29-Figure 31). In addition, the quantification of number of neurons revealed no differences between experimental and respective control groups (Molinaro et al., 2016).

NCX1 immunosignal was reduced in cortex, amygdala and in both dorsal and ventral hippocampal subregions of *NCX1*^{ko} mice and increased in the same regions of *NCX1.4*^{over} mice (Figure 29-Figure 31). In addition, phosphorylated CREB at Ser133 (pCREB) and the active form of phosphorylated CaMKII at Thr286 (pCaMKII_T286), were significantly reduced in hippocampus (Figure 35, Figure 36, Figure 39, Figure 40), amygdala (Figure 34, Figure 38) and cortex (Figure 33, Figure 37) of *NCX1*^{ko} and increased in same brain regions of *NCX1.4*^{over} mice. Accordingly, western blot analysis confirmed that pCREB was reduced in hippocampus (Figure 41 A) and cortex (Figure 42A) of *NCX1*^{ko} and was increased in same brain regions of *NCX1.4*^{over}. Similarly, pCaMKII_T286 was reduced in the hippocampus of *NCX1*^{ko} and increased in same brain region of *NCX1.4*^{over} (Figure 41 B). On the other hand, no variation of pCaMKII_T286 was detected in cortex of the two genetic modified mice (Figure 42 B). In addition, the inactive phosphorylated form of CaMKII (pCaMKII_T305) was reduced in the hippocampus of *NCX1*^{ko} (Figure 41 B) and in the cortex of *NCX1.4*^{over} mice (Figure 42 B).

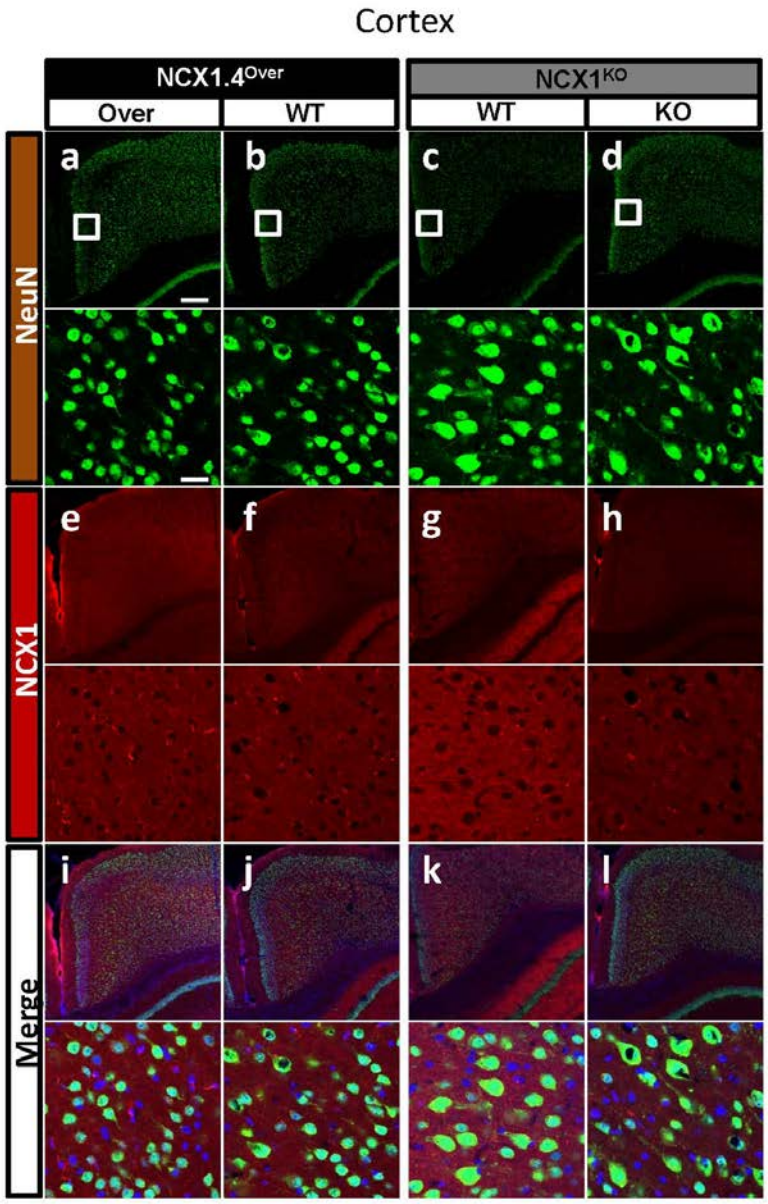

Figure 29. *NCX1 immunosignal in the cortex of NCX1^{ko} and NCX1.4^{over} mice. Immunofluorescence images showing cortex of NCX1.4^{over} (Over), NCX1.4$^{+/+}$ (WT), NCX1^{ko} (KO) and NCX1$^{+/+}$ (WT) mice. Overview pictures and high-magnification photomicrographs showing the colocalization of NeuN (green: a, b, c, d) and NCX1 (red: e, f, g, h) in amygdala. Scale bars, 200 µm or 25 µm.*

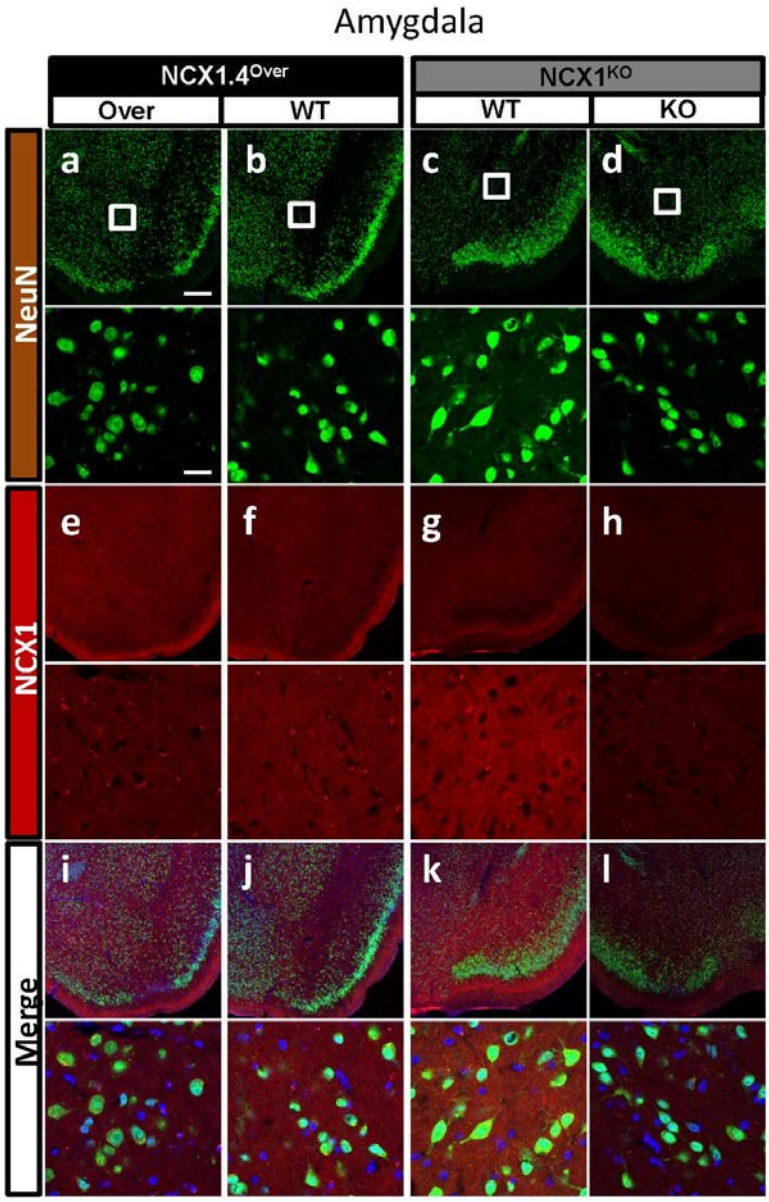

***Figure 30**. NCX1 immunosignal in the amygdala of NCX1^{ko} and NCX1.4^{over} mice. Immunofluorescence images showing amygdala of NCX1.4^{over} (Over), NCX1.4$^{+/+}$ (WT), NCX1^{ko} (KO) and NCX1$^{+/+}$ (WT) mice. Overview pictures and high-magnification photomicrographs showing the colocalization of NeuN (green: a, b, c, d) and NCX1 (red: e, f, g, h) in amygdala. Scale bars, 200 µm or 25 µm.*

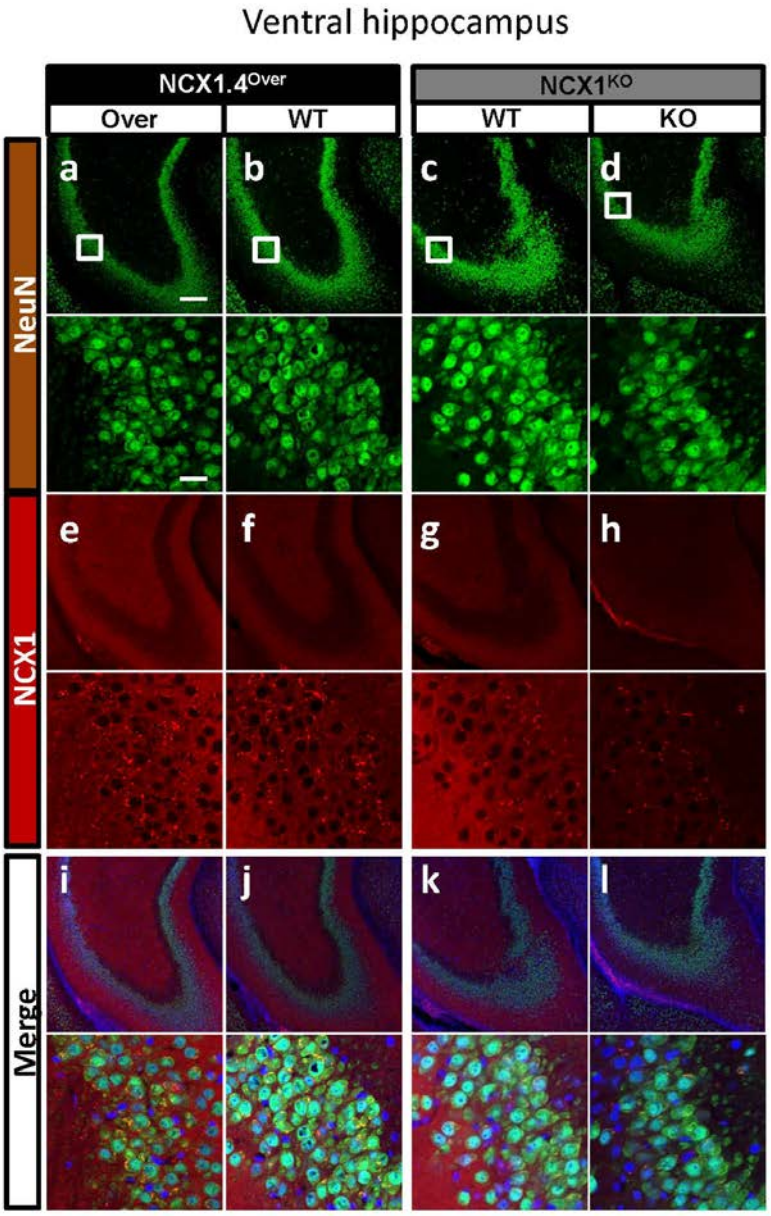

***Figure 31**. NCX1 immunosignal in ventral hippocampus of NCX1^{ko} and NCX1.4^{over} mice. Immunofluorescence images showing ventral hippocampus of NCX1.4^{over} (Over), NCX1.4$^{+/+}$ (WT), NCX1^{ko} (KO) and NCX1$^{+/+}$ (WT) mice. Overview pictures and high-magnification photomicrographs showing the colocalization of NeuN (green: a, b, c, d) and NCX1 (red: e, f, g, h) in ventral hippocampus. Scale bars, 200 µm or 25 µm.*

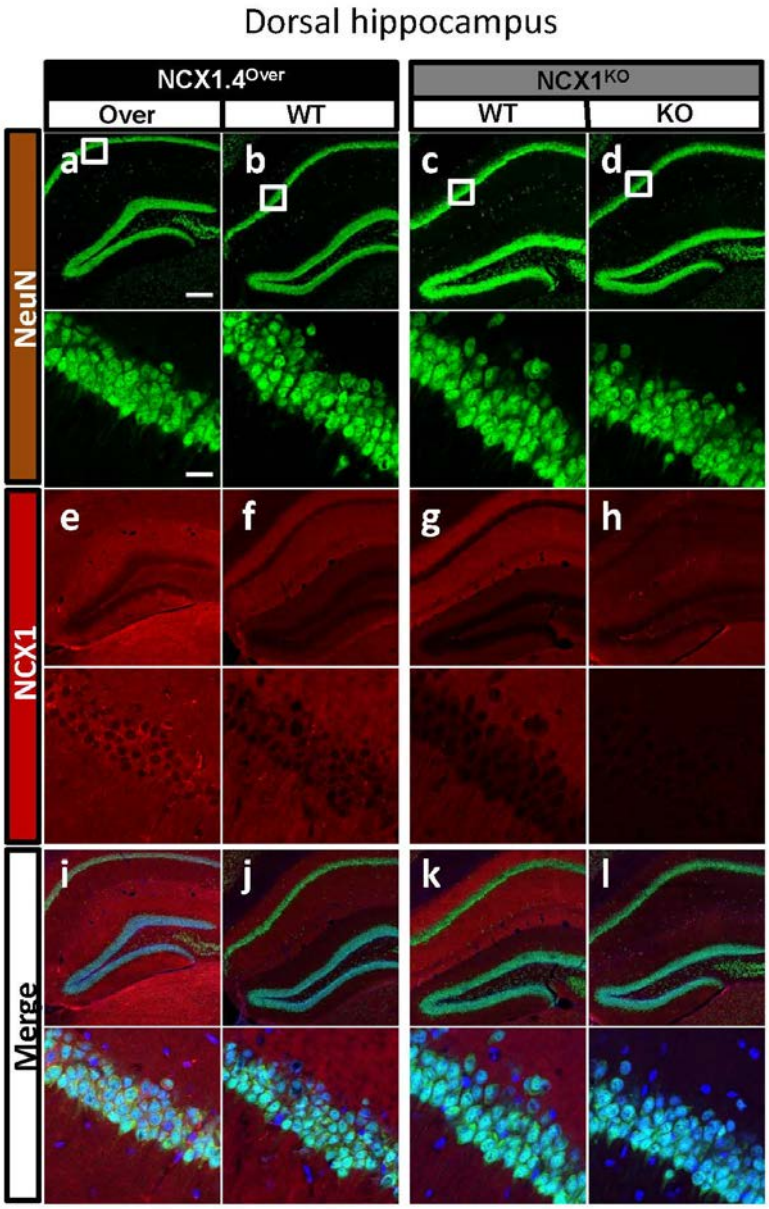

***Figure 32**. NCX1 immunosignal in dorsal hippocampus of NCX1^{ko} and NCX1.4^{over} mice. Immunofluorescence images showing dorsal hippocampus of NCX1.4^{over} (Over), NCX1.4$^{+/+}$ (WT), NCX1^{ko} (KO) and NCX1$^{+/+}$ (WT) mice. Overview pictures and high-magnification photomicrographs showing the colocalization of NeuN (green: a, b, c, d) and NCX1 (red: e, f, g, h) in dorsal hippocampus. Scale bars, 200 µm or 25 µm.*

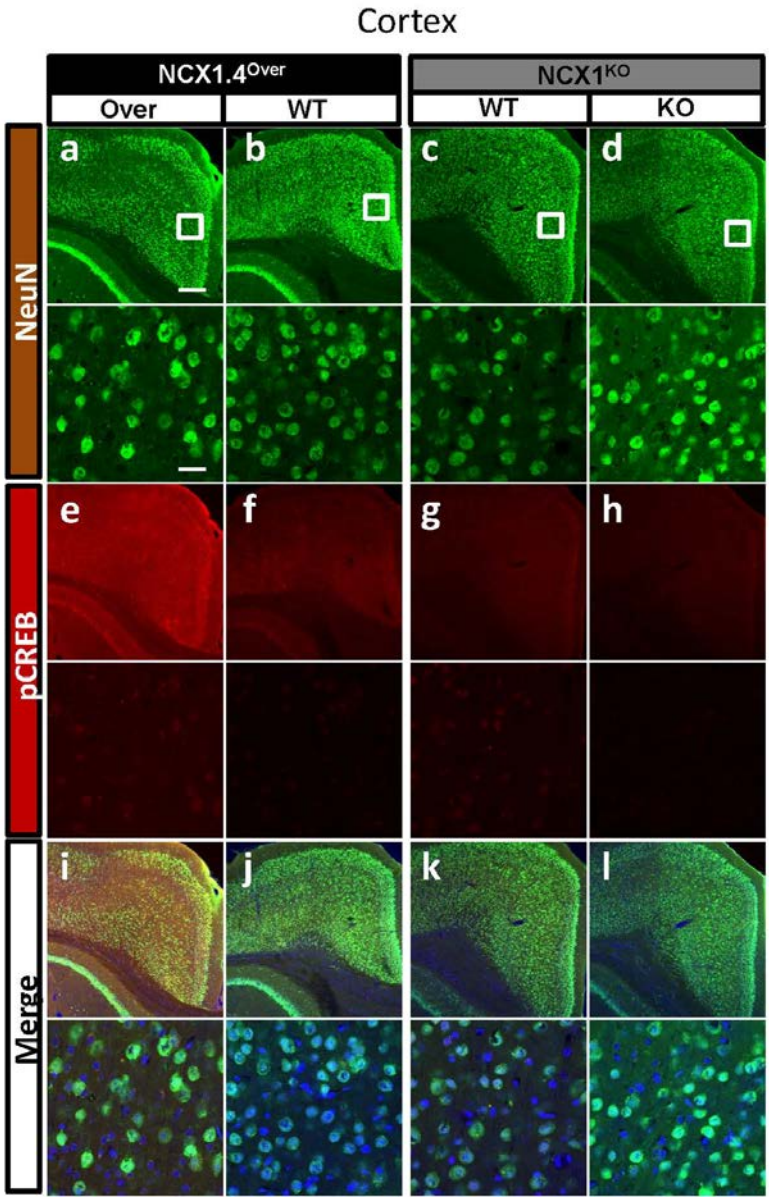

***Figure 33**. pCREB_S133 immunosignal in cortex of NCX1^{ko} and NCX1.4^{over} mice. Immunofluorescence images showing cortex of NCX1.4^{over} (Over), NCX1.4$^{+/+}$ (WT), NCX1^{ko} (KO) and NCX1$^{+/+}$ (WT) mice. Overview pictures and high-magnification photomicrographs showing the colocalization of NeuN (green: a, b, c, d) and pCREB_S133 (red: e, f, g, h) in cortex. Scale bars, 200 µm or 25 µm.*

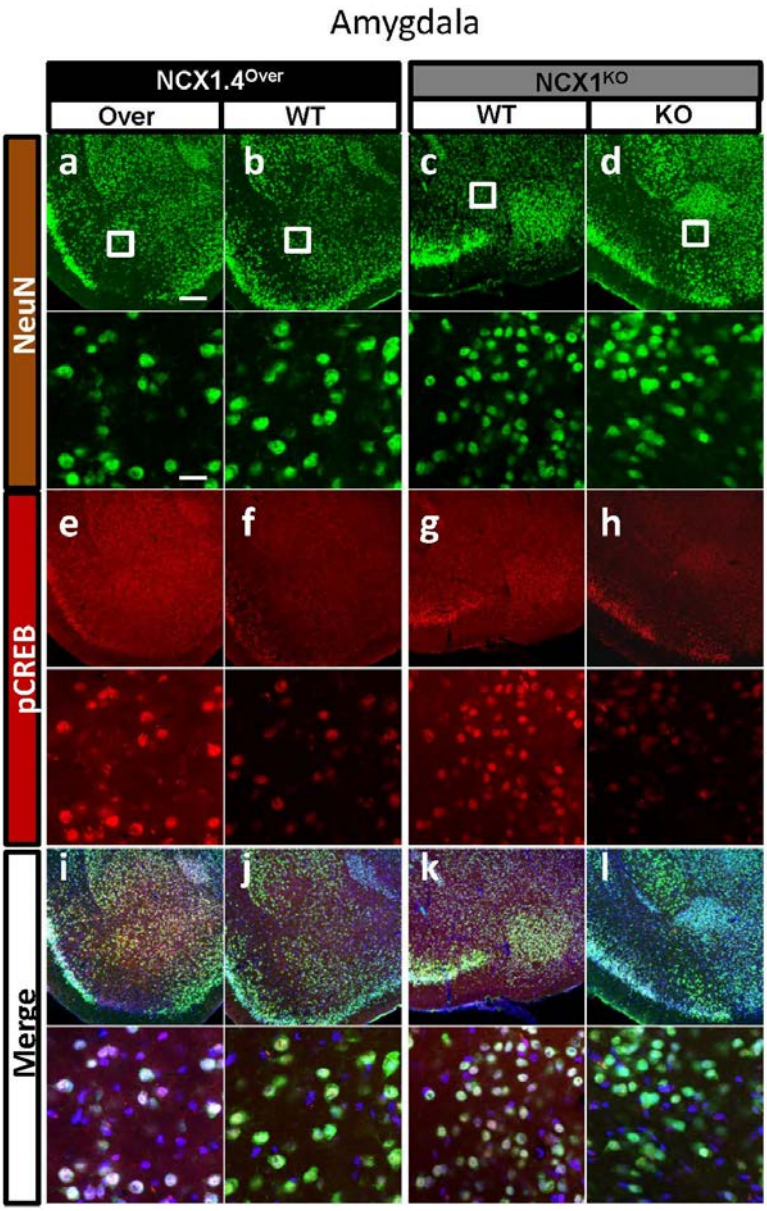

***Figure 34**. pCREB_S133 immunosignal in amygdala of NCX1^{ko} and NCX1.4^{over} mice. Immunofluorescence images showing amygdala of NCX1.4^{over} (over), NCX1.4$^{+/+}$ (WT), NCX1^{ko} (KO) and NCX1$^{+/+}$ (WT) mice. Overview pictures and high-magnification photomicrographs showing the colocalization of NeuN (green: a, b, c, d) and pCREB_S133 (red: e, f, g, h) in amygdala. Scale bars, 200 μm or 25 μm.*

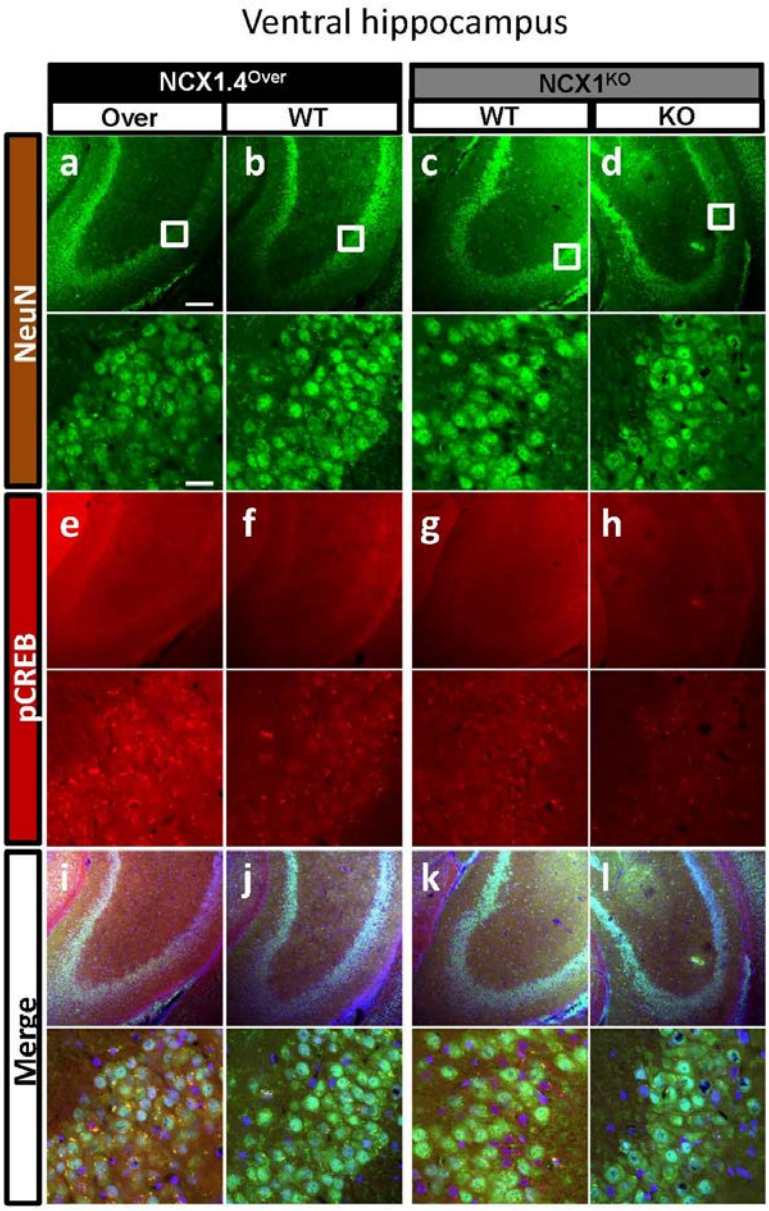

***Figure 35**.pCREB_S133 immunosignal in ventral hippocampus of NCX1^{ko} and NCX1.4^{over}. Immunofluorescence images showing ventral hippocampus of NCX1.4^{over} (Over), NCX1.4$^{+/+}$ (WT), NCX1^{ko} (KO) and NCX1$^{+/+}$ (WT) mice. Overview pictures and high-magnification photomicrographs showing the colocalization of NeuN (green: a, b, c, d) and pCREB_S133 (red: e, f, g, h) in ventral hippocampus. Scale bars, 200 µm or 25 µm.*

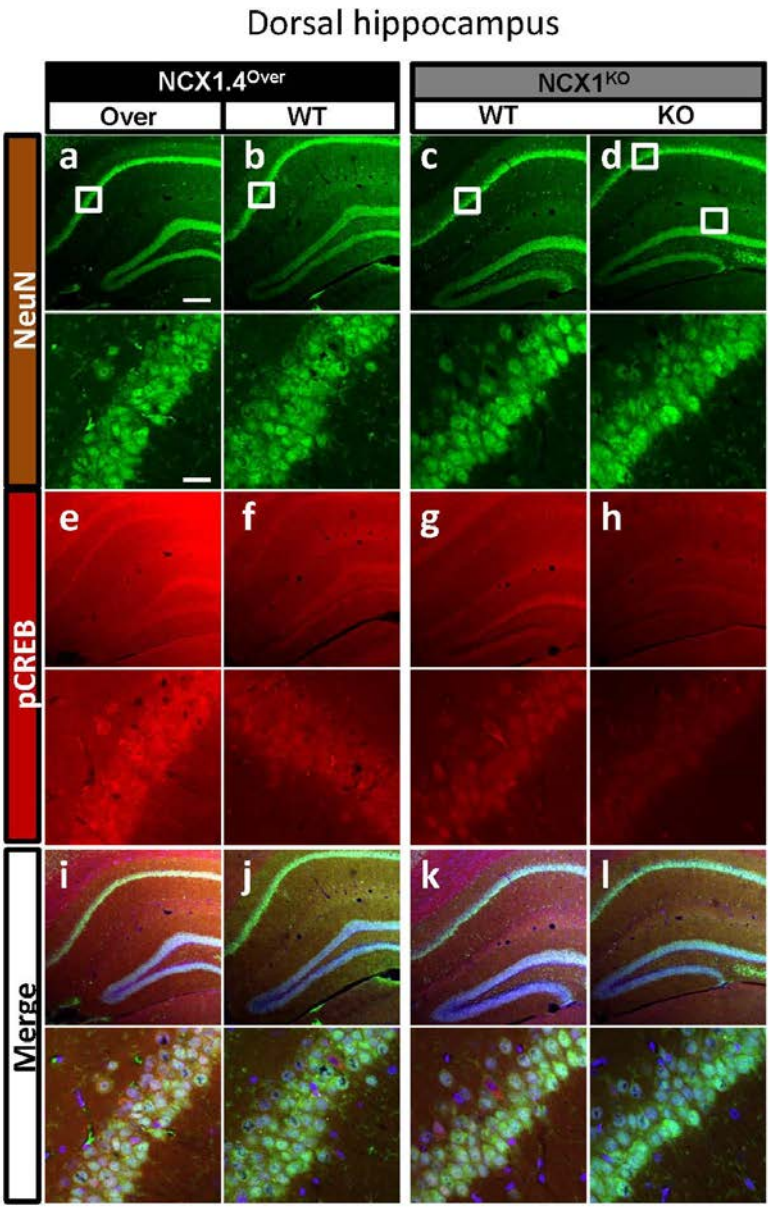

***Figure 36**. pCREB_S133 immunosignal in dorsal hippocampus of NCX1^{ko} and NCX1.4^{over}. Immunofluorescence images showing dorsal hippocampus of NCX1.4^{over} (Over), NCX1.4$^{+/+}$ (WT), NCX1^{ko} (KO) and NCX1$^{+/+}$ (WT) mice. Overview pictures and high-magnification photomicrographs showing the colocalization of NeuN (green: a, b, c, d) and pCREB_S133 (red: e, f, g, h) in dorsal hippocampus. Scale bars, 200 μm or 25 μm.*

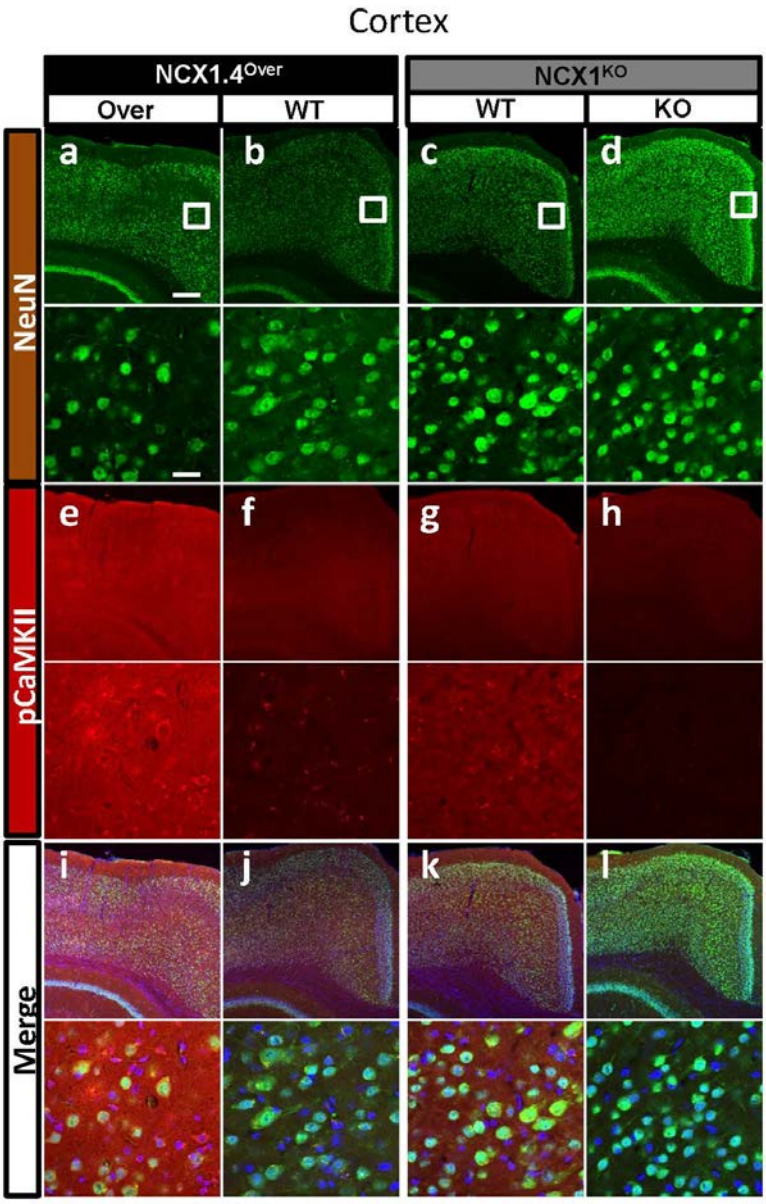

***Figure 37**. pCaMKII_T286 immunosignal in cortex of NCX1^{ko} and NCX1.4^{over} mice. Immunofluorescence images showing cortex of NCX1.4^{over} (Over) NCX1.4$^{+/+}$ (WT), NCX1^{ko} (KO) and NCX1$^{+/+}$ (WT) mice. Overview pictures and high-magnification photomicrographs showing the colocalization of NeuN (green: a, b, c, d) and pCaMKII_T286 (red: e, f, g, h) in cortex. Scale bars, 200 µm or 25µm.*

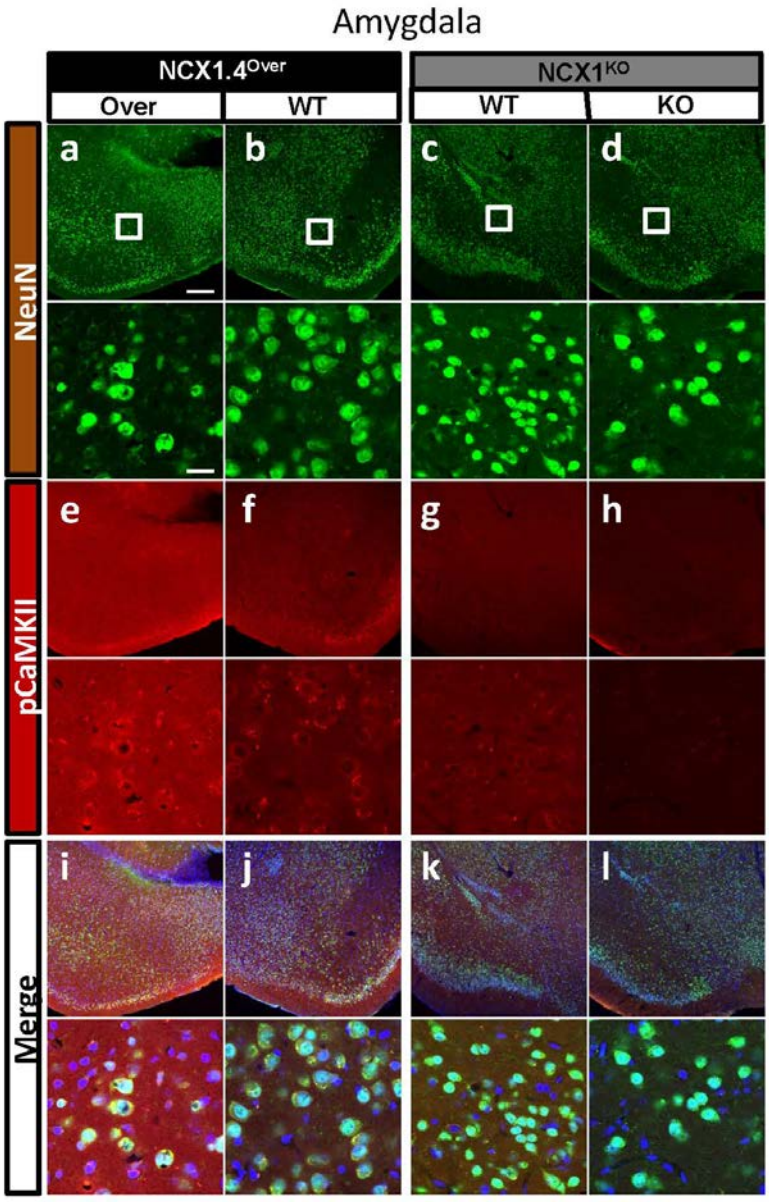

***Figure 38**. pCaMKII_T286 immunosignal in amygdala of NCX1^{ko} and NCX1.4^{over} mice. Immunofluorescence images showing amygdala of NCX1.4^{over} (Over), NCX1.4$^{+/+}$ (WT), NCX1^{ko} (KO) and NCX1$^{+/+}$ (WT) mice. Overview pictures and high-magnification photomicrographs showing the colocalization of NeuN (green: a, b, c, d) and pCaMKII_T286 (red: e, f, g, h) in amygdala. Scale bars, 200 µm or 25 µm.*

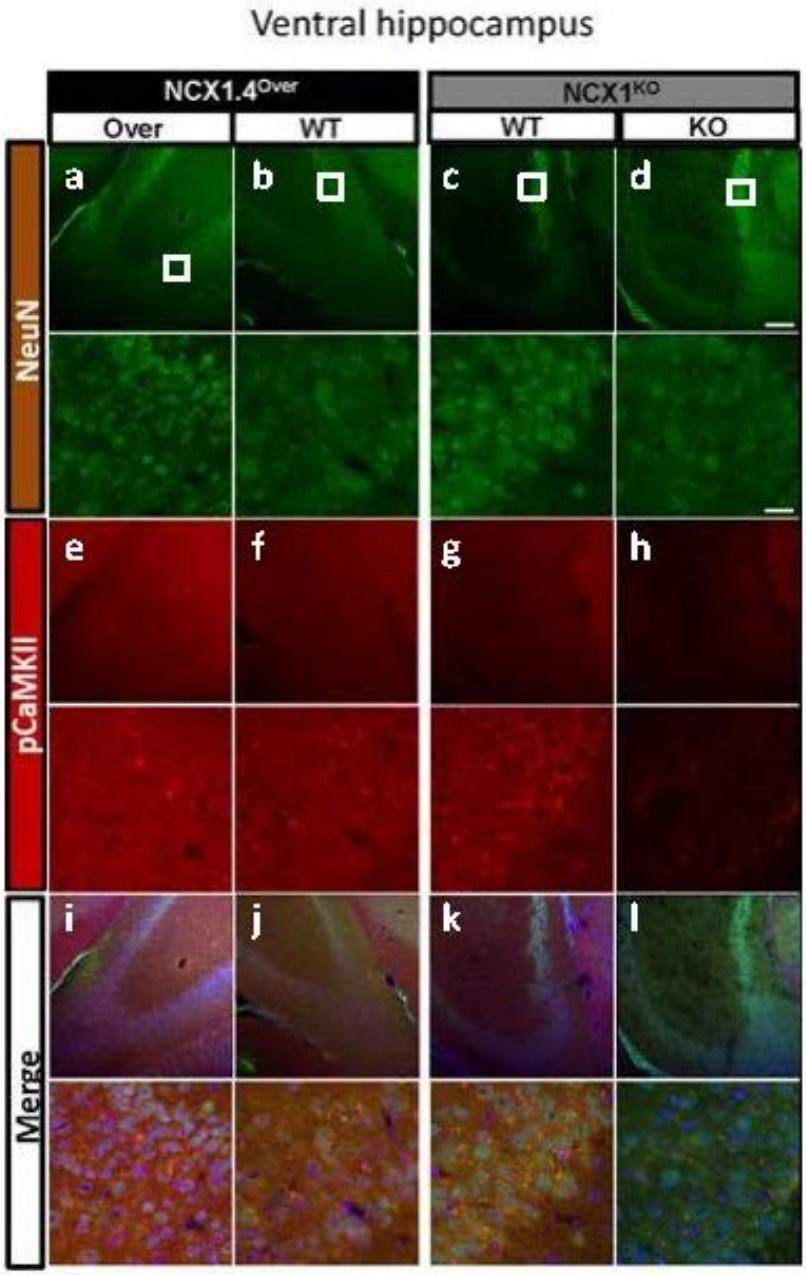

***Figure 39**. pCaMKII_T286 immunosignal ventral hippocampus of NCX1^{ko} and NCX1.4^{over} mice.*

Immunofluorescence images showing ventral hippocampus of NCX1.4^{over} (Over), NCX1.4$^{+/+}$ (WT), NCX1^{ko} (KO) and NCX1$^{+/+}$ (WT) mice. Overview pictures and high-magnification photomicrographs showing the colocalization of NeuN (green: a, b, c, d) and pCaMKII_T286 (red: e, f, g, h) in ventral hippocampus. Scale bars, 200 µm or 25 µm.

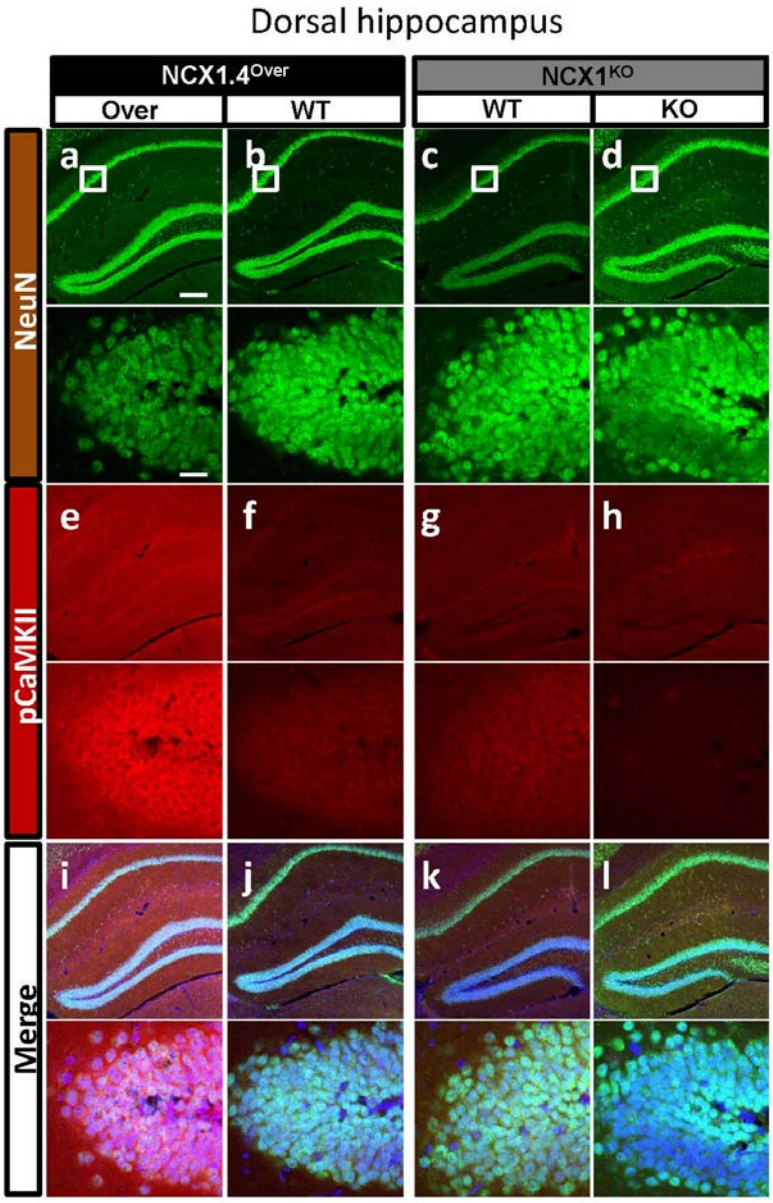

***Figure 40**. pCaMKII_T286 immunosignal dorsal hippocampus of NCX1^{ko} and NCX1.4^{over} mice.*

Immunofluorescence images showing dorsal hippocampus of NCX1.4^{over} (Over), NCX1.4$^{+/+}$ (WT), NCX1^{ko} (KO) and NCX1$^{+/+}$ (WT) mice. Overview pictures and high-magnification photomicrographs showing the colocalization of NeuN (green: a, b, c, d) and pCaMKII_T286 (red: e, f, g, h) in dorsal hippocampus. Scale bars, 200 µm or 25 µm.

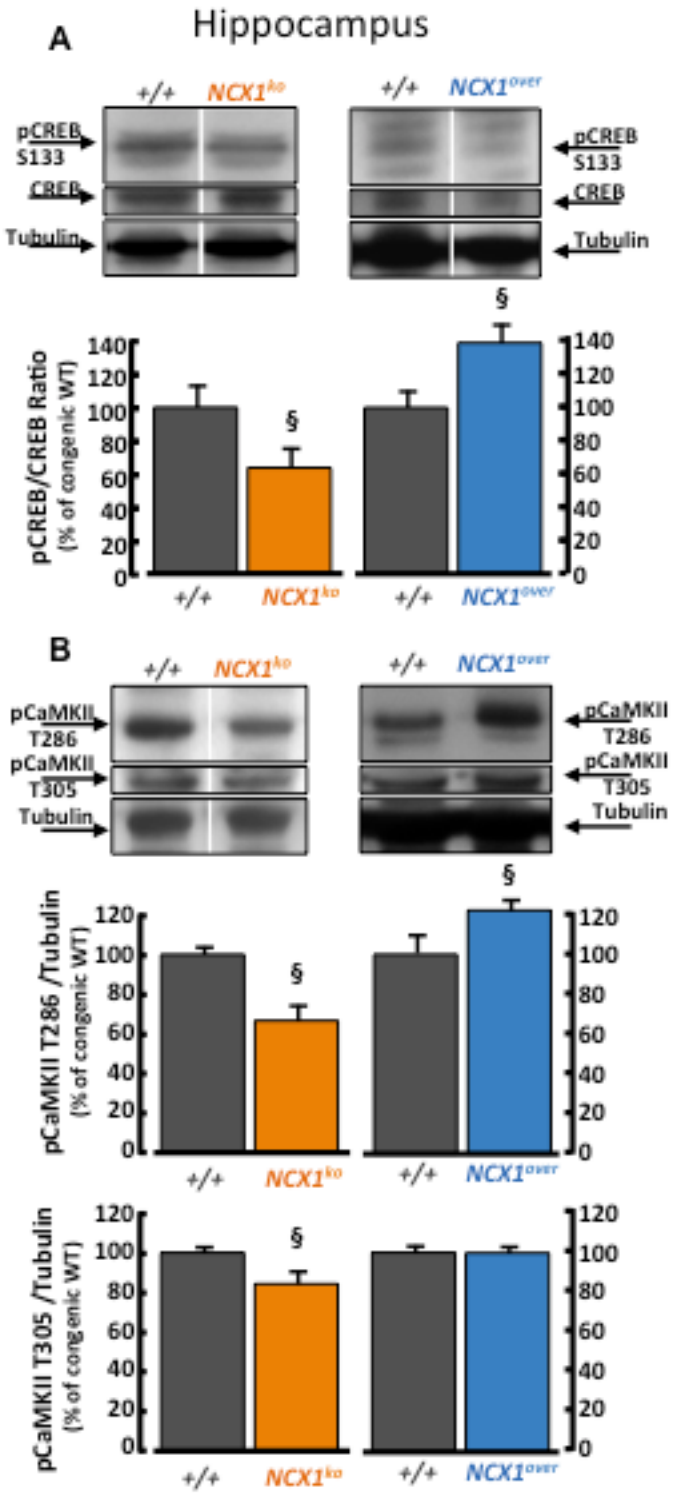

Figure 41. *Quantification of pCREB_S133 and pCaMKII286 expression in hippocampus of NCX1^{ko} and NCX1.4^{over} mice.*

(A) Quantification of pCREB_S133 in hippocampus of genetic modified mice NCX1^{ko} (n=8), NCX1$^{+/+}$ (n=8), NCX1.4^{over} (n=8) and NCX1.4$^{+/+}$ (n=8) normalized for total CREB and

expressed as percentage of control. [§], p<0.05 vs congenic wild-type mice, unpaired Student's t test.

(B) Quantification of pKaMKII_T286 and pCaMKII_T305 in the hippocampus of genetic modified mice $NCX1^{ko}$ (n=8), $NCX1^{+/+}$ (n=8), $NCX1.4^{over}$ (n=8) $NCX1.4^{+/+}$ (n=8) normalized for tubulin and expressed as percentage of control. [§], p<0.05 vs congenic wild-type mice, unpaired Student's t test.

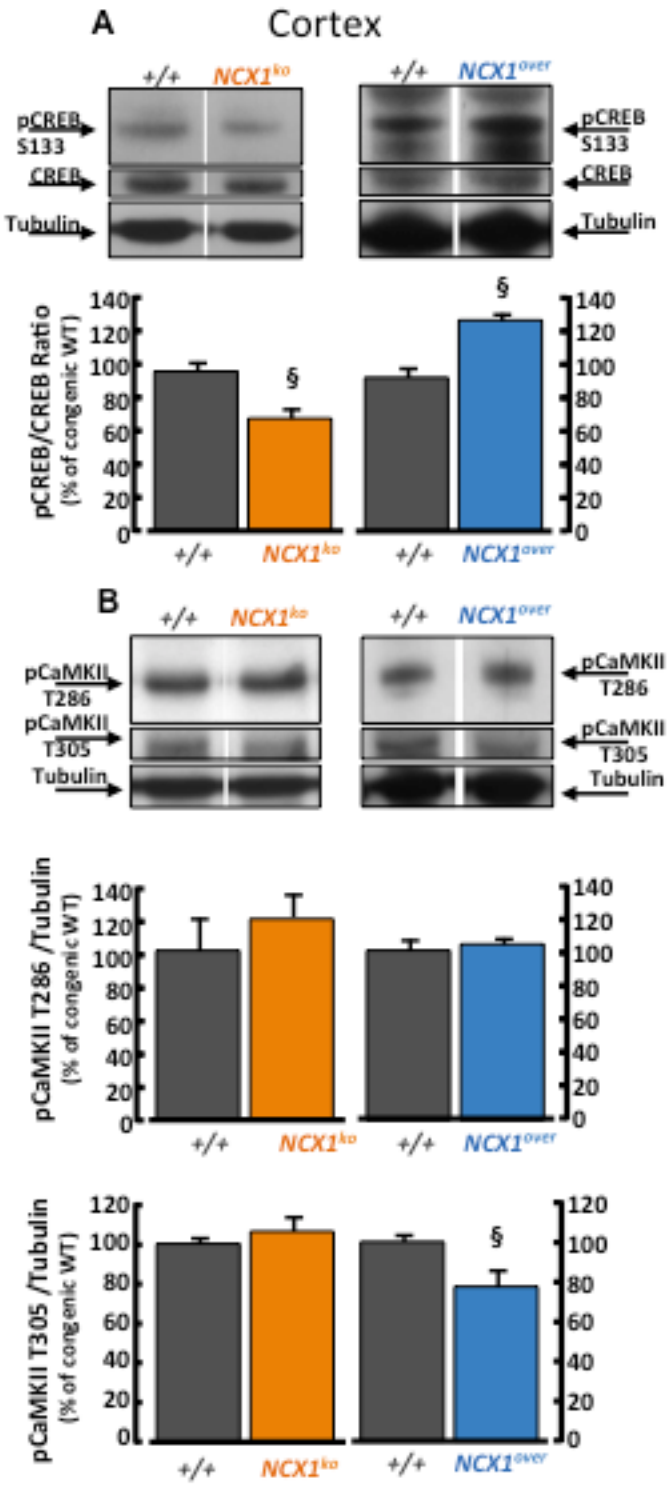

Figure 42. *Quantification of pCREB_S133 and p CaMKII286 expression in cortex of NCX1^{ko} and NCX1.4^{over} mice.*

(A) Quantification of pCREB_S133 in cortex of genetic modified mice $NCX1^{ko}$ (n=8), $NCX1^{+/+}$ (n=8), $NCX1.4^{over}$ (n=8) and $NCX1.4^{+/+}$ (n=8) normalized for total CREB and expressed as percentage of control. §, p<0.05 vs congenic wild-type mice, unpaired Student's t test.

(B) Quantification of pKaMKII_T286 and pCaMKII_T305 in cortex of genetic modified mice $NCX1^{ko}$ (n=8), $NCX1^{+/+}$ (n=8), $NCX1.4^{over}$ (n=8) $NCX1.4^{+/+}$ (n=8) normalized for tubulin and expressed as percentage of control. §, p<0.05 vs congenic wild-type mice, unpaired Student's t test.

4.8 NCX1^{ko} AND NCX1.4^{over} MICE DO NOT DISPLAY IMPAIREMENT OF LOCOMOTOR ACTIVITY

Locomotor activity of genetically modified mice were evaluated in the open field test and in rotarod test. In particular, *NCX1^{ko}* mice did not show variations in total freezing time (Figure 43 A), total moving time (Figure 43 B), total distance travelled (Figure 43 C), and in normalized speed (Figure 44B) in the open field test and latency to fall in rotarod test (Figure 44 D), as compared with congenic wild-type mice. By contrast, *NCX1.4^{over}* mice, in open field, displayed an increase of the total freezing time (Figure 43 D) with a reduction of both total moving time (Figure 43 E) and total distance travelled (Figure 43F) as compared with its congenic wild-type mice. On the other hand, no differences were observed in normalized speed (Figure 44 C) and in rotarod test (Figure 44 D).

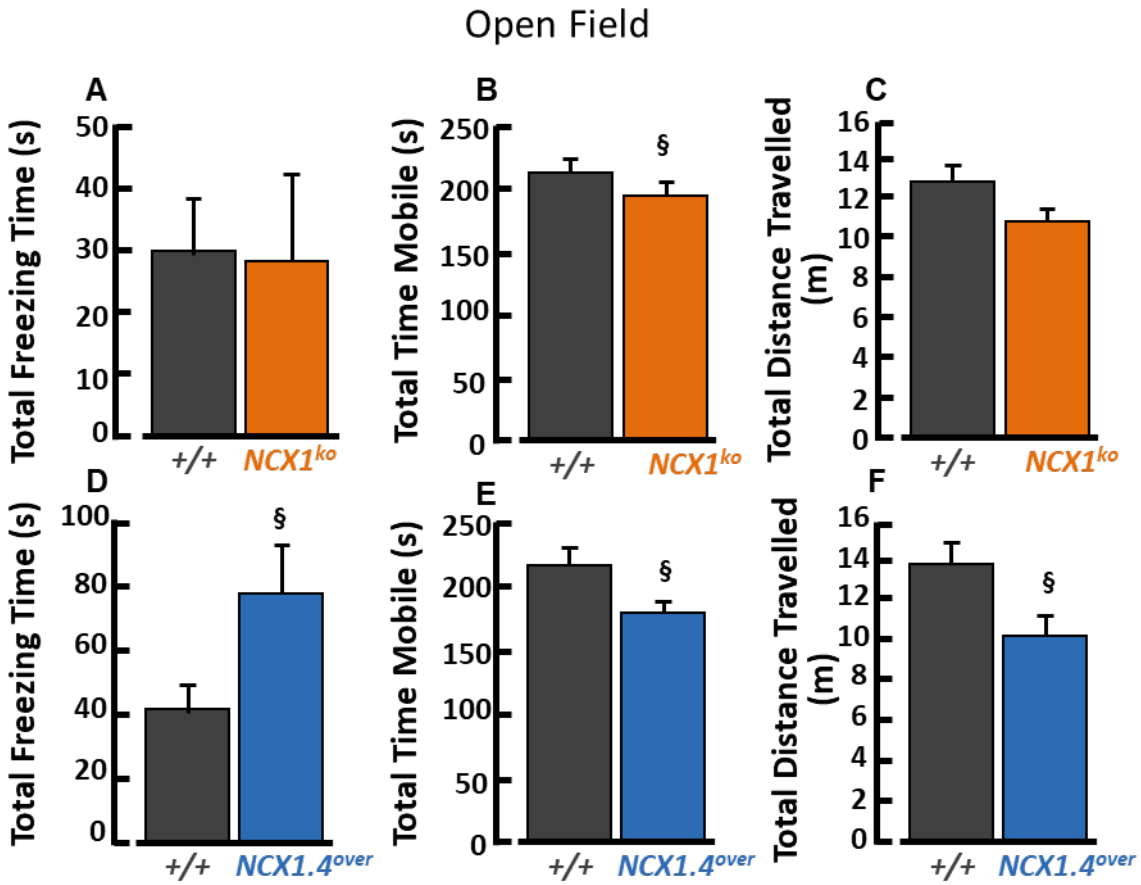

Figure 43. Evaluation of locomotor activity in open field test.

(A and D) Quantification of total time spent in freezing during open field test expressed in seconds in NCX1$^{+/+}$ (31s ±3, n = 19), NCX1^{ko} (29s ±5, n = 17) (A), NCX1.4$^{+/+}$ (42s ±8, n = 12), and NCX1.4^{over} (80s ±13, n = 13) mice (D) expressed in seconds. §, p<0,05 vs respective congenic wild-type mice, unpaired Student's t-test.

(B and E) Quantification of total time spent moving in open field test in NCX1$^{+/+}$ (215.35s ± 5.89, n = 19), NCX1^{ko} (196.71s ±7.01, n = 17) (B), NCX1.4$^{+/+}$ (218.41s ± 10.39, n = 12), and NCX1.4^{over} (181.65s ± 9.44, n = 13) (D) expressed in seconds. §, p<0,05 vs respective congenic wild-type mice, unpaired Student's t-test.

(C and F) Total distance travelled in the open field test in NCX1$^{+/+}$ (12.976m ±0.829, n = 19), NCX1^{ko} (10.957m ±0.653, n = 17) (C) NCX1.4$^{+/+}$ (218.41s ± 10.39, n = 12), and NCX1.4^{over} (181.65s ± 9.44, n = 13) (D) expressed in meters. §, p<0.05 vs respective congenic wild-type mice, unpaired student's t test.

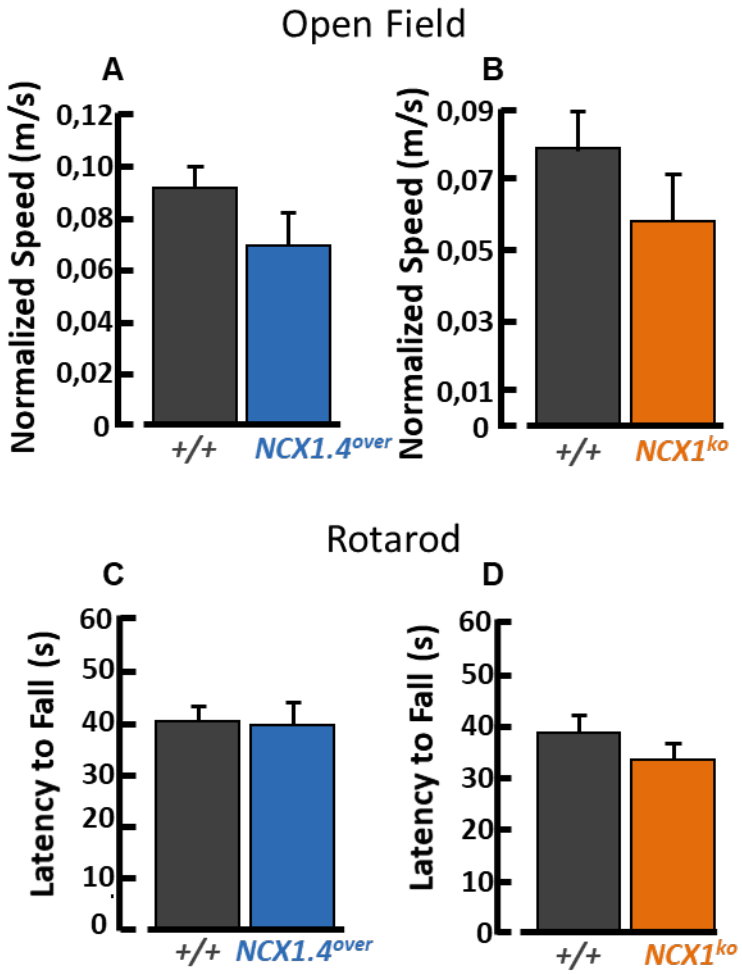

***Figure 44**. Evaluation of locomotor activity in open field and rotarod test.*

(A and B) Total distance travelled normalized for the total time spent moving expressed in meters per seconds in NCX1.4$^{+/+}$ (0.09 m/s ± 10.39, n = 12) and NCX1.4^{over} (181.65s ± 9.44, n = 13) (A), NCX1$^{+/+}$ (0.08 m/s ±0.01, n = 19) and NCX1^{ko} (0.06 m/s ± 0.06, n = 17) (B).

(C and D) Average of time to fall in test session of rotarod task of NCX1.4$^{+/+}$ (40.1s ±3.5, n = 13) and NCX1.4^{over} (40.2s ±4.3, n = 13) (C), NCX1$^{+/+}$ (39.1s ±3.3, n = 18) and NCX1^{ko} (34.2s ±2.9, n = 17) (D) mice expressed in seconds.

4.9 NCX1^{ko} SHOW IMPAIRED, WHEREAS NCX1.4^{over} MICE DISPLAY IMPROVED LONG-TERM MEMORY PERFORMANCE IN NOVEL OBJECT RECOGNITION, BARNES MAZE AND TRACE FEAR CONDITIONING TESTS

The novel object recognition test allowed to evaluate spatial learning and memory by quantifying the time spent exploring a novel object 1h or 24h after a training session. During the training session both *NCX1^{ko}* and *NCX1.4^{over}* showed no preference for one object over another as compared with their congenic wild-type, suggesting that all experimental groups were equally motivated to explore each object (Figure 45). *NCX1^{ko}* mice showed impaired spatial learning and memory as measured by the reduced time of exploration of novel object 1h and 24h after the training session (Figure 45 A). By contrast, *NCX1.4^{over}* mice displayed an enhancement of time spent exploring the novel object after 24h as compared with its congenic wild-type littermates (Figure 45 B). In Barnes maze test, during the learning phase (trials 1-5), *NCX1^{ko}* mice required more time than congenic wild-type to find the escape box in the last two days of the test (Figure 46 A). By contrast, *NCX1.4^{over}* mice showed a slightly amelioration of long-term spatial memory in the last two days of the learning phase (Figure 46 B).

In addition, in the memory recall phase (trial 6) the escape box was removed, the platform was virtually divided in 4 quadrants (Figure 47) and it was calculated the time spent in each one. NCX1^{ko} mice spent less time in the quadrant of the platform that contained the escape box during the learning phase (Q1) (Figure 47 A) and displayed a reduced time of permanence in the probe zone (Figure 47 B). Accordingly, *NCX1.4^{over}* spent more time in Q1 (Figure 47 C) and showed an increased time of permanence in the probe zone (Figure 47 D).

In the trace fear conditioning test, both *NCX1*^{ko} and *NCX1.4*^{over} mice increased freezing time after a single 0.8s foot-shock administered during the training trial (Figure 48).

In addition, *NCX1*^{ko} mice 30 minutes and 4 days after the training did not show any differences of freezing time than congenic wild-type in the same environment where they received the foot-shock (Figure 49 A and B). By contrast, *NCX1.4*^{over} mice significantly increased their freezing time 30 minutes after foot-shock in the context trial (Figure 49 C). This effect was almost lost at 4 days where only the time segment 180-240s was significant greater as compared with congenic wild-type (Figure 49 D).

However, in a new environment (cue trial) *NCX1*^{ko}, *NCX1.4*^{over} mice and their respective congenic wild-type displayed an increased freezing time when exposed to the conditioned stimulus (sound) (Figure 50 A and B).

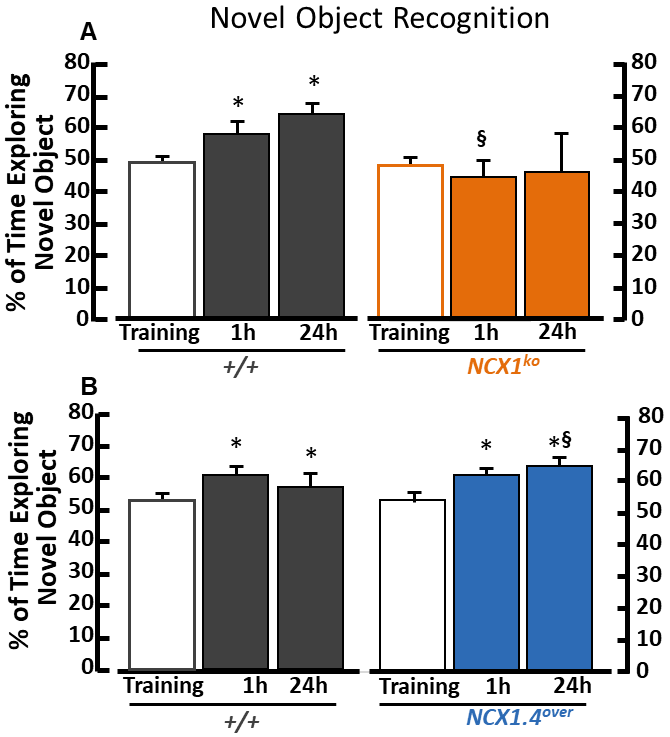

***Figure 45**. Impairment of memory performance for NCX1^{ko} and improvement of memory performance for NCX1.4^{over} mice in novel object recognition test*

*(A) Mean exploratory preference during the training session and each retention time (1h and 24h) in NCX1^{ko} (n = 16) and congenic wild-type (n = 17) mice. Data are expressed as time spent exploring novel object versus total exploring time for both objects. *, p < 0.05 vs respective group in training session, ANOVA followed by Student-Newman-Keuls post-hoc test; Genotype F(1,31)=7.7019, p=0.009; Time F(2,62)=6.1929, p=0.004; §, p < 0.05 vs congenic wild-type, Student's t test.*

*(B) Mean exploratory preference during the training session and each retention time (1h and 24h) in NCX1.4^{over} (n = 10) and congenic wild-type (n = 12) mice. Data are expressed as time spent exploring novel object versus total exploring time for both objects. *, p < 0.05 vs respective group in training session, ANOVA followed by Student-Newman-Keuls post-hoc test; Genotype F(1,20)=0.00001, p=0.994; Time F(2,40)=1.5667, p=0.221; §, p < 0.05 vs congenic wild-type, Student's t test.*

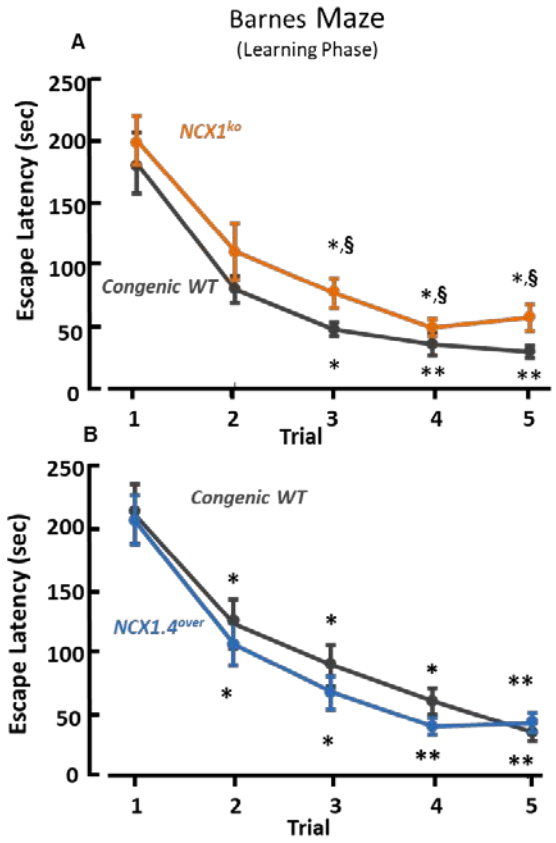

Figure 46. *NCX1^{ko} mice shows an impairment, whereas NCX1.4^{over} mice display an improvement, of spatial learning performance during trial 1-5 of Barnes Maze.*

*(A) Results of escape latency during trial 1-5 of Barnes maze in NCX1^{ko} (n = 17) and congenic wild-type (n = 18) mice. Data are expressed in seconds. *, p<0.05 vs trial 1, **, p<0.05 vs trial 2, ANOVA followed by Dunn's post-hoc test in all pairwise multiple comparison procedure; Genotype F(1,29) = 4.7223, p=0.038; Time F(4,116) = 35.0442, p=0.000; §, p<0.05 vs congenic wild-type, unpaired Student's t test.*

*(B) Results of escape latency during trial 1-5 of Barnes maze in NCX1.4^{over} (n = 20) and congenic wild-type (n = 19) mice. Data are expressed in seconds. *, p<0.05 vs trial 1, **, p<0.05 vs trial 2, ANOVA followed by Dunn's post-hoc test in all pairwise multiple comparison procedure. Genotype F(1,29) = 0.4033, p=0.530; Time F(4,116)=33.1803, p<0.0001.*

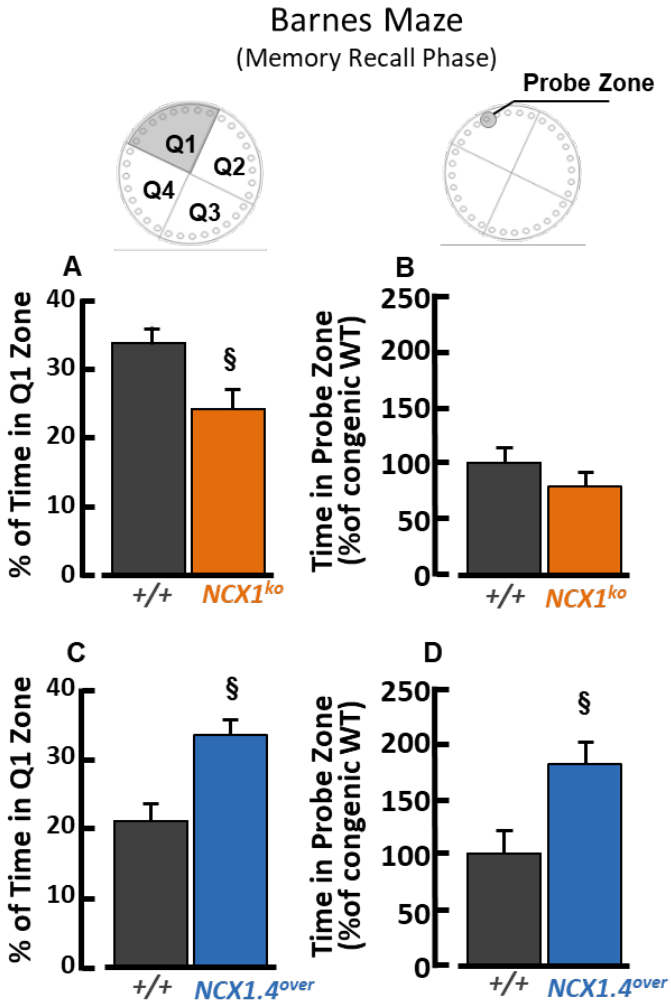

Figure 47. *NCX1^{ko} mice shows an impairment, whereas NCX1.4^{over} mice display an improvement, of spatial learning performance during trial 6 of Barnes Maze.*

(A and C) Quantification of the time spent by NCX1$^{+/+}$ (33.8% ±2.4, n = 18) and NCX1^{ko} (23.8% ±3.2, n = 17) (A), NCX1.4$^{+/+}$ (20.9% ±3.2, n = 19) and NCX1.4^{over} (33.4% ±2.4, n = 20) (C) mice in Q1 zone of the platform where before was located the escape box. Time is expressed as percentage of the total test duration. §, p < 0.05 vs respective congenic wild-type mice, unpaired Student's t test.

(B and D) Quantification of the time spent by NCX1$^{+/+}$ (100% ±11) and NCX1^{ko} (73% ±14) (B), NCX1.4$^{+/+}$ (100% ±22) and NCX1.4^{over} (183% ±18) (D) mice in the probe zone during trial 6, expressed as percentage of congenic wild-type mice. §, p < 0.05 vs respective congenic wild-type mice, unpaired Student's t test.

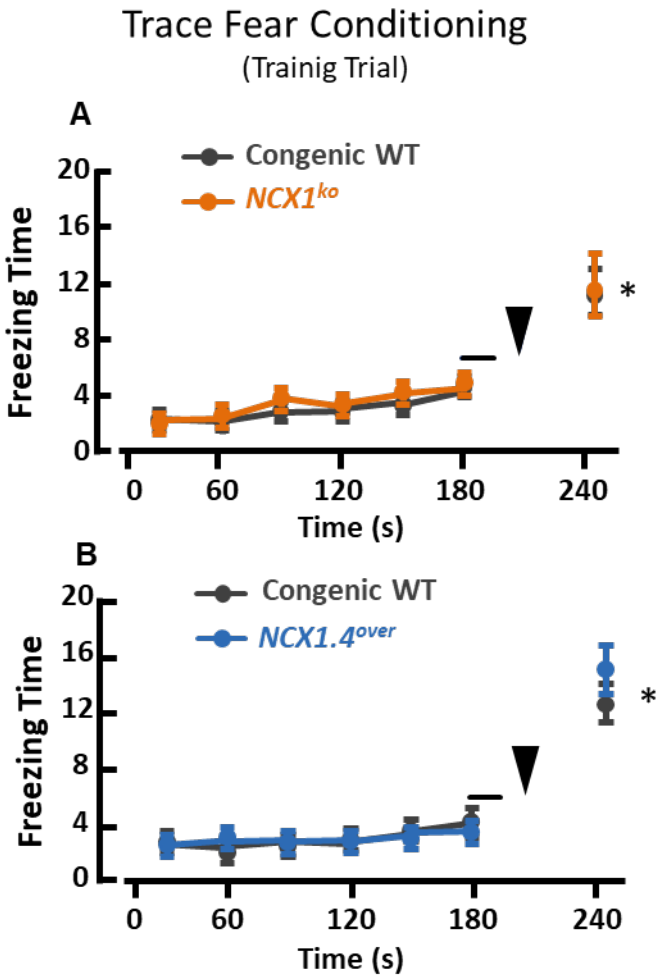

***Figure 48**. Training trial of the trace fear conditioning test.*

*(A and B) Freezing behavior of NCX1^{ko} (n = 27) and NCX1$^{+/+}$ (n = 28) mice (A), NCX1.4^{over} (n = 30) and NCX1.4$^{+/+}$ (n = 28) (B) during training session of trace fear conditioning test. Solid line indicates the duration of CS (tone, 15 s) and the triangle indicates US (foot-shock, 0.8s). *, p<0.05 vs all segments of time, ANOVA followed by Dunn's in all pairwise multiple comparison procedure.*

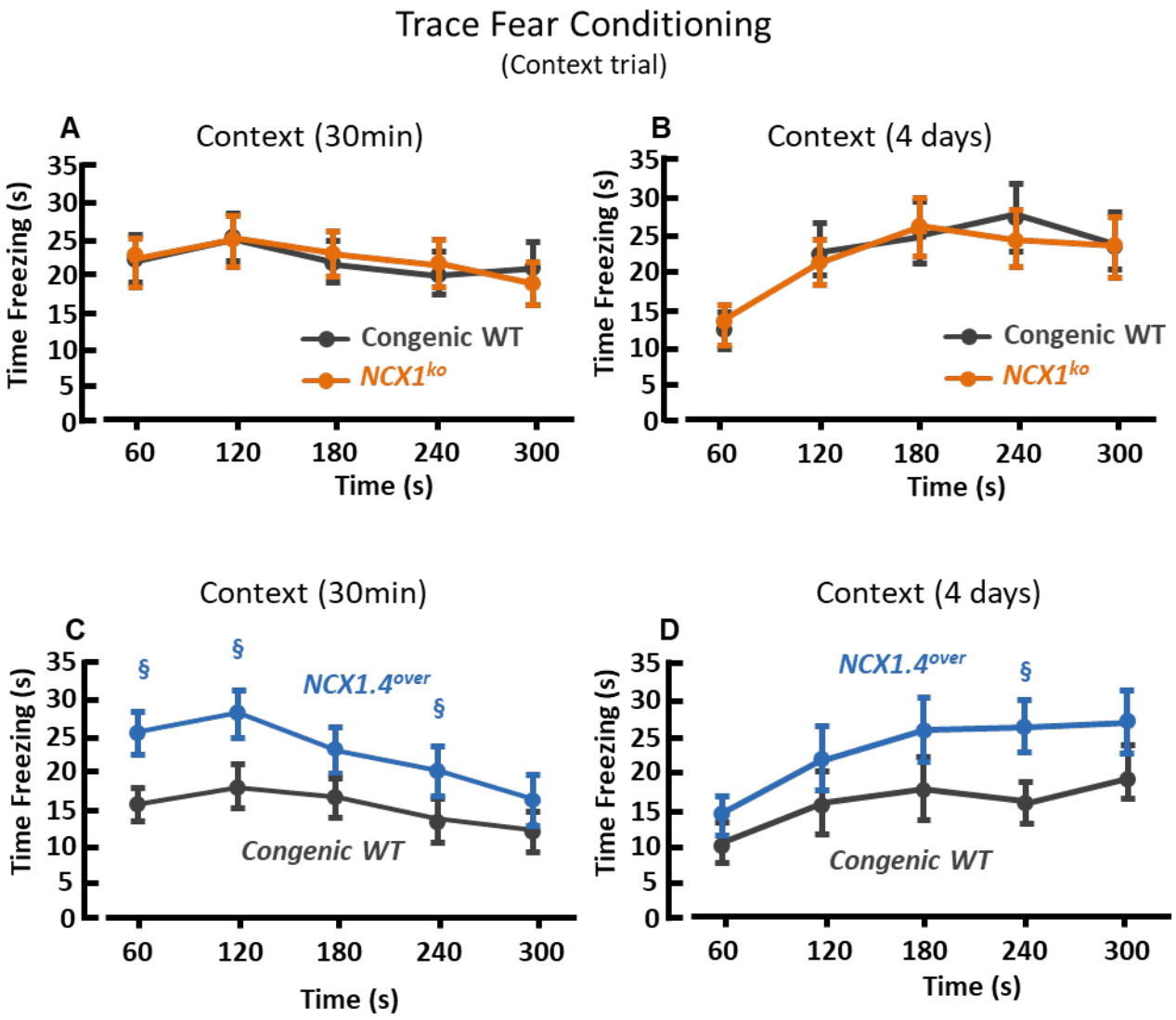

***Figure 49**. NCX1.4^{over} mice display an improvement of memory performance in context trials.*

(A and B) Quantification of freezing behavior in the same environment where NCX1^{ko} (n = 27) and NCX1$^{+/+}$ (n = 28) mice received the foot-shock 30 minutes before (A) and after 4 days (B) from the traing phase.

(C and D) Quantification of freezing behavior in the same environment where and NCX1.4^{over} (n = 30) and NCX1.4$^{+/+}$ (n = 28) mice received the foot-shock after 30 minutes (C) and after 4 days (D) from the traing phase. §, p<0.05 vs the corresponding time-segment of congenic wild-type, unpaired Student's t test.

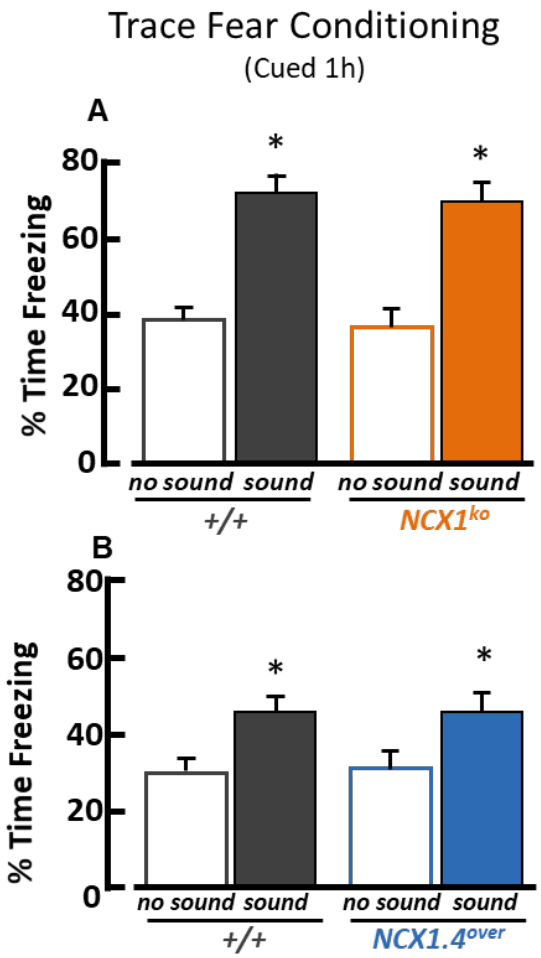

***Figure 50**. Cued trace fear conditioning.*

*(A and B) Quantification of freezing behavior, of NCX1$^{+/+}$ (38.3% ±3.2, 71.7% ±3.3, n = 28), NCX1^{ko} (37.4% ±3.7, 69.8% ±4.0, n = 27) (A), NCX1.4$^{+/+}$ (30.7% ±2.6, 45.2% ±3.8, n = 28), and NCX1.4^{over} (31.6% ±3.6, 45.8% ±4.1, n = 30) (B) 60 minutes after training, in a new environment (represented by empty histograms) and in a new environment in presence of the acoustic stimulus (represented by full histograms). Data are represented as percentage of the session duration (180s). *, p < 0.05 vs respective basal conditions, paired Student's t test*

4.10 NCX1.4^{over} MICE SHOW AN INCREASE IN ANXIETY SUSCEPTIBILITY IN OPEN FIELD, ZERO MAZE, BARNES MAZE, DARK/LIGHT BOX AND IN CORTICOSTERONE LEVELS

The behavior of genetically modified mice was analyzed in open field and zero maze tests to evaluate their anxiety levels under basal conditions. The open arena of open field was virtually subdivided in three concentric zones and it was calculated the time spent in each one. *NCX1*^{ko} mice showed no differences in the time spent in the external, intermediate and inner zone as compared to their congenic wild-type (Figure 51 A); whereas, *NCX1.4*^{over} significantly spent more time in the external zone and less time in central zone (Figure 51 B).

Moreover, *NCX1*^{ko} showed no differences in time spent in open zone of zero maze (Figure 52 A), whereas *NCX1.4*^{over} increased their residence time in the open zone (Figure 52 B), as compared to their respectively congenic wild-type littermates.

In addition, during the trial 6 of Barnes maze, *NCX1*^{ko} displayed increased time immobile in the inner zone of the platform (Figure 53 A and B) and *NCX1.4*^{over} mice stayed significantly longer time in the external zone of the platform as compared to their congenic wild-type (Figure 53 C and D).

In dark/light box test there was no difference in the total time spent in light zone between each genetic modified mouse, *NCX1*^{ko} (Figure 54Figure 53 A) and *NCX1.4*^{over} (Figure 54 B), and the respective wild-type group under basal conditions. However, *NCX1.4*^{over} mice displayed a significant reduction of the time spent in the light zone after a single foot-shock (Figure 54 B).

The corticosterone levels, evaluated in peripheral blood of mice, significantly reduced in *NCX1*^{ko} (Figure 55 A) and increased in *NCX1.4*^{over} (Figure 55 B) at 12:00 p.m. On

the other hand, no difference was observed at 6:00 a.m., 6:00 p.m. and 12:00 a.m. between genetic modified mice and their wild-type littermates.

In addition, all experimental groups increased their corticosterone levels 1h after foot-shock as compared to the pre-shock trial, whereas they returned to basal levels after 24h (Figure 56).

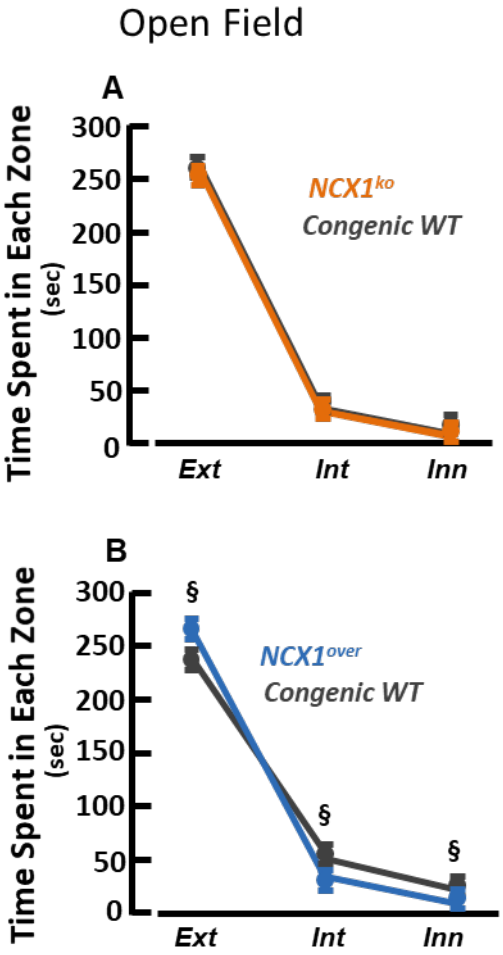

***Figure 51**. NCX1.4^{over} mice display an increased anxiety levels in open field test.*

(A and B) Quantification of the time spent by animals in three concentric areas measured as anxious behavior test of NCX1$^{+/+}$ (262s ±4, 31s ±3, 7s ±1, n = 19), NCX1^{ko} (258s ±5, 33s ±5, 9s ±1, n = 17) (A), NCX1.4$^{+/+}$ (238s ±10, 52s ±9, 10s ±1, n = 12) and NCX1.4^{over} (262s ±4, 32s ±4, 6s ±1, n = 13) mice (B). Time is expressed in seconds. §, p<0.05 vs respective congenic wild-type mice, unpaired Student's t test.

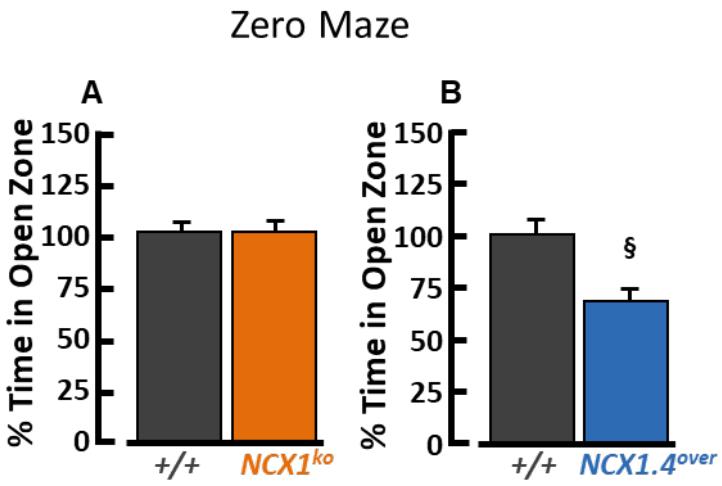

Figure 52. *NCX1.4^{over} mice display an increased anxiety levels in zero maze test.*

(A and B) Total time spent in the open zone of zero maze of NCX1$^{+/+}$ (100% ±6.4, n = 18), NCX1^{ko} (100% ±7.7, n = 17) (A), NCX1.4$^{+/+}$ (100% ±4.1, n = 12), and NCX1.4^{over} (67.9% ±6.2, n = 13) (B) mice expressed as percentage of respective congenic wild-type mice. §, p<0.05 vs respective congenic wild-type mice, unpaired Student's t test.

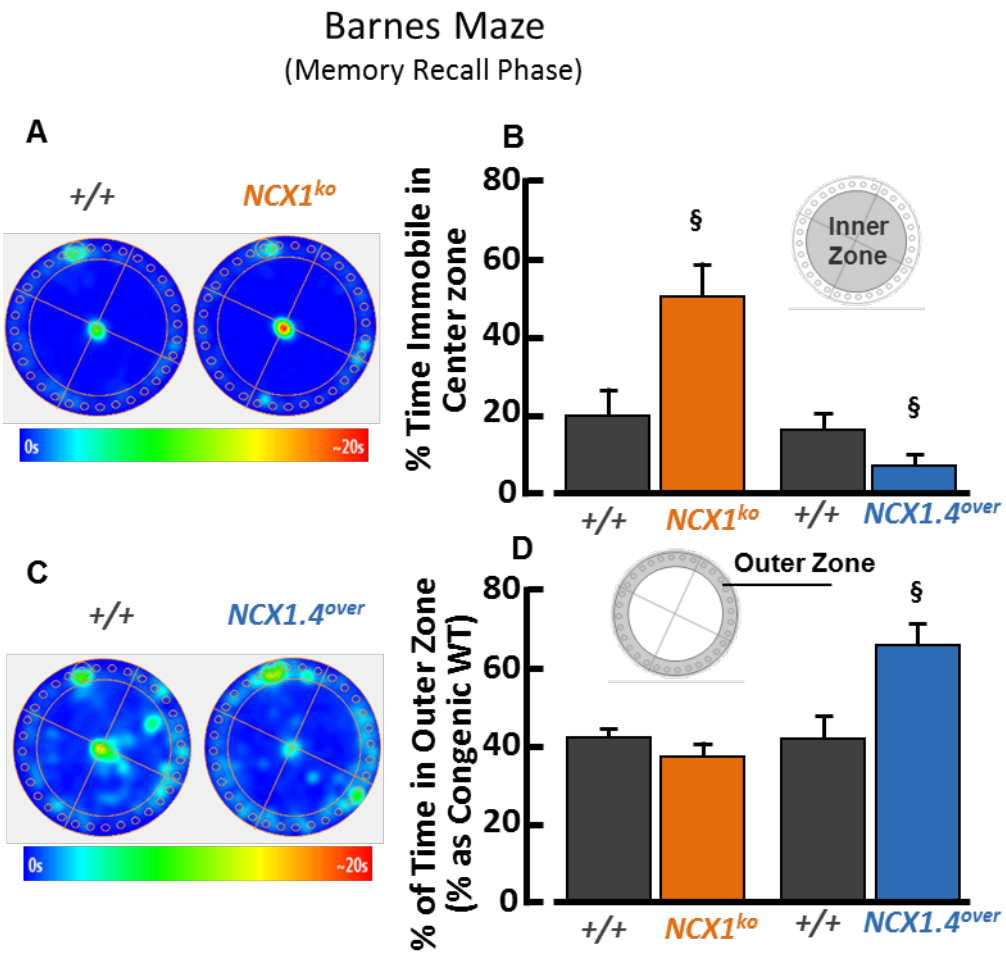

Figure 53. *NCX1.4^{over} mice increase anxiety levels during the trial 6 of Barnes maze test.*

(A and C) Heat maps of mouse position on Barnes maze platform for NCX1^{ko} (n = 17) and NCX1$^{+/+}$ (n = 18) (A), NCX1.4^{over} (n = 20) and NCX1.4$^{+/+}$ (n = 19) (C) mice.

(B) Quantification of the total immobile time spent by NCX1$^{+/+}$ (20.8s ±5.7), NCX1^{ko} (52.0 ±8.3), NCX1.4$^{+/+}$ (16.7s ±3.6), and NCX1.4^{over} (6.6s ±2.1) mice in the inner zone of Barnes maze platform during trial 6, expressed as percentage of test duration. §, p<0.05 vs respective congenic wild-type mice, unpaired Student's t test.

(D) Quantification of the total time spent by NCX1$^{+/+}$ (65.4s ±3.8), NCX1^{ko} (59.1 ±4.6), NCX1.4$^{+/+}$ (41.3% ±6.8), and NCX1.4^{over} (67.0s ±4.4) in the peripheral zone of Barnes maze platform during trial 6, expressed as percentage of congenic wild-type. §, p<0.05 vs respective congenic wild-type mice, unpaired Student's t test.

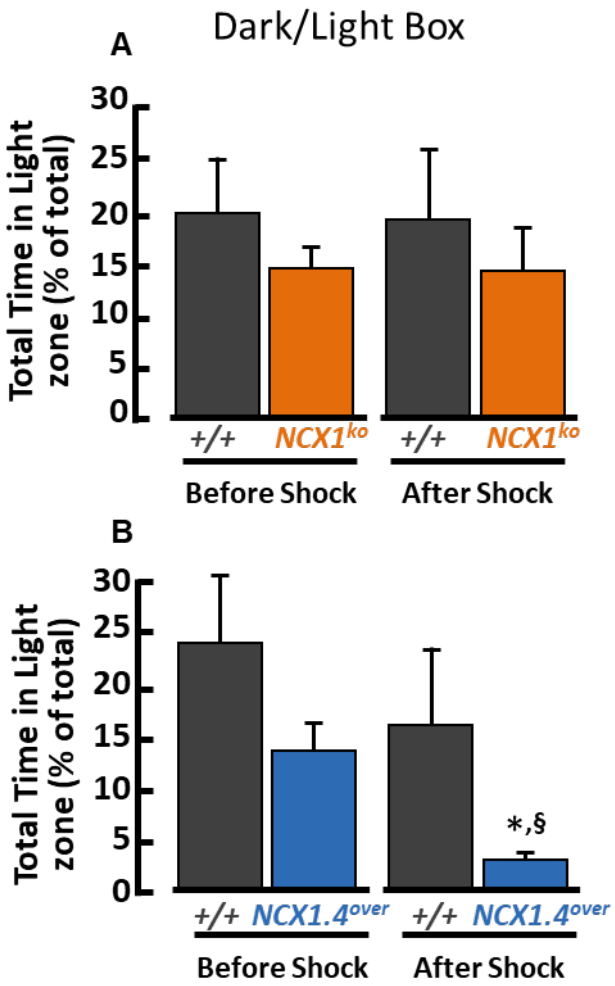

***Figure 54**. NCX1.4^{over} mice display an increased anxiety levels in dark-light box after foot-shock.*

(A) Quantification of total time spent in the light box by full body before the foot-shock (on the left) in NCX1$^{+/+}$ (21% ±4, n = 12), NCX1^{ko} (15% ±2, n = 10), and after foot-shock (on the right) in NCX1$^{+/+}$ (18% ±8, n = 12), NCX1^{ko} (14% ±5, n = 10). Time is expressed as percentage of total test time (5min).

*(B) Quantification of total time spent in the light box by full body before the foot-shock (on the left) in NCX1.4$^{+/+}$ (25% ±7, n = 10), and NCX1.4^{over} (14% ±3, n = 8) and after foot-shock (on the right) in NCX1.4$^{+/+}$ (17% ±7, n = 10) and NCX1.4^{over} (3% ±1, n = 8). Time is expressed as percentage of total test time (5min). §, p<0.05 vs congenic wild-type mice, unpaired Student's t test; *, p<0.05 vs respective non-shocked group, paired Student's t test.*

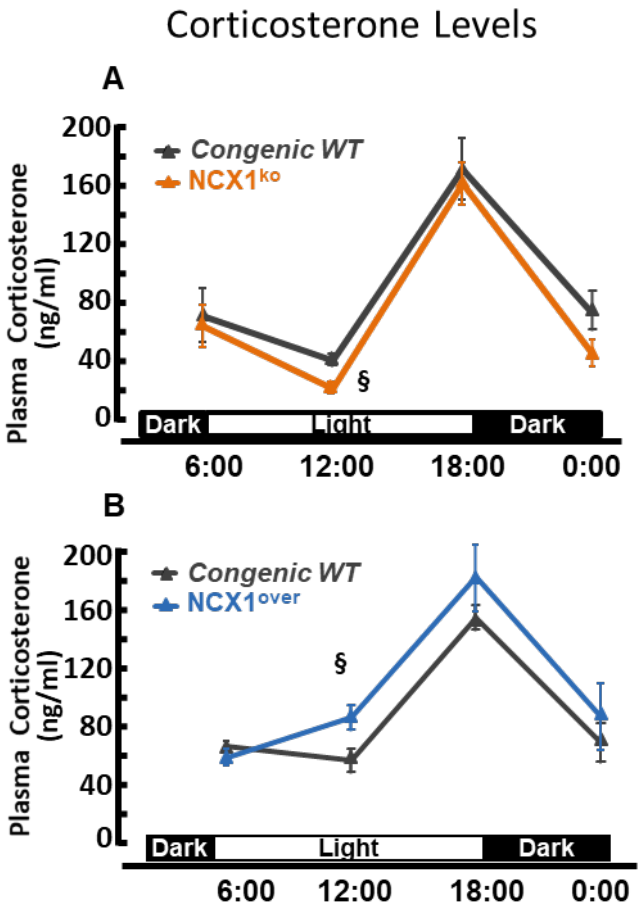

***Figure 55**. Corticosterone levels measured during circadian rhythm.*

(A and B) Concentrations of serum corticosterone in $NCX1^{ko}$ and $NCX1^{+/+}$ (A), $NCX1.4^{over}$ and $NCX1.4^{+/+}$ (B) male mice at different time of day. §, $p<0.05$ vs respective congenic wild-type mice, unpaired Student's t test

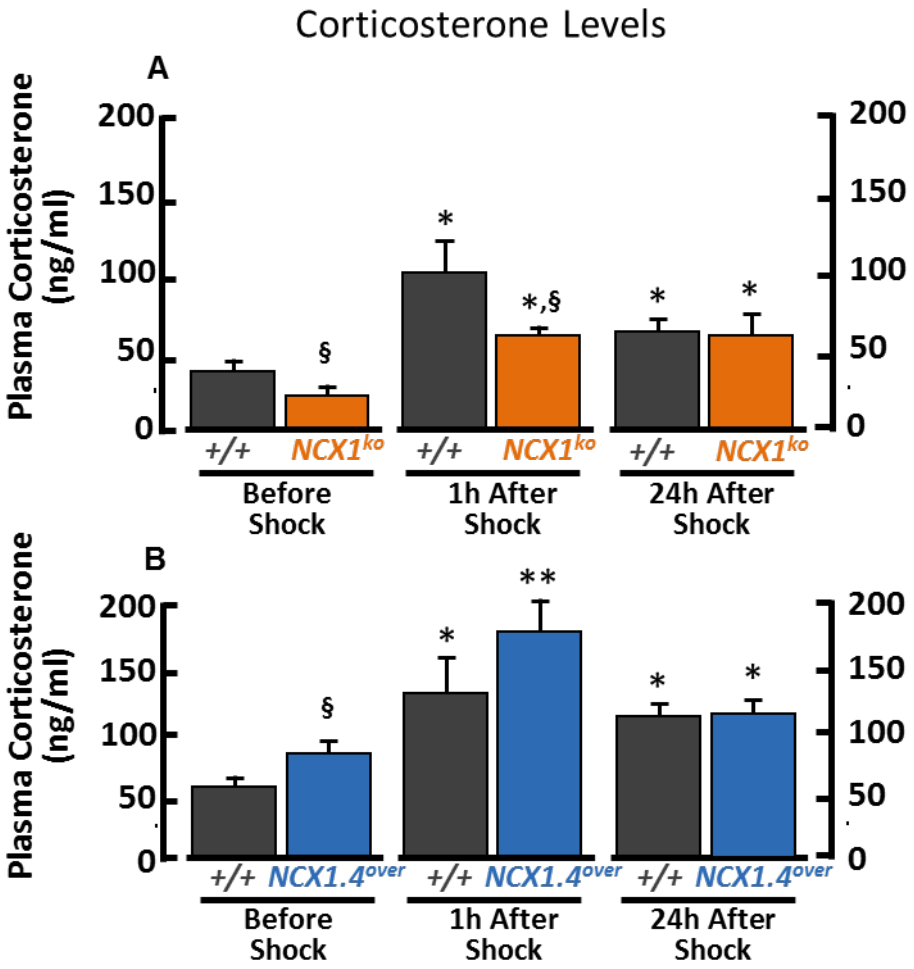

Figure 56. *Corticosterone levels measured after foot-shock.*

*(A) Concentration of serum corticosterone levels under basal conditions (12:00 p.m. of circadian rhythm) and 1h and 24h after the foot-shock in NCX1$^{+/+}$ and NCX1^{ko} mice. §, p<0.05 vs respective congenic wild-type mice, unpaired Student's t test. *, p<0.05 vs respective control group, unpaired Student's t test.*

*(B) Concentration of serum corticosterone levels under basal conditions (12:00 p.m. of circadian rhythm) and 1h and 24h after the foot-shock in NCX1.4$^{+/+}$ and NCX1.4^{over} mice. §, p<0.05 vs respective congenic wild-type mice, unpaired Student's t test. *, p<0.05 vs respective control group, unpaired Student's t test, **, p<0.05 vs respective control group at 24h after foot-shock.*

5. DISCUSSION

The main conclusions of the present study are: (1) to have designed, synthetized and characterized a novel potent activator of NCX1, named compound 2; (2) NCX1 plays a role in some cognition processes such as spatial memory and anxiety response.

5.1 THE ADDITION OF CLORYDE IN POSITION 2 ON NEUROUNINA 1 SCAFFOLD LEDS TO THE GENERATION OF A NOVEL POTENT ACTIVATOR OF NCX1

Different modifications on the chemical backbone of neurounina-1 were made to obtain novel compounds able to selectively affect each of the three different isoforms of NCX. From a preliminary screening, based on $^{45}Ca^{2+}$ radiotracer assay and fura-2 technique (Figure 2), three groups of modifications emerged as most promising: the addition of chloride in position 2 or 7 and the elongation of molecular chain in position 1 (Figure 1). In particular, molecules characterized by addition of chloride residue, compounds 2 and 3, showed an increased selectivity on NCX1 activity; derivatives generated by elongation of molecular chain in position 1, compounds II and IX, displayed inhibitory effects on NCX2 activity; compound III, generated by elongation of molecular chain in position 1, was chosen for its activator effects on NCX3 activity. More detailed experiments, such as concentration-effect curves, revealed that compound 2, was the most potent and selective modulator of NCX1 (Figure 3), whereas the other four compounds showed weak efficacy to regulate the activity of each NCX isoforms.

5.2 COMPOUND 2 AMELIORATES INDICES OF SPATIAL LEARNING AND MEMORY

The effects of the five selected compounds were assessed in behavioral tests specific for cognition processes evaluation since some studies demonstrate importance of NCX2 and NCX3 in learning and memory performance (Jeon et al., 2003; Molinaro et al., 2011). None of the new compounds showed neither *in vitro* toxicity, as measured by cell viability after 10 nM or 10 μM incubation, nor *in vivo* toxicity measured by body weight loss after one and two weeks of treatment (Figure 6 A and B).

In novel object recognition test, one of the most common behavioral test used for learning and memory performance (Ennaceur and Delacour, 1988; Leger et al., 2013), compound IX ameliorated long term memory (Figure 11) accordingly to the results obtained in NCX2 knock-out mice (Jeon et al., 2003). Moreover, this compound also induced an increase of novel object exploration 1h after the training session as compared with vehicle-treated mice; this could be due to the effects of the temporally inhibition of NCX2 that increases paired pulse facilitation (PPF) and transient enhancement of neurotransmitter release; there are some pieces of evidence demonstrating that during to the novel object test there is an increase of neurotransmitter release in hippocampus during novel object recognition phase (Stanley et al., 2012).

Compound III, the one selected as activator of NCX3, didn't show any amelioration in novel object recognition test (Figure 12) probably because of its weak, and less selective, effects on NCX3 activity.

Interestingly, mice treated with compound 2 increased the exploration time of novel object in both 1h and 24h trials, even if, until now, there is no evidence for the role played by NCX1 in learning and memory processes (Figure 10).

None of the selected compounds showed amelioration of escape time in Barnes maze test during learning phase. However, mice treated with compound IX or 2 displayed an amelioration of spatial learning and memory performance during the memory recall phase. In particular, compound IX-treated mice increased the time spent in the probe zone suggesting improvement of spatial memory as compared with vehicle-treated mice (Figure 17). In addition, compound 2-treated mice displayed an increase of: (a) total time spent in the quadrant where was located the escape box (Q1), (b) total time spent in the probe zone, (c) number of entries in probe zone (Figure 16). Taken together these results suggest a strong consolidation of spatial memory for mice treated with compound 2.

Also results obtained in trace fear conditioning test confirmed the consolidation of spatial memory for mice treated with compound 2 during the context trial performed 30 minutes after the training, whereas compound IX didn't induce amelioration of memory (Figure 19) possibly because of the low levels of NCX2 expression in the amygdala, a crucial brain region for this test (Kwapis et al., 2011; Baysinger et al., 2012; Gilmartin et al., 2012).

In conclusion of the first part of the present study, compound 2 was found to be the most promising, among all the new generated compounds, since it was able to ameliorate spatial learning and memory performance in mice. In addition, this could represent a starting point for the study of the role played by NCX1 in these cognition processes.

5.3 THE INCREASE OF NCX1 EXPRESSION/ACTIVITY INDUCES ACTIVATION OF CREB AND CAMKII

To deeper investigate the improvement of memory dependent on NCX1 expression/activity we analyzed typical molecular markers of memory, such as pCREB and pCAMKII_T286 in cortex, hippocampus and amygdala of all mouse groups. In particular, results obtained in NCX1 genetically modified mice suggest that NCX1 positively correlates with the activation of CaMKII/CREB molecular markers, possibly via intracellular Ca^{2+}-dependent pathways (Ma et al., 2015). In addition, the activation of CREB, observed in the amygdala of *NCX1.4*^{over} mice could be ascribed to the CaMKII activity, where they participate in a memory reconsolidation process (Jarome et al., 2016).

5.4 NCX1 OVEREXPRESSION IMPROVES, WHEREAS NCX1 KNOCKOUT IMPAIRS LEARNING AND MEMORY PERFORMANCE

Since it was observed that the activation of NCX1 improved spatial learning and memory performance and the increase of NCX1 activity or expression enhanced the phosphorylation of markers of memory, the role of NCX1 played in learning and memory process was deeper investigated. *NCX1.4*^{over} and *NCX1*^{ko} mice were subjected to several behavioral tests. Their motor coordination and locomotor activity were evaluated in open field and rotarod test (Bohlen et al., 2009; Tatem et al., 2014). Among these mouse groups, only *NCX1.4*^{over} mice significantly travelled less distance (Figure 43), probably because they spent more time in a freezing status since no differences was observed in normalized speed, calculated as the total

distance travelled during time mobile (Figure 44). Moreover, rotarod test displayed no differences in time latency to fall for all genetic modified animals.

In novel object recognition test *NCX1*^{ko} mice showed an impairment of memory hippocampus dependent as measured by novel object recognition test (Antunes and Biala, 2012), whereas *NCX1.4*^{over} mice, in the same test showed a slight amelioration of reconsolidation memory. In addition, *NCX1.4*^{over} mice showed an increased the time spent in the Q1 and the specific area in which previously was located the escape box suggesting a strong consolidation of spatial memory (Figure 47) during the memory recall phase. Opposite results were obtained with *NCX1*^{ko} mice under the same conditions if compared with their congenic wild-type controls. In addition, these results were reinforced by similar data obtained in trace fear conditioning test suggesting an improvement of spatial memory for *NCX1.4*^{over} mice. In line with these data, C57BL/6 mice treated with compound 2 showed an improvement of spatial memory under the same conditions. Nobably, both genetically modified mice for NCX1 and mice treated with compound 2 showed a significant increase of freezing time only in the same context where they received the footshock delivery 30 minutes before if compared with respective control group. On the other hand, the effect was almost lost at 4 days after footshock delivery. It is should be mentioned that the contextual memory evaluated by trace fear conditioning is dependent by the neural communication among amygdala, hippocampus and medial prefrontal cortex (Maren et al., 2013), three brain regions of *NCX1.4*^{over} mice in which there is a significant increase of NCX1 expression (Figure 30).

5.5 NCX1 INCREASES ANXIETY LEVELS

An increase of anxiety levels was observed in *NCX1.4*^{over} mice subjected to open field, zero maze, Barnes maze and dark/light box test. In particular, *NCX1.4*^{over} mice spent significantly more time in the external zone in open field, avoiding the open zone in the zero maze test and the central region of Barnes maze platform during trial 6. On the other hand, these results were not observed in C57BL/6 mice treated with compound 2 probably because the acute effect compared to the chronic increased expression/activity of NCX1 in genetic modified mice. Thus, in the case of the treatment with compound 2 it would be necessary a stimulus for the occurrence of anxiety dependent by NCX1. In fact, it was observed an increase of anxiety levels comparable for both mouse groups in the dark/light box test performed after the foot-shock delivery.

6. REFERENCES

Aneiros E, Philipp S, Lis A, Freichel M, Cavalie A (2005) Modulation of Ca2+ signaling by Na+/Ca2+ exchangers in mast cells. J Immunol 174:119-130.

Annunziato L, Pignataro G, Di Renzo GF (2004) Pharmacology of brain Na+/Ca2+ exchanger: from molecular biology to therapeutic perspectives. Pharmacol Rev 56:633-654.

Annunziato L, Pignataro G, Boscia F, Sirabella R, Formisano L, Saggese M, Cuomo O, Gala R, Secondo A, Viggiano D, Molinaro P, Valsecchi V, Tortiglione A, Adornetto A, Scorziello A, Cataldi M, Di Renzo GF (2007) NCX1, ncx2, and ncx3 gene product expression and function in neuronal anoxia and brain ischemia. Ann N Y Acad Sci 1099:413-426.

Antunes M, Biala G (2012) The novel object recognition memory: neurobiology, test procedure, and its modifications. Cogn Process 13:93-110.

Anzilotti S, Tornincasa M, Gerlini R, Conte A, Brancaccio P, Cuomo O, Bianco G, Fusco A, Annunziato L, Pignataro G, Pierantoni GM (2015) Genetic ablation of homeodomain-interacting protein kinase 2 selectively induces apoptosis of cerebellar Purkinje cells during adulthood and generates an ataxic-like phenotype. Cell Death Dis 6:e2004.

Anzilotti S, Brancaccio P, Simeone G, Valsecchi V, Vinciguerra A, Secondo A, Petrozziello T, Guida N, Sirabella R, Cuomo O, Cepparulo P, Herchuelz A, Amoroso S, Di Renzo G, Annunziato L, Pignataro G (2018) Preconditioning, induced by sub-toxic dose of the neurotoxin L-BMAA, delays ALS progression in mice and prevents Na. Cell Death Dis 9:206.

Bach ME, Hawkins RD, Osman M, Kandel ER, Mayford M (1995) Impairment of spatial but not contextual memory in CaMKII mutant mice with a selective loss of hippocampal LTP in the range of the theta frequency. Cell 81:905-915.

Bangasser DA, Waxler DE, Santollo J, Shors TJ (2006) Trace conditioning and the hippocampus: the importance of contiguity. J Neurosci 26:8702-8706.

Baysinger AN, Kent BA, Brown TH (2012) Muscarinic receptors in amygdala control trace fear conditioning. PLoS One 7:e45720.

Blaustein MP, Lederer WJ (1999) Sodium/calcium exchange: its physiological implications. Physiol Rev 79:763-854.

Bliss TV, Gardner-Medwin AR (1973) Long-lasting potentiation of synaptic transmission in the dentate area of the unanaestetized rabbit following stimulation of the perforant path. J Physiol 232:357-374.

Bliss TV, Collingridge GL (1993) A synaptic model of memory: long-term potentiation in the hippocampus. Nature 361:31-39.

Bohlen M, Cameron A, Metten P, Crabbe JC, Wahlsten D (2009) Calibration of rotational acceleration for the rotarod test of rodent motor coordination. J Neurosci Methods 178:10-14.

Boscia F, Besozzi G, Recchimurzo N, Sborgia L, Furino C (2011) Cauterization for the prevention of leaking sclerotomies after 23-gauge transconjunctival pars plana vitrectomy: an easy way to obtain sclerotomy closure. Retina 31:988-990.

Boscia F, Gala R, Pannaccione A, Secondo A, Scorziello A, Di Renzo G, Annunziato L (2009) NCX1 expression and functional activity increase in microglia invading the infarct core. Stroke 40:3608-3617.

Bouron A, Reuter H (1996) A role of intracellular Na+ in the regulation of synaptic transmission and turnover of the vesicular pool in cultured hippocampal cells. Neuron 17:969-978.

Bourtchuladze R, Frenguelli B, Blendy J, Cioffi D, Schutz G, Silva AJ (1994) Deficient long-term memory in mice with a targeted mutation of the cAMP-responsive element-binding protein. Cell 79:59-68.

Bridge JH, Smolley JR, Spitzer KW (1990) The relationship between charge movements associated with ICa and INa-Ca in cardiac myocytes. Science 248:376-378.

Canitano A, Papa M, Boscia F, Castaldo P, Sellitti S, Taglialatela M, Annunziato L (2002) Brain distribution of the Na+/Ca2+ exchanger-encoding genes NCX1, NCX2, and NCX3 and their related proteins in the central nervous system. Ann N Y Acad Sci 976:394-404.

Carlezon WA, Jr., Duman RS, Nestler EJ (2005) The many faces of CREB. Trends Neurosci 28:436-445.

Cho CH, Kim SS, Jeong MJ, Lee CO, Shin HS (2000) The Na+ -Ca2+ exchanger is essential for embryonic heart development in mice. Mol Cells 10:712-722.

Cobar LF, Yuan L, Tashiro A (2017) Place cells and long-term potentiation in the hippocampus. Neurobiol Learn Mem 138:206-214.

Crespo LM, Grantham CJ, Cannell MB (1990) Kinetics, stoichiometry and role of the Na-Ca exchange mechanism in isolated cardiac myocytes. Nature 345:618-621.

D'Adamo P, Welzl H, Papadimitriou S, Raffaele di Barletta M, Tiveron C, Tatangelo L, Pozzi L, Chapman PF, Knevett SG, Ramsay MF, Valtorta F, Leoni C, Menegon A, Wolfer DP, Lipp HP, Toniolo D (2002) Deletion of the mental retardation gene Gdi1 impairs associative memory and alters social behavior in mice. Hum Mol Genet 11:2567-2580.

Desmedt A, Marighetto A, Garcia R, Jaffard R (2003) The effects of ibotenic hippocampal lesions on discriminative fear conditioning to context in mice: impairment or facilitation depending on the associative value of a phasic explicit cue. Eur J Neurosci 17:1953-1963.

Du K, Montminy M (1998) CREB is a regulatory target for the protein kinase Akt/PKB. J Biol Chem 273:32377-32379.

Ennaceur A, Delacour J (1988) A new one-trial test for neurobiological studies of memory in rats. 1: Behavioral data. Behav Brain Res 31:47-59.

Figurov A, Pozzo-Miller LD, Olafsson P, Wang T, Lu B (1996) Regulation of synaptic responses to high-frequency stimulation and LTP by neurotrophins in the hippocampus. Nature 381:706-709.

Fujioka Y, Hiroe K, Matsuoka S (2000) Regulation kinetics of Na+-Ca2+ exchange current in guinea-pig ventricular myocytes. J Physiol 529:611-623.

Fukunaga K, Muller D, Miyamoto E (1995) Increased phosphorylation of Ca2+/calmodulin-dependent protein kinase II and its endogenous substrates in the induction of long-term potentiation. J Biol Chem 270:6119-6124.

Fukunaga K, Stoppini L, Miyamoto E, Muller D (1993) Long-term potentiation is associated with an increased activity of Ca2+/calmodulin-dependent protein kinase II. J Biol Chem 268:7863-7867.

Giampà C, Laurenti D, Anzilotti S, Bernardi G, Menniti FS, Fusco FR (2010) Inhibition of the striatal specific phosphodiesterase PDE10A ameliorates striatal and cortical pathology in R6/2 mouse model of Huntington's disease. PLoS One 5:e13417.

Giese KP, Mizuno K (2013) The roles of protein kinases in learning and memory. Learn Mem 20:540-552.

Gilmartin MR, Kwapis JL, Helmstetter FJ (2012) Trace and contextual fear conditioning are impaired following unilateral microinjection of muscimol in the ventral hippocampus or amygdala, but not the medial prefrontal cortex. Neurobiol Learn Mem 97:452-464.

Grynkiewicz G, Poenie M, Tsien RY (1985) A new generation of Ca2+ indicators with greatly improved fluorescence properties. J Biol Chem 260:3440-3450.

Gunthorpe MJ, Smith GD, Davis JB, Randall AD (2001) Characterisation of a human acid-sensing ion channel (hASIC1a) endogenously expressed in HEK293 cells. Pflugers Arch 442:668-674.

Hasegawa H, Muraoka M, Matsui K, Kojima A (2003) Discovery of a novel potent Na+/Ca2+ exchanger inhibitor: design, synthesis and structure-activity relationships of 3,4-dihydro-2(1H)-quinazolinone derivatives. Bioorg Med Chem Lett 13:3471-3475.

HEBB CO, KONZETT H (1949) The effect of certain analgesic drugs on synaptic transmission as observed in the perfused superior cervical ganglion of the cat. Q J Exp Physiol Cogn Med Sci 35:213-217.

Herchuelz A, Diaz-Horta O, van Eylen F (2002) Na/Ca exchange and Ca2+ homeostasis in the pancreatic beta-cell. Diabetes Metab 28:3S54-60; discussion 53S108-112.

Huerta PT, Sun LD, Wilson MA, Tonegawa S (2000) Formation of temporal memory requires NMDA receptors within CA1 pyramidal neurons. Neuron 25:473-480.

Iwamoto T, Kita S, Katsuragi T (2004) Endothelin-1 aggravates hypoxia/reoxygenation-induced injury in renal epithelial cells through the activation of a Na+/Ca2+ exchanger. J Cardiovasc Pharmacol 44 Suppl 1:S462-466.

James W (1890) Origin of Right-handedness. Science 16:275.

Jarome TJ, Ferrara NC, Kwapis JL, Helmstetter FJ (2016) CaMKII regulates proteasome phosphorylation and activity and promotes memory destabilization following retrieval. Neurobiol Learn Mem 128:103-109.

Jeon D, Yang YM, Jeong MJ, Philipson KD, Rhim H, Shin HS (2003) Enhanced learning and memory in mice lacking Na+/Ca2+ exchanger 2. Neuron 38:965-976.

Jimenez JC, Su K, Goldberg AR, Luna VM, Biane JS, Ordek G, Zhou P, Ong SK, Wright MA, Zweifel L, Paninski L, Hen R, Kheirbek MA (2018) Anxiety Cells in a Hippocampal-Hypothalamic Circuit. Neuron 97:670-683.e676.

Kandel ER (2012) The molecular biology of memory: cAMP, PKA, CRE, CREB-1, CREB-2, and CPEB. Mol Brain 5:14.

Kang TM, Hilgemann DW (2004) Multiple transport modes of the cardiac Na+/Ca2+ exchanger. Nature 427:544-548.

Kassed CA, Herkenham M (2004) NF-kappaB p50-deficient mice show reduced anxiety-like behaviors in tests of exploratory drive and anxiety. Behav Brain Res 154:577-584.

Kazlauckas V, Schuh J, Dall'Igna OP, Pereira GS, Bonan CD, Lara DR (2005) Behavioral and cognitive profile of mice with high and low exploratory phenotypes. Behav Brain Res 162:272-278.

Koushik SV, Wang J, Rogers R, Moskophidis D, Lambert NA, Creazzo TL, Conway SJ (2001) Targeted inactivation of the sodium-calcium exchanger (NCX1) results in the lack of a heartbeat and abnormal myofibrillar organization. FASEB J 15:1209-1211.

Kulkarni SK, Singh K, Bishnoi M (2007) Elevated zero maze: a paradigm to evaluate antianxiety effects of drugs. Methods Find Exp Clin Pharmacol 29:343-348.

Kwapis JL, Jarome TJ, Schiff JC, Helmstetter FJ (2011) Memory consolidation in both trace and delay fear conditioning is disrupted by intra-amygdala infusion of the protein synthesis inhibitor anisomycin. Learn Mem 18:728-732.

Larson J, Wong D, Lynch G (1986) Patterned stimulation at the theta frequency is optimal for the induction of hippocampal long-term potentiation. Brain Res 368:347-350.

Leger M, Quiedeville A, Bouet V, Haelewyn B, Boulouard M, Schumann-Bard P, Freret T (2013) Object recognition test in mice. Nat Protoc 8:2531-2537.

Li Z, Matsuoka S, Hryshko LV, Nicoll DA, Bersohn MM, Burke EP, Lifton RP, Philipson KD (1994) Cloning of the NCX2 isoform of the plasma membrane Na(+)-Ca2+ exchanger. J Biol Chem 269:17434-17439.

Lo Iacono L, Gross C (2008) Alpha-Ca2+/calmodulin-dependent protein kinase II contributes to the developmental programming of anxiety in serotonin receptor 1A knock-out mice. J Neurosci 28:6250-6257.

Lu YM, Jia Z, Janus C, Henderson JT, Gerlai R, Wojtowicz JM, Roder JC (1997) Mice lacking metabotropic glutamate receptor 5 show impaired learning and reduced CA1 long-term potentiation (LTP) but normal CA3 LTP. J Neurosci 17:5196-5205.

Lüscher C, Nicoll RA, Malenka RC, Muller D (2000) Synaptic plasticity and dynamic modulation of the postsynaptic membrane. Nat Neurosci 3:545-550.

Lynch MA (2004) Long-term potentiation and memory. Physiol Rev 84:87-136.

Ma H, Li B, Tsien RW (2015) Distinct roles of multiple isoforms of CaMKII in signaling to the nucleus. Biochim Biophys Acta 1853:1953-1957.

Maine de Biran P (1929) The influence of habit on the faculty of thinking, (first published in 1804) Edition: Baltimore.

Maren S, Phan KL, Liberzon I (2013) The contextual brain: implications for fear conditioning, extinction and psychopathology. Nat Rev Neurosci 14:417-428.

Matthews BR (2015) Memory dysfunction. Continuum (Minneap Minn) 21:613-626.

McEchron MD, Bouwmeester H, Tseng W, Weiss C, Disterhoft JF (1998) Hippocampectomy disrupts auditory trace fear conditioning and contextual fear conditioning in the rat. Hippocampus 8:638-646.

Milner B, Taylor L, Sperry RW (1968) Lateralized suppression of dichotically presented digits after commissural section in man. Science 161:184-186.

Miyamoto E (2006) Molecular mechanism of neuronal plasticity: induction and maintenance of long-term potentiation in the hippocampus. J Pharmacol Sci 100:433-442.

Mizuno M, Yamada K, Maekawa N, Saito K, Seishima M, Nabeshima T (2002) CREB phosphorylation as a molecular marker of memory processing in the hippocampus for spatial learning. Behav Brain Res 133:135-141.

Molinaro P, Pannaccione A, Sisalli MJ, Secondo A, Cuomo O, Sirabella R, Cantile M, Ciccone R, Scorziello A, di Renzo G, Annunziato L (2015) A New Cell-penetrating Peptide That Blocks the Autoinhibitory XIP Domain of NCX1 and Enhances Antiporter Activity. Mol Ther 23:465-476.

Molinaro P, Viggiano D, Nistico R, Sirabella R, Secondo A, Boscia F, Pannaccione A, Scorziello A, Mehdawy B, Sokolow S, Herchuelz A, Di Renzo GF, Annunziato L (2011) Na+ -Ca2+ exchanger (NCX3) knock-out mice display an impairment in hippocampal long-term potentiation and spatial learning and memory. J Neurosci 31:7312-7321.

Molinaro P, Sirabella R, Pignataro G, Petrozziello T, Secondo A, Boscia F, Vinciguerra A, Cuomo O, Philipson KD, De Felice M, Di Lauro R, Di Renzo G, Annunziato L (2016) Neuronal NCX1 overexpression induces stroke resistance while knockout induces vulnerability via Akt. J Cereb Blood Flow Metab 36:1790-1803.

Molinaro P, Cuomo O, Pignataro G, Boscia F, Sirabella R, Pannaccione A, Secondo A, Scorziello A, Adornetto A, Gala R, Viggiano D, Sokolow S, Herchuelz A, Schurmans S, Di Renzo G, Annunziato L (2008a) Targeted disruption of Na+/Ca2+ exchanger 3 (NCX3) gene leads to a worsening of ischemic brain damage. Journal of Neuroscience 28:1179-1184.

Molinaro P, Cuomo O, Pignataro G, Boscia F, Sirabella R, Pannaccione A, Secondo A, Scorziello A, Adornetto A, Gala R, Viggiano D, Sokolow S, Herchuelz A, Schurmans S, Di Renzo G, Annunziato L (2008b) Targeted disruption of Na+/Ca2+ exchanger 3 (NCX3) gene leads to a worsening of ischemic brain damage. J Neurosci 28:1179-1184.

Molinaro P, Cantile M, Cuomo O, Secondo A, Pannaccione A, Ambrosino P, Pignataro G, Fiorino F, Severino B, Gatta E, Sisalli MJ, Milanese M, Scorziello A, Bonanno G, Robello M, Santagada V, Caliendo G, Di Renzo G, Annunziato L (2013) Neurounina-1, a novel compound that increases Na+/Ca2+ exchanger activity, effectively protects against stroke damage. Mol Pharmacol 83:142-156.

Moser MB, Rowland DC, Moser EI (2015) Place cells, grid cells, and memory. Cold Spring Harb Perspect Biol 7:a021808.

Nicoll DA, Longoni S, Philipson KD (1990) Molecular cloning and functional expression of the cardiac sarcolemmal Na(+)-Ca2+ exchanger. Science 250:562-565.

Nicoll DA, Quednau BD, Qui Z, Xia YR, Lusis AJ, Philipson KD (1996) Cloning of a third mammalian Na+-Ca2+ exchanger, NCX3. J Biol Chem 271:24914-24921.

Otto T, Eichenbaum H, Wiener SI, Wible CG (1991) Learning-related patterns of CA1 spike trains parallel stimulation parameters optimal for inducing hippocampal long-term potentiation. Hippocampus 1:181-192.

Pannaccione A, Castaldo P, Ficker E, Annunziato L, Taglialatela M (2002) Histidines 578 and 587 in the S5-S6 linker of the human Ether-a-gogo Related Gene-1 K+ channels confer sensitivity to reactive oxygen species. J Biol Chem 277:8912-8919.

Papa M, Canitano A, Boscia F, Castaldo P, Sellitti S, Porzig H, Taglialatela M, Annunziato L (2003) Differential expression of the Na+-Ca2+ exchanger transcripts and proteins in rat brain regions. J Comp Neurol 461:31-48.

Philipson KD, Nicoll DA (2000) Sodium-calcium exchange: a molecular perspective. Annu Rev Physiol 62:111-133.

Pintado AJ, Herrero CJ, Garcia AG, Montiel C (2000) The novel Na(+)/Ca(2+) exchange inhibitor KB-R7943 also blocks native and expressed neuronal nicotinic receptors. Br J Pharmacol 130:1893-1902.

Quednau BD, Nicoll DA, Philipson KD (1997) Tissue specificity and alternative splicing of the Na+/Ca2+ exchanger isoforms NCX1, NCX2, and NCX3 in rat. Am J Physiol 272:C1250-1261.

Reeves JP, Hale CC (1984) The stoichiometry of the cardiac sodium-calcium exchange system. J Biol Chem 259:7733-7739.

Reuter H, Porzig H (1995) Localization and functional significance of the Na+/Ca2+ exchanger in presynaptic boutons of hippocampal cells in culture. Neuron 15:1077-1084.

Reuter H, Henderson SA, Han T, Ross RS, Goldhaber JI, Philipson KD (2002a) The Na+-Ca2+ exchanger is essential for the action of cardiac glycosides. Circ Res 90:305-308.

Reuter H, Henderson SA, Han T, Matsuda T, Baba A, Ross RS, Goldhaber JI, Philipson KD (2002b) Knockout mice for pharmacological screening: testing the specificity of Na+-Ca2+ exchange inhibitors. Circ Res 91:90-92.

Roozendaal B, McEwen BS, Chattarji S (2009) Stress, memory and the amygdala. Nat Rev Neurosci 10:423-433.

Rose GM, Dunwiddie TV (1986) Induction of hippocampal long-term potentiation using physiologically patterned stimulation. Neurosci Lett 69:244-248.

Secondo A, Staiano RI, Scorziello A, Sirabella R, Boscia F, Adornetto A, Valsecchi V, Molinaro P, Canzoniero LM, Di Renzo G, Annunziato L (2007) BHK cells transfected with NCX3 are more resistant to hypoxia followed by reoxygenation than those transfected with NCX1 and NCX2: Possible relationship with mitochondrial membrane potential. Cell Calcium 42:521-535.

Secondo A, Pannaccione A, Molinaro P, Ambrosino P, Lippiello P, Esposito A, Cantile M, Khatri PR, Melisi D, Di Renzo G, Annunziato L (2009a) Molecular Pharmacology of the Amiloride Analog 3-Amino-6-chloro-5- (4-chloro-benzyl)amino -N- (2,4-dimethylbenzyl)amin o iminomethyl -pyrazinecarboxamide (CB-DMB) as a Pan Inhibitor of the Na(+)-Ca(2+) Exchanger Isoforms NCX1, NCX2, and NCX3 in Stably Transfected Cells. Journal of Pharmacology and Experimental Therapeutics 331:212-221.

Secondo A, Pannaccione A, Molinaro P, Ambrosino P, Lippiello P, Esposito A, Cantile M, Khatri PR, Melisi D, Di Renzo G, Annunziato L (2009b) Molecular pharmacology of the amiloride analog 3-amino-6-chloro-5-[(4-chloro-benzyl)amino]-n-[[(2,4-dimethylbenzyl)-amino]iminomethyl]-pyrazinecarboxamide (CB-DMB) as a pan inhibitor of the Na+-Ca2+ exchanger isoforms NCX1, NCX2, and NCX3 in stably transfected cells. J Pharmacol Exp Ther 331:212-221.

Secondo A, Esposito A, Petrozziello T, Boscia F, Molinaro P, Tedeschi V, Pannaccione A, Ciccone R, Guida N, Di Renzo G, Annunziato L (2018a) Na + /Ca 2+ exchanger 1 on nuclear envelope controls PTEN/Akt pathway via nucleoplasmic Ca 2+ regulation during neuronal differentiation. Cell Death Discov 4:12.

Secondo A, Esposito A, Petrozziello T, Boscia F, Molinaro P, Tedeschi V, Pannaccione A, Ciccone R, Guida N, Di Renzo G, Annunziato L (2018b) Na. Cell Death Discov 4:12.

Secondo A, Esposito A, Sirabella R, Boscia F, Pannaccione A, Molinaro P, Cantile M, Ciccone R, Sisalli MJ, Scorziello A, Di Renzo G, Annunziato L (2015) Involvement of the Na+/Ca2+ exchanger isoform 1 (NCX1) in neuronal growth factor (NGF)-induced neuronal differentiation through Ca2+-dependent Akt phosphorylation. J Biol Chem 290:1319-1331.

Seeger T, Fedorova I, Zheng F, Miyakawa T, Koustova E, Gomeza J, Basile AS, Alzheimer C, Wess J (2004) M2 muscarinic acetylcholine receptor knock-out mice show deficits in behavioral flexibility, working memory, and hippocampal plasticity. J Neurosci 24:10117-10127.

Shepherd JK, Grewal SS, Fletcher A, Bill DJ, Dourish CT (1994) Behavioural and pharmacological characterisation of the elevated "zero-maze" as an animal model of anxiety. Psychopharmacology (Berl) 116:56-64.

Silva AJ, Stevens CF, Tonegawa S, Wang Y (1992) Deficient hippocampal long-term potentiation in alpha-calcium-calmodulin kinase II mutant mice. Science 257:201-206.

Sokolow S, Luu SH, Headley AJ, Hanson AY, Kim T, Miller CA, Vinters HV, Gylys KH (2011) High levels of synaptosomal Na(+)-Ca(2+) exchangers (NCX1, NCX2, NCX3) co-localized with amyloid-beta in human cerebral cortex affected by Alzheimer's disease. Cell Calcium 49:208-216.

Squire LR (1992) Declarative and nondeclarative memory: multiple brain systems supporting learning and memory. J Cogn Neurosci 4:232-243.

Squire LR, Stark CE, Clark RE (2004) The medial temporal lobe. Annu Rev Neurosci 27:279-306.

Stanley EM, Wilson MA, Fadel JR (2012) Hippocampal neurotransmitter efflux during one-trial novel object recognition in rats. Neurosci Lett 511:38-42.

Sui L, Wang J, Li BM (2008) Role of the phosphoinositide 3-kinase-Akt-mammalian target of the rapamycin signaling pathway in long-term potentiation and trace fear conditioning memory in rat medial prefrontal cortex. Learn Mem 15:762-776.

Sun P, Enslen H, Myung PS, Maurer RA (1994) Differential activation of CREB by Ca2+/calmodulin-dependent protein kinases type II and type IV involves phosphorylation of a site that negatively regulates activity. Genes Dev 8:2527-2539.

Tatem KS, Quinn JL, Phadke A, Yu Q, Gordish-Dressman H, Nagaraju K (2014) Behavioral and locomotor measurements using an open field activity monitoring system for skeletal muscle diseases. J Vis Exp:51785.

Tolman EC (1948) Cognitive maps in rats and men. Psychol Rev 55:189-208.

Wakimoto K, Kobayashi K, Kuro-O M, Yao A, Iwamoto T, Yanaka N, Kita S, Nishida A, Azuma S, Toyoda Y, Omori K, Imahie H, Oka T, Kudoh S, Kohmoto O, Yazaki Y, Shigekawa M, Imai Y, Nabeshima Y, Komuro I (2000) Targeted disruption of Na+/Ca2+ exchanger gene leads to cardiomyocyte apoptosis and defects in heartbeat. J Biol Chem 275:36991-36998.

Walters ET, Byrne JH (1984) Post-tetanic potentiation in Aplysia sensory neurons. Brain Res 293:377-380.

Watano T, Harada Y, Harada K, Nishimura N (1999) Effect of Na+/Ca2+ exchange inhibitor, KB-R7943 on ouabain-induced arrhythmias in guinea-pigs. Br J Pharmacol 127:1846-1850.

Wong CW (1997) Two circuits to convert short-term memory into long-term memory. Med Hypotheses 49:375-378.

Wood-Kaczmar A, Deas E, Wood NW, Abramov AY (2013) The role of the mitochondrial NCX in the mechanism of neurodegeneration in Parkinson's disease. Adv Exp Med Biol 961:241-249.

Zucker RS, Regehr WG (2002) Short-term synaptic plasticity. Annu Rev Physiol 64:355-405.